REMOVAL OF CONTAMINANTS OF VARIOUS TYPES FROM MODEL SOLUTIONS AND SEWAGES - PHYSICOCHEMICAL AND SPECTROSCOPIC STUDIES

Zbigniew HUBICKI, Marek MAJDAN, Dorota KOŁODYŃSKA, Monika WAWRZKIEWICZ, Anna WOŁOWICZ, Agnieszka GŁADYSZ-PŁASKA, Magdalena MAKARSKA-BIAŁOKOZ, Grzegorz WÓJCIK, Justyna BĄK, Marzena GĘCA, Agnieszka LIPKE, Weronika SOFIŃSKA-CHMIEL
DEPARTMENT OF INORGANIC CHEMISTRY

It is very important to develop research related to innovative and efficient methods of removing pollutants from the environment in particular from waters and wastewaters in the next few years. The challenges involve new, more efficient and selective adsorbents. To meet these requirements, new trends point to the development of adsorbents of a combined or hybrid nature. Organic-inorganic composite materials have found numerous applications in the areas of chemistry, biochemistry, engineering, and material science. The combination of organic and inorganic precursors yields hybrid materials of mechanical properties not present in the pure materials therefore, organic-inorganic composite ion exchange materials show the improvement in their properties that makes them more suitable for the application in the environmental protection. Besides the traditional methods used for this purpose research on preparation and economical use of mineral and organic adsorbents is carried out. Here lignin occupies an important part as a cheap and readily available biosorbent waste [1], and above all, the material that can be easily modified [2]. It can be used for heavy metal ions, dyes and organic pollutants removal. Lignin can also be modified by synthetic adsorbents such as oxides. In this group of particular interest are: (i) oxides and oxide systems (such as silicon dioxide, magnesium oxide, aluminum trioxide, iron oxide(II,III), titanium dioxide), (ii) hybrids (containing e.g. chitin, chitosan, oxide systems), and (iii) polymers.

In this paper we attempted to use TiO_2/lignin and TiO_2-SiO_2/lignin hybrid materials so far, not reported in the literature, with the potential sorbents of Pb(II) ions from model solutions. The obtained TiO_2/lignin and TiO_2-SiO_2/lignin hybrid materials were applied for the adsorption of lead(II) ions from aqueous systems. Lead nitrate, $Pb(NO_3)_2$, was used as the source of lead(II) ions. It was determined how parameters such as: (i) the phase contact time from 1 to 180 min. for the solutions at the concentrations 25, 50, 75 and 100 mg/L, pH 5 and mass of the adsorbents of 0.5 g, at a temperature 293 K, (ii) the reaction system pH value from 3 to 7 for the solutions at concentrations 50 mg/L, mass of the adsorbents of 0.5 g, at temperature 293 K and the phase contact time 180 min. as well as (iii) the mass of the adsorbents from 0.5 to 5 g for the solutions at concentrations 50 mg/L, at pH value 5, at a temperature 293 K influence on the effectiveness of lead(II) ions removal.

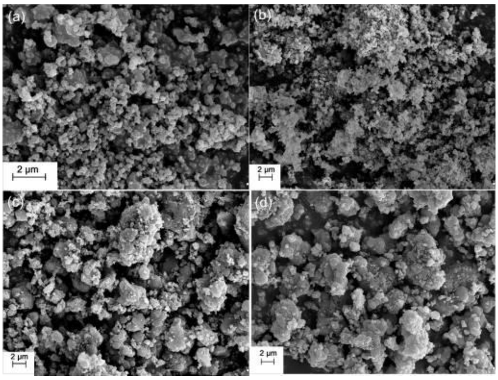

Fig.1. SEM images of titanium dioxide (a), TiO2/lignin hybrid material (b), titania-silica oxide system (c) and TiO2-SiO2/lignin hybrid (d).

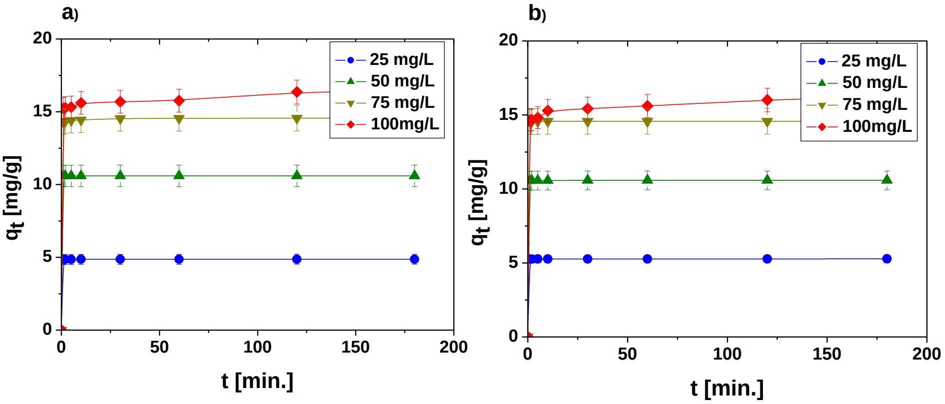

Fig.2. Kinetic data for the adsorption of Pb(II) ions at different initial concentrations on TiO2/lignin (a, c, e) and TiO2-SiO2/lignin (b, d, f) sorbents.

It was found that the most promising removal of Pb(II) ions occurs at pH 5 and the amount of adsorbent 0.5 g. In all cases sorption capacity (q_t) of the studied materials increases with the increasing initial concentration of Pb(II). Moreover, with the phase contact time passage the value q_t also increases. The highest sorption capacity 16.48 mg/g and 16.27 mg/gm in the Pb(II) ions sorption was obtained on the TiO_2/lignin and TiO_2-SiO_2/lignin adsorbents, respectively. These values correspond the minimal value of sorption percentage for the concentration range 25-100 mg/L. For the lead-TiO_2/lignin and lead-TiO_2-SiO_2/lignin systems the sorption process can be well defined by the Langmuir isotherm model. The obtained results showed the highest efficiency of lead(II) removal onto TiO_2-SiO_2/lignin compared with TiO_2/lignin. It can also be concluded that the process was spontaneous, favourable and exothermic in nature.

References:

[1] Y. Lei, Y. Huizhen, *Adv. Mater. Res.*, **622** (2013) 1646-1650.
[2] Y. Ge, Z. Li, Y. Kong, Q. Song, K. Wang, *J. Ind. Eng. Chem.*, **20** (2014) 4429-4436.

STUDIES OF ELECTRODE PROCESSES AND PRECONCENTRATION OF TRACE ELEMENTS AND BIOLOGICALLY ACTIVE COMPOUNDS AND ITS EXPLOITATION FOR ANALYTICAL PURPOSES

Mieczysław KOROLCZUK, Małgorzata GRABARCZYK, Iwona GĘCA,
Mateusz OCHAB
DEPARTMENT OF ANALYTICAL CHEMISTRY
AND INSTRUMENTAL ANALYSIS

The application of double deposition and stripping steps was utilized to decrease the detection limit of Se(IV) determination by anodic stripping voltammetry (ASV). Gold film macroelectrode and an ensemble of five gold microelectrodes were used during the first and the second deposition step, respectively. As the deposition step at the first electrode was finished, the first electrode was shifted to the bottom of the vessel at a short distance opposite an ensemble of microelectrodes. After that stage the first stripping step was performed and then the analyte stripped from the first electrode was deposited on the second one. Because of the fact that the volume of the space between electrodes was very small, concentration of analyte in the solution between electrodes was much higher than in the depth of the solution and, consequently, the detection limit was decreased. The application of double deposition and stripping step was used to decrease the detection limit and to minimize the interference effect of Se(IV) determination. The optimized procedure was used for determining selenium traces in natural water samples.

Preparation of gold film electrode

The gold film was plated onto the glassy carbon electrode from the solution containing 1.25×10^{-4} mol L^{-1} Au(III) + 0.025 mol L^{-1} HCl + 4 g L^{-1} urea at the potential of -0.3 V for 120 s. Then the gold film was polarized at the potential of 0.2 V within 15 s for stripping impurities from the film and finally it was washed with purified water.

The Se(IV) determination procedure consists of the following steps: The sample was pippeted to the voltammetric cell and the following reagents were added: 600 µL 1 mol L^{-1} H_2SO_4 and water to the volume of 30 mL. Firstly the potential of 1.2 V for 15 s was applied to the first electrode in order to clean the surface of electrode after the preceding measurement. The deposition of elemental Se at the first electrode with large surface area was carried out at -0.1 V for 180 s from the stirred solution. Stirring was performed using a magnetic stirring bar. Next the stirring was stopped, the stirrer was directed near the wall of the vessel using a stir bar retriever placed outside the cell and the electrode was moved near an ensemble of microelectrodes and the deposited Se was oxidized to Se(IV) by applying the potential of 1.3 V for 15 s. The first electrode was disconnected and the potential of -0.15 V for 120 s was applied to the second electrode in order to perform the second deposition step at this electrode. Then, a square wave voltammogram was recorded at a frequency of 20 Hz, while the potential was changed from -0.2 to 1.05 V. The amplitude and the potential step were equal to 25 and 2 mV, respectively. The measurements were carried out without solution deoxygenation. After each measurement a conditioning step of 20 s at 1.0 V (with solution stirring) was used to remove the target metals from an ensemble of microelectrodes.

The procedure optimization

The concentration of H_2SO_4 was changed from 0.005 to 0.1 mol L^{-1} and its influence on selenium analytical signal was studied. The selenium peak current was observed to attain the maximal value when H_2SO_4 concentration was equal to 0.02 mol L^{-1} and so this value was chosen for further study. The optimum deposition potentials were found to be -0.1 V and -0.15 V at the first and second electrode, respectively. Another parameter influencing the Se(IV) signal was the time of deposition. At first deposition time at the first electrode was changed from 90 to 600 s while deposition time at the second electrode was 120 s. For further measurements deposition time at the first electrode equal to 180 s was chosen because at such deposition time the maximum value of the Se(IV) peak current was observed. Similar measurements were performed at constant deposition time at the first electrode equal to 180 s and deposition time at the second electrode was changed in the range from 30 to 300 s. The Se(IV) peak current in this case increased only as deposition time was prolonged to 120 s.

The calibration graph for Se(IV) in the optimized conditions was linear in the range from 5×10^{-9} to 1×10^{-7} mol L^{-1} with the linear correlation coefficient $r = 0.9987$. The relative standard deviation from seven determinations of Se(IV) at a concentration of 5×10^{-8} mol L^{-1} was 4.3 %. The limit of detection of Se(IV) determination estimated from (3σ) for the lowest studied concentration of Se(IV) was 8.5×10^{-10} mol L^{-1} for deposition time of 180 and 120 s at the first and the second electrode, respectively.

The influence of foreign ions and surfactants on the determination of Se(IV) was studied for a Se(IV) concentration of 5×10^{-8} mol L^{-1}. The results show that at least 1000-fold amounts of As(V) and Mo(VI), 500-fold amounts of As(III), Cd(II), Co(II), Fe(III), Se(VI) and Zn(II), 200-fold amounts of Pb(II) and Ni(II), 50-fold amounts of Sb(III), 25-fold amounts of Cu(II), 5-fold amounts of Bi(III) and 2-fold amounts of Hg(II) do not influence selenium peak current. The influence of surfactants as interfering organic species on the Se(IV) peak current was studied using Triton X-100, CTAB and SDS. It was observed that Triton X-100 at a concentration of 1 mg L^{-1} and SDS at a concentration of 5 mg L^{-1} did not influence the Se(IV) peak current, whereas CTAB at a concentration of 0.5 mg L^{-1} caused a decrease of the Se(IV) peak current to 91 % of its original value.

The proposed procedure was used for Se(IV) determination in certified reference material SPS-SW1 synthetic freshwater (certified value for selenium was equal to 2.00 ± 0.02 μg L^{-1}). Determinations were carried out using the method of standard additions. The obtained result of 2.09 μg L^{-1} with a standard deviation 4.4 % ($n = 3$) confirmed the accuracy of the proposed method and indicates that this procedure can be used for Se(IV) determination in natural water samples. Additionally, Se(IV) was determined in the Bystrzyca river and Lake Zemborzyce water samples. Because the Se(IV) content in the river and lake water samples was below the detection limit of the procedure, the recoveries of added Se(IV) were studied. The recoveries for Se(IV) from the river and lake water samples added at a concentration of 2.5×10^{-8} and 5×10^{-8} mol L^{-1} ranged from 95 % to 103 %, so the proposed procedure can be applied for analyses of Se(IV) in natural water samples.

Ryszard DOBROWOLSKI, Joanna DOBRZYŃSKA
DEPARTAMENT OF ANALYTICAL CHEMISTRY
AND INSTRUMENTAL ANALYSIS

Gold is a precious metal widely used in various areas of the human activity. Being a toxic element it may cause the allergic egzematous dermatitis. However chosen gold organic compounds e.g. auranofin act as antitumor drugs. Due to the widespread application of gold in industry and medicine the development of precise and trustworthy procedures of its determination in samples of various matrix is necessary. The analytical methods ensuring the low detection limits such as GF AAS, ICP-OES and ICP-MS are usually employed for the gold determination in environmental, industrial and biological samples. However, taking into account the matrix interferences and low concentration of gold, the obtaining of the reliable results is often impossible without the separation and preconcentration of the noble metal. The preconcentration and separation of gold may be realized by solid-phase extraction (SPE). Recently, the attention of scientists focus ion-imprinted polymers (IIP) which are characterized by the presence of the specific ion recognition sites in the polymeric matrix. Despite the numerous advantages (the high recognition property, chemical and mechanical stability, selectivity towards specific analytes) IIP are characterized by low active surface which is the reason of low sorption capacities exhibited towards specific ions. This problem may be overcome by the application of silica as a matrix. The main advantage of silica-based ion imprinted materials is the possibility of the surface functionalization, which leads to the increase of the adsorption capacities.

In this work the organosilica of SBA-15 type was applied as a matrix to prepare the new ion-imprinted material dedicated to the enrichment of Au(III) ions. The parameters affecting the adsorption of Au(III), such as pH of the solution, contact time and interfering ions were investigated. The possibility of gold desorption from the ion-imprinted silica was studied using nitric acid, hydrochloric acid and thiourea solution.

In the model synthesis, 2 g of P123 was mixed with 60 mL of 2 M HCl and 11 mL of deionized water under stirring at 40°C. After 8 h $AuCl_3$ (0.15 g), tetraethoxysilane TEOS (18 mmol) and thiocyanatopropyltriethoxysilane TCTES (2 mmol) were added. The mixture was stirred at 40°C for 24 h and aged at 100°C for next 48 h. The obtained solid was washed with deionized water, filtered and dried at 100°C. Pluronic123 was removed by three-time extraction with the acidified ethanol (99.8 %) at 78 °C. The template Au(III) ions were removed from the materials using 0.5 M thiourea in 5 % HCl, until Au was not detected (GF AAS) in the leaching solution. The control adsorbent was similarly synthesized in the absence of $AuCl_3$. The ion imprinted and non-ion imprinted sorbents were marked as Au(III)TCTES and TCTES, respectively.

The adsorption/desorption experiments were carried out using batch mode. The effect of equilibrium pH on Au(III) adsorption onto the Au(III)TCTES and TCTES was investigated in the range between 0.5 and 4.5 for the adsorption system consisting of 50 mL of 50 mg/L Au(III) solution and 50 mg of sorbents. In the case of Au(III)TCTES the adsorption does not depend on the pH value for the studied range. In the adsorption equilibrium state Au(III) ions were completely adsorbed onto sorbent surface for all studied systems. In the case for TCTES material the complete adsorption was observed between 2.0 and 4.5, whereas the decrease of pH from 2 to 0.5 resulted in the decrease of the adsorption from 50 to 35 mg/g.

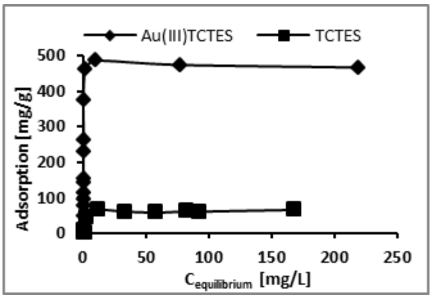

Fig.1. Adsorption isotherms of Au(II onto Au(III)TCTES and TCTES; m 0.005 g, V = 5 mL, $t_{Au(III)TCTES}$ = 3h, t_{TC} = 24 h, T = 25°C, $pH_{initial}$ = 2.0

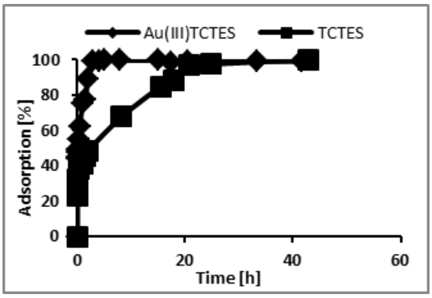

Fig.2. Adsorption kinetics of Au(III) onto Au(III)TCTES and TCTES; m=0.005 mg, V=5 mL, c_{Au} =100 mg/L, pH=2

Based on kinetic studies (Fig.2) it was stated that the adsorption equilibrium was achieved after 3 and 24 hours for Au(III)TCTES and TCTES, respectively. The acceleration of the process observed in the case of ion-imprinted material was the result of the absence of steric hindrance, which allows rapid contact of Au(III) ions with imprinting sites. In the both cases the sorption process was found to follow pseudo second-order kinetic model. Based on the adsorption isotherms it was stated that the maximum static adsorption capacity of Au(III)TCTES reached 485 mg/g and was 7.5 times higher than in the case of non imprinted sorbent (Fig.1). The experimental data could be successfully fitted to the linear Langmuir equation. Due to the fact that before the analysis the environmental samples are usually digested in inorganic acids, the impact of chlorides and nitrates (present in aqua regia) on the adsorption of Au(III) was investigated carefully. It was stated that even 1 M solution of NO_3^- ions do not influence on the adsorption of Au(III) onto Au(III)TCTES and TCTES, whereas 1 M solution of Cl^- ions drastically (about 85%) decrease the adsorption of Au(III) when TCTES sorbent is used. In the case of Au(III)TCTES the decrease of the adsorption is not observed in the presence of chlorides. It was found that the effectiveness of gold desorption from Au(III)TCTES in the presence of concentrated nitric, hydrochloric acid and thiourea solution was significantly lower than from TCTES. Due to incomplete desorption of Au from Au(III)TCTES the slurry sampling graphite furnace atomic absorption spectrometry was proposed for determination of gold in real samples after its enrichment on Au(III)TCTES.

Jolanta NIESZPOREK, Dorota GUGAŁA-FEKNER, Dorota SIEŃKO
DEPARTMENT OF ANALYTICAL CHEMISTRY
AND INSTRUMENTAL ANALYSIS

Surfactants are substances having the ability to adsorb on the electrode/electrolyte interface and thus the ability to change the properties of electrode surface. As a result surfactants can change the rate of electrode processes. Recent studies showed that the cationic surfactant octyltrimethylammonium bromide [1] and nonionic surfactants N-octanoyl-N-methylglucamine and N-decanoyl-N-methylglucamine [2] have an inhibiting effect on the Zn^{2+} electroreduction rate on the mercury electrode. Surfactant particles adsorbed on mercury electrode close down the access of depolarizer ions to the electrode and thus hinder their electroreduction. Quite different ability have anionic surfactants: sodium 1-octanesulfonate (SOS) and sodium 1-decanesulfonate (SDS), they cause the increase of the rate of above mentioned electrode process.

Table 1. The changes in the difference between the anodic peak potential and the cathodic peak potential $\Delta E=E_a-E_k$ [V] and the values of the lowest charge transfer resistance R_a [$\Omega \cdot cm^2$] determined at the formal potential for the process of Zn^{2+} ion electroreduction in 1 $mol \cdot dm^{-3}$ $NaClO_4$ in the presence and absence of sodium 1-octanesulfonate and sodium1-decanesulfonate at 288K and 298K.

c_{SOS}/M	SOS				c_{SDS}/M	SDS			
	T=288K		T=298K			T=288K		T=298K	
	ΔE	R_a	ΔE	R_a		ΔE	R_a	ΔE	R_a
0	0.098	12.03	0.077	6.60	0	0.098	12.03	0.077	6.60
$1.0 \cdot 10^{-3}$	0.098	11.66	0.072	6.51	$2.5 \cdot 10^{-4}$	0.097	9.37	0.077	5.36
$3.0 \cdot 10^{-3}$	0.088	8.93	0.067	5.06	$4.0 \cdot 10^{-4}$	0.088	8.28	0.077	5.10
$5.0 \cdot 10^{-3}$	0.080	7.54	0.058	4.10	$6.0 \cdot 10^{-4}$	0.076	7.20	0.060	4.06
$1.0 \cdot 10^{-2}$	0.072	7.22	0.057	3.97	$7.5 \cdot 10^{-4}$	0.065	5.97	0.058	3.81
$3.0 \cdot 10^{-2}$	0.058	5.21	0.051	2.95	$9.0 \cdot 10^{-4}$	0.063	6.25	0.054	3.79
$7.0 \cdot 10^{-2}$	0.052	4.05	0.050	2.41	$1.0 \cdot 10^{-3}$	0.060	5.78	0.052	3.22
$1.0 \cdot 10^{-1}$	0.052	3.72	0.048	2.56	-	-	-	-	-

It has been proved by the differences between the potentials of the anodic and cathodic peaks (ΔE) on the cyclic voltamperogram (CV), the decrease of the values of the charge-transfer resistance (R_a) obtained at the formal potential using the faradaic impedance method and the increase of the standard electroreduction rate constants caused by the increase of SOS and SDS concentrations. The catalytic activity of aforementioned anionic surfactants is caused by the formation on the electrode surface an unstable active complex between depolarizer ions and surfactant particle. The complex facilitates the exchange of electrons between Zn^{2+} ions and electrode. More effective catalysts for Zn^{2+} electroreduction on the mercury electrode is the anionic surfactant with longer hydrocarbon chain like sodium 1-decanesulfonate. Also an increase in temperature of the solution has favorable effect on the Zn^{2+} electroreduction rate.

The Tafel plots show that the dependences ln k_f vs. f(E) are nonlinear and the slopes of curves change with the change of potentials and surfactants concentrations. Thus the Zn^{2+} electroreduction in the presence of SOS and SDS surfactants is a multi-stage process. The mechanism of Zn^{2+} electroreduction on the mercury electrode in the presence of SOS and SDS have been considered using Fawcett models [3, 4]: EE (electron transfer – electron transfer), IA (ion transfer – adsorption), IE (ion transfer – electron transfer) and CE (chemical step – electron transfer). The EE model has been ruled out and three other CE, IE and IA seem to be acceptable to describe the mechanism of Zn^{2+} ion electroreduction on the mercury electrode.

The independent studies were devoted to the pH influence on the adenine adsorption on mercury electrode in the presence of acetate buffer.

References:

[1] J. Nieszporek, *J. Electroanal. Chem.,* **706** (2013) 108-116.
[2] J. Nieszporek, K. Dagci, *Electrochim. Acta,* **125** (2014) 473-481.
[3] W.R. Fawcett, *J. Electroanal.Chem.*, **302** (1991) 13.
[4] W.R. Fawcett, *J. Electroanal.Chem.,* **310** (1991) 13.

Katarzyna TYSZCZUK-ROTKO
DEPARTMENT OF ANALYTICAL CHEMISTRY
AND INSTRUMENTAL ANALYSIS

The aim of the study was to develop voltammetric procedure for the determination of biologically active compounds with the use of electrodes modified with polymer and bismuth particles. The bismuth particles were deposited by an in situ method at Nafion covered boron-doped diamond electrode (BDDE) from 0.1 mol L^{-1} sulphuric acid solution containing metal ions and different concentrations of paracetamol and caffeine. The obtained oxidation peaks of paracetamol and caffeine appear at 0.78 and 1.44 V (vs. Ag/AgCl), respectively. The obtained detection limits for paracetamol and caffeine were 2.62×10^{-8} and 1.14×10^{-9} mol L^{-1}, respectively. The comparison to other electrochemical sensors proposed for the simultaneous paracetamol and caffeine assays shows that bismuth nanoparticles Nafion covered BDDE provides lower [1-5] detection limits of both compounds and the widest linear range. In one case [6] the paracetamol and caffeine detection limits are significantly lower than those obtained by the presented procedure. However, the proposed procedure of the sensor preparation is much simpler than the procedure described in [6].

The optimized voltammetric procedure was used for the simultaneous determination of paracetamol and caffeine in commercially available pharmaceutical formulation containing both of these compounds. The standard addition method was adopted in order to minimize possible matrix effects of other substances present in the sample. No significant differences between the data supplied by the manufactures and the data obtained by the proposed voltammetric method were observed. The extracts of different types of tea and coffee were also analyzed in order to determine caffeine employing the proposed heroin differential-pulse voltammetric method and adsorptive stripping voltammetric method using Nafion covered lead film glassy carbon electrode [7] for comparison. Moreover, both of the methods were used to determine caffeine in the weight loss supplement. The obtained results were found to be satisfactory.

References:

[1] J. Zen, Y. Ting, *Analitica Chimica Acta,* **342** (1997) 175.
[2] T. R. Saciloto, P. Cervini, É. T. G. Cavalheiro, *Journal of the Brazilian Chemical Society,* **24** (2013) 1461.
[3] B. Habibi, M. Jahanbakhshi, M. Abazari, *Journal of the Iranian Chemical Society,* **11** (2014) 511.
[4] A. Câmpean, M. Tertiş, R. Săndulescu, *Central European Journal of Chemistry,* **9** (2011) 688.
[5] M. Amiri-Aref, J. B. Raoof, R. Ojani, *Sensors and Actuators B: Chemical,* **192** (2014) 634.
[6] R. N. Goyal, A. R. S. Rana, H. Chasta, *Journal of the Electrochemical Society,* **60** (2013) G3014.
[7] K. Tyszczuk-Rotko, I. Bęczkowska, *Food Chemistry,* **172** (2015) 24.

Joanna LENIK, Cecylia WARDAK
DEPARTMENT OF ANALYTICAL CHEMISTRY
AND INSTRUMENTAL ANALYSIS

Cyclodextrins belong to the group of cyclical oligosaccharides and they are formed from α-D-glucopyranose units linked together by α-(1,4) acetal bonds. The most common cyclodextrins are α-, β- and γ-cyclodextrins, which consist of 6-, 7-, and 8-glucose units respectively. α-, β- and γ-cyclodextrins occur in the form of white crystal powders of a delicate sweetish taste. They are capable of interacting with a large variety of guest molecules: organic compounds, ions, and even structures as small as radicals to form inclusion complexes; therefore they are widely used in different branches of industry [1, 2].

The scientific novelty of the presented work was the incorporation of selected β-cyclodextrin derivatives heptakis (2,3,6-tri-O-methyl)-β-cyclodextrin (HSMβCD), heptakis (2,3,6-tri-O-benzoyl)-β-cyclodextrin (HSBβCD), (2-hydroxypropyl)-β-cyclodextrin (HPβCD), 2-hydroxypropyltrimethylammonium-β-CD - quaternary ammonium β-cyclodextrin (QAβCD) as electroactive material of ion-selective naproxen electrodes.

The formation of inclusive complexes of these cyclodextrins was confirmed by IR spectroscopy. The naproxen molecule as the guest was partially or completely incorporated into the cavity of the host-cyclodextrin molecule.

The optimum membrane of ion-selective electrode contains heptakis(2,3,6-tri-O-benzoyl)-β-cyclodextrin, o-nitrophenyloctyl ether and tetraoctylammonium chloride as a lipophilic salt. The electrode is characterized by a Nernstian response slope of 59.0 ±0.5 mV decade^{-1} over the linear range of 5.0×10^{-5}–1.0×10^{-2} mol L^{-1} and the detection limit 1.0×10^{-5} mol L^{-1}, as well as the response time 10 s. It can be used in the pH range 6.2–8.5 for 10 months without any considerable deterioration. The high selectivity, which is perhaps the most valuable advantage of the constructed sensors, is also worth mentioning. The use of functionalized β-cyclodextrin in the polymeric membrane increased the selectivity coefficients.

Also, the electrode is cheap and easy to construct and use for determination of naproxen in the pharmaceutical and milk samples with good accuracy and precision. It provides an attractive, alternative method for naproxen determination in quality control laboratories.

References:

[1] H. Dodziuk, Cyclodextrins and Their Complexes, Wiley-VCh Verlag GmbhH & Co. KGaA, Weinheim, 2006.
[2] W. Śliwa, Cyclodextrins, Wydawnictwo Częstochowa, 2001.

Agnieszka NOSAL - WIERCIŃSKA
DEPARTMENT OF ANALYTICAL CHEMISTRY
AND INSTRUMENTAL ANALYSIS

The electroreduction of metal ions in aqueous solutions is highly dependent not only on the type and concentration of the supporting electrolyte, but also on the presence of trace amounts of organic substances. Organic substances may either inhibit or accelerate the electrode process, or they may not affect its course.

Lovrič and co-workers [1 – 2], investigating the Bi(III) ions electroreduction in chlorates(VII), demonstrated that the Bi(III) ion electroreduction process is significantly affected by water particles. The authors assumed the three-step mechanism of Bi(III) electroreduction with the gradual transition of single electrons.

The Bi(III) ion hydrolysis limits the pH range that allows investigating the electroreduction of these ions [3]. It was found that a change in the chloric(VII) acid /sodium chlorate(VII) ratio in the basic electrolyte, affects the structure of both the bismuth aqua ion and the molecule of the selected amino acid, and, consequently, the course of the electrode process [4 – 5].

Homocysteine, according to the cap-pair rule, catalyses the process of Bi(III) ion electroreduction. Also, changes in the double layer parameters at the electrode/ chlorates(VII) interface, and a correlation between the rate of Bi(III) ion electroreduction in the presence of homocysteine and water activity under conditions of varying protonation of the catalysing substance were observed. The catalytic activity of homocysteine increases with an increasing amount of $NaClO_4$ in a basic electrolyte solution. The highest catalytic activity of homocysteine was observed for 2 $mol \cdot dm^{-3}$ chlorates(VII). The multistage process is confirmed by the not rectilinear $\ln k_f = f(E)$ dependences. In this mechanism, the chemical stages of $Bi–Hg(SR)_2$ complexes formation with the participation of homocysteine, which is a mediator in the formation of these complexes, and water can be distinguished. The composition of these complexes is diversified in solutions that differ in the degree of amino acid protonation.

References:

[1] Š. Komorsky – Lovrić, M. Lovrić and M. Branica, *J. Electrochem. Soc.,* **140** (1993) 1850.
[2] M. Lovrić and M. Branica, *Indian J. Chem.,* **29A** (1990) 435.
[3] A. Nosal – Wiercińska, *Electrochim. Acta,* **92** (2013) 397.
[4] A. Nosal – Wiercińska, M. Grochowski, M. Wiśniewska, K. Tyszczuk – Rotko, S. Skrzypek, M. Brycht, D. Guziejewski, *Electrocatalysis*, **6** (2015) 315.
[5] M. Grochowski, A. Nosal – Wiercińska, M. Wiśniewska, A. Szabelska, B. Gołębiowska, *Electrochim. Acta,* **207** (2016) 48.

STUDIES OF INTERIAL PHENOMENA AT DIFFERENT INTERFACES INCLUDING THE SYSTEMS WITH SURFACTANTS AND BIOSURFACTANTS

EFFECT OF LOW-TEMPERATURE PLASMA ON CHITOSAN-COATED POLYETHERETHERKETONE WETTABILITY

Agnieszka Ewa WIĄCEK, Małgorzata JURAK, Konrad TERPIŁOWSKI,
Aleksandra SZCZEŚ, Lucyna HOŁYSZ, Emil CHIBOWSKI
DEPARTMENT OF INTERFACIAL PHENOMENA

Polyetheretherketone (PEEK) is one of a few plastic polymers of the polyaryletherketones family (PAEK). It is evident that PEEK exhibits higher strength and greater resistance to both chemical and physical degradation than other well-known polymers. This polymer is largely resistant to thermal degradation as well as to the attack of inorganic and organic substances. Moreover, polyetheretherketone has the advantage to be formed into many different shapes because of its excellent mechanical properties. PEEK is also one of the promising alternative materials instead of metallic biomaterials because it is characterized by good chemical resistance and mechanical properties similar to those of human bones [1-4]. Due to satisfactory mechanical, thermal and surface properties, polyetheretherketone has found numerous applications in different kinds of industries. However, the main aspect of the biomaterial characteristics must be its biocompatibility, cells adhesion to the polymer, which should be also mechanically strong and biodegradable. PEEK meets fully conditions but the only disadvantage can be poor adhesive properties because polyetheretherketone like many other polymers has a low surface free energy that results in poor adhesion. It is known that the relatively low surface energy of PEEK can limit osseointegration, potentially leading to fibrous encapsulation and reduced wound healing in applications requiring integration. The way of excluding this difficulty is surface modification which leads to obtain useful properties [1-4].

Surface treatment by low-temperature plasma is especially effective for long-chain polymers, because such materials can be processed in a simple way. The efficiency of surface modification depends on plasma power, its contact time and concentration of active species. It is significant that physicochemical modification of the first few molecular layers of the surface during plasma action does not change the excellent properties of PEEK polymer bulk phase. During plasma treatment of PEEK surface hydrogen separation from polymeric chains and free radical creation are possible. Subsequently the radicals are able to interact with gas components and thus the new functional groups can be included into the PEEK surface.

The interesting trend of polymer research is the chemistry of biocompatible substances applicable for medical production. Antibacterial chitosan was used for PEEK modification because it has also many extra functions: forming a translucent film on the surface, blocking transpiration and decreasing a moisture loss. The film of this active substance can reduce activity of relevant enzyme during the storage period of different kinds of products and improve stability of the cellular membrane. Chitosan molecules can also induce a series of defensive reaction mechanism and blocking attack of pathogenic bacteria. On the other hand, chitosan-coated materials could be also applied as a pharmaceutical material because of its wound healing functions. Wettability of base and chitosan-coated polymer surfaces before and after plasma modification was investigated via contact angle measurements of three probe liquids (water, formamide and diiodomethane). The contact angles allowed evaluation of the total surface free energy and its components (Lifshitz-van der Waals component γ_S^{LW}, electron-donor γ_S^- and electron-acceptor γ_S^+ parameters) for different systems based on the theoretical approach proposed by van Oss et al. (LWAB) [5]. The XPS technique was used to analyse the surface carbon, oxygen and nitrogen contents of different PEEK probes. Plasma modification causes formation of free radicals and/or additional groups (mainly C–O-, C=O and O=C–O-) on its surface. The low-temperature plasma treatment of polyetheretherketone polymer resulted mainly in the increase of oxygen and nitrogen amounts on the surface which was confirmed by the XPS analysis. Both forms of plasma treated PEEK and plasma treated PEEK with the chitosan film contained similar quantities of carbon on the surface. The appearance of functional hydrophilic group caused a sharp increase of polar interactions and significant increase in the surface roughness. The treated PEEK surface was more hydrophilic, more rugged and rougher than base untreated PEEK. This was also verified by wettability and profilometer measurements. As follows from the calculations of the surface apparent free energy, the increased polar component was responsible for wettability changes of the studied polymer surfaces. The apolar component of the surface free energy remained almost the same. Some correlations between the changes in surface roughness and the values of contact angles measured on these surfaces can be obtained. The considerable rise in the surface roughness of polyetheretherketone after the plasma treatment extended the PEEK adhesive attributes and formation of compact chitosan film was attainable.

The presented results can be helpful to design the modified PEEK materials with the stable tridimensional surface structure and special antibacterial properties which can potentially be suitable for pharmaceutical and medical applications.

References:

[1] P. Patela, T. R. Hulla, R. E. Lyonb, S. I. Stoliarovc, R. N. Waltersb, S. Crowleyb and N. Safronava, *Polymer Degradation and Stability,* **96** (2010) 12.

[2] E.T.J. Rochford, A.H.C. Poulsson, J. Salavarrieta Varela, P. Lezuo, R.G. Richards and T.F. Moriarty, *Colloids Surfaces B.*, **113** (2014) 213.

[3] A. Murari and A. Barzon, *Vacuum,* **72** (2003) 327.

[4] M.C. Kuo, C.M. Tsai, J.C. Huang and M. Chen, *Materials Chemistry and Physics,* **90** (2005) 185.

[5] C.J. van Oss, M.K. Chaudhury and R.J. Good, *Chemical Reviews,* **88** (1988) 927.

STUDIES OF INTERIAL PHENOMENA AT DIFFERENT INTERFACES INCLUDING THE SYSTEMS WITH SURFACTANTS AND BIOSURFACTANTS

MUTUAL INFLUENCE OF RHAMNOLIPID AND ETHYL ALCOHOL ON THEIR ADSORPTION AND AGREGATION PROPERTIES

Anna ZDZIENNICKA, Katarzyna SZYMCZYK, Joanna KRAWCZYK,
Bronisław JAŃCZUK
DEPARTMENT OF INTERFACIAL PHENOMENA

Besides tendency to form micelles and adsorb at various interfaces, biosurfactants are also characterized by low toxicity and high biodegradability as well as high tolerance to environmental changes. These features are an alternative to the conventional surfactants obtained by chemical synthesis. One of the biosurfactants of great importance is rhamnolipid which as a non-toxic, biocompatible with human skin and mucous membranes compound, is added to cosmetic and food products. Ethanol is a compound commonly used in cosmetics. It is one of the oldest known antiseptic compounds which cleans and degreases the skin surface, dries up wounds and sores, and at the same time also acts antiedematously [1,2]. Ethanol is often added to the surfactant solutions and, depending on the concentration, can act as a co-surfactant or co-solvent [3]. The presence of ethanol can affect such properties as the CMC of surfactants, the number of aggregation or the degree of hydration. Therefore in this work volumetric and adsorptive properties of ethanol and rhamnolipid (RL) mixture were examined. These studies were carried out by measuring the surface tension, density and viscosity of aqueous solutions of rhamnolipid with the fixed concentrations of 0.00625, 0.5 and 20 mg/l and in the range of ethanol concentration from zero to 17.13 M (mole fraction equal to unity)

On the basis of the obtained results the mutual influence of rhamnolipid and ethyl alcohol on their adsorption at the solution-air interface and critical micelle concentration (CMC) were discussed. It appeared that in the RL concentration range corresponding to its unsaturated monolayer in the absence of ethanol [4] and the ethanol concentration range in the absence of rhamnolipid from 0 to its critical concentration of aggregation (CAC) [5], the independent adsorption of rhamnolipid and ethanol takes place. The surface tension of the solution above CAC is practically the same as the ethanol aqueous solutions. If the concentration of rhamnolipid is close to its CMC in the absence of ethanol and corresponds to the saturated monolayer at the solution-air interface then in the range of ethanol concentration from 0 to CAC [5] rhamnolipid plays a the decisive role in the reduction of water surface tension. However, the values of surface tension of the three-component solution are somewhat higher than that for the aqueous solution of rhamnolipid if the ethanol concentration is close to its CAC. Over the ethanol CAC the influence of rhamnolipid on the solution surface tension is not observed. It means that the values of solution surface tension are close to those of individual ethanol solution. As a result the adsorption of rhamnolipid at the solution-air interface is small if the concentration of ethanol is higher than its CAC. The above mentioned adsorption behaviour was confirmed by the standard Gibbs free energy of adsorption of ethanol and rhamnolipid calculated using different methods. The values of this energy at the RL concentration corresponding to the unsaturated monolayer at the water-air interface in the absence of ethanol and ethanol concentration lower than its CAC practically are the same as for individual solutions of rhamnolipid and ethanol. At the concentration of rhamnolipid and ethanol higher than the above mentioned there is mutual influence of rhamnolipid and ethanol on their tendency to adsorb at the solution-air interface.

Rhamnolipid does not significantly influence on the CAC of ethanol. The obtained values of surface tension, density and viscosity of the studied solutions showed that the values of ethanol CAC are practically the same as the solution of ethanol in the absence of rhamnolipid, however, there are some differences between CAC obtained based on the surface tension, density and viscosity isotherms. This confirms the suggestions of some investigators that the CAC is not one value but a range of concentrations.

Based on the results obtained from the density measurements, it appeared also that rhamnolipid did not influence on the apparent and partial molar volumes of water and ethanol. It is interesting that in the solution in which the ratio of water to ethanol molecules is 1 to 1, then the minimal excess of the solution volume in comparison to ideal mixing takes place. The values of partial molar volume obtained from the density data were compared to those calculated based on the bonds length and angle between them as well as the average distance between the molecules of alcohol and water. It proved that there is a good agreement between the volume values obtained from the density data and those calculated.

References:

[1] T. Stipcevic, A. Piljac, G. Piljac, *Burns*, **32** (2006) 24.
[2] T. Stipcevic, T. Piljac, R. R. Isseroff, J. *Dertmatol. Sci*. **40** (2005) 141.
[3] J.M. Rosen, *Surfactants and Interfacial Phenomena*, Wiley-Interscience, New York, 2004.
[4] D. Mańko, A. Zdziennicka, B. Jańczuk, *Appl. Surf. Sci,,* **120** (2017) 117.
[5] A. Chodzińska, A. Zdziennicka, B. Jańczuk,. *J Sol Chem.*, **41** (2012) 2226.

CHROMATOGRAPHIC AND SPECTROSCOPIC PROCEDURES IN ANALYSIS OF ORGANIC, BIOACTIVE COMPOUNDS

Andrzej L. DAWIDOWICZ, Irena CHOMA, Jadwiga SKUBISZEWSKA-ZIĘBA, Dorota WIANOWSKA, Barbara CHARMAS, Rafał TYPEK, Michał DYBOWSKI, Piotr BOROWSKI, Małgorzata OLSZOWY, Katarzyna BERNACIK
DEPARTAMENT OF CHROMATOGRAPHIC METHODS

Modified HS-SPME for determination of quantitative relations between low-molecular oxygen compounds in plant matrices

Essential oils (EOs) are highly complex fragrance mixtures of compounds, such as hydrocarbons (terpenes and sesquiterpenes) and oxygenated compounds (alcohols, aldehydes, acids, ketones, phenols, lactones, oxides, ethers and esters), varying in biological activity. Naturally synthesized by some plants, they are widely used in pharmaceutical, food, cosmetic and fragrance industries. As the quality of the final products containing EOs frequently depends on the type and quality of the source material, quality evaluation of plant material is required. Steam distillation (SD) is a routine method recommended by pharmacopoeias for the isolation of essential oils from plant materials to estimate their value as essential oil sources. This standard method is very time-consuming, and thus not efficient enough in the aroma composition analysis of numerous plant samples. Moreover, many EO components, when exposed to heat, light and oxygen (typical factors for the distillation process), easily decompose into substances which initially do not exist in the examined plants. Due to these limitations, some research attention has recently been given to the environmentally friendly method, i.e. solid phase microextraction (SPME), in which sample component degradation is eliminated. This method is routinely used in the head-space (HS) analysis of volatiles in different sample types: environmental, foodstuffs and plants. It is based on the sorption of analytes on fiber coating. After establishing equilibria between the headspace above the sample (plant) and fiber coating, the components are desorbed from the fiber to a chromatography column. The main limitation in the standard HS-SPME application for the evaluation of plants as sources of EOs are different quantitative relations of EO components from those obtained by direct analysis of EO which was got in the SD process from the same plant (hereafter named EO/SD). As demonstrated for the system consisting of Polydimethylsiloxane (PDMS) fiber and silica oil plant suspension, the replacement of the plant material by its suspension in oil of the same physicochemical character as that of SPME fiber coating allows to get similar quantitative relations of EO components to those in EO/SD [1]. The question appears at this moment if this idea can be transferred to the system of polar SPME fiber coating/plant suspension in a proper polar liquid. A few SPME fiber coatings are commercially available. The selection of proper liquid to each SPME fiber may seem problematic. However, the application of the system consisting of SPME fiber with Carbowax and plant suspension in polyethylene glycol (PEG) complies with the assumptions of the considered approach: plant suspension in liquid of the same physicochemical character as that of SPME fiber coating. The question seems to be justified as the interactions involved in distribution of EO components between suspending liquid/HS phase and HS phase/SPME fiber are different for silica oil plant suspension/PDMS fiber (mainly dispersive interactions) and plant suspended in PEG/Carbowax fiber (mainly specific interactions).

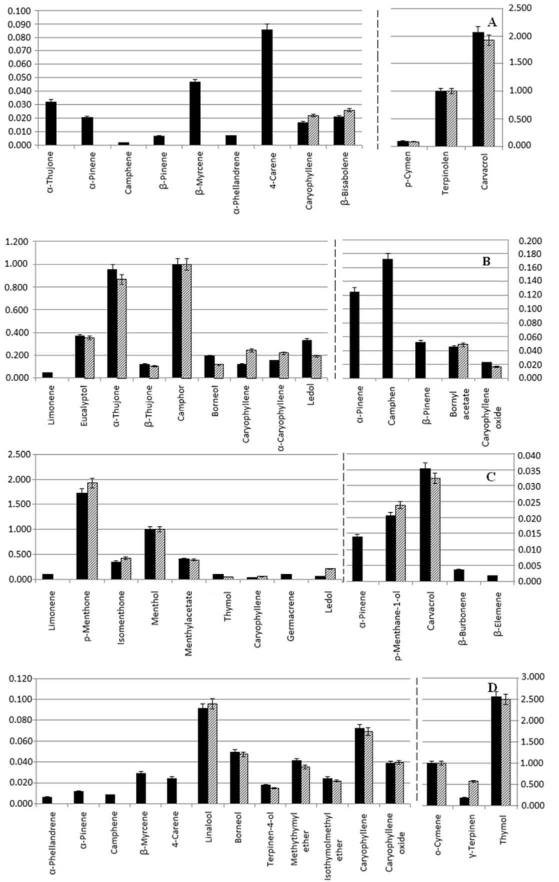

Fig. 1. presents the relative peak areas of the main EO components (n=5), estimated by direct injection of individual herb EO/SD (black bars) and HS-SPME procedure of the same herb suspended in PEG (gray bars). Parts A–D concern four different plants: savory, sage, mint, and thyme. The presented data were obtained in optimal HS-SPME conditions: extraction time, equilibrium time and temperature, and sample mass for each plant material (A – 15 min, 10 min, 60 °C, 500 mg; B – 25 min, 10 min, 75 °C, 500 mg; C – 5 min, 15 min, 60 °C, 500 mg; D – 10 min, 15 min, 60 °C, 500 mg) [2].

The obtained results confirm the utility of the tested procedure. They also prove its applicability not only for the sample suspension/SPME fiber system in which dispersive interactions exist (PDMS fiber over sample suspension/emulsion in methyl silica oil), but also for system with specific interactions (Carbowax fiber over sample suspension/emulsion in PEG). The application of presented procedure to systems in which the equilibrium state is determined by specific interactions significantly shortens HS-SPME optimization, but only in the case of polar constituents mixtures.

Determining the true content of quercetin and its derivatives in plants employing SSDM and LC-MS analysis

Quercetin is one of the most widely distributed polyphenolics in plants. This aglycone compound occurs in fruits, vegetables, leaves and grains, often in the form of glycoside derivatives. Rutin, isoquercitrin and quercitrin are the most ubiquitous quercetin glycosides. In view of the antioxidant, anti-inflammatory and anti-cancer properties of quercetin and its glycosides, research interest in the natural occurrence and medical properties of these compounds has been growing.

Reliable plant analysis is a challenging task due to the physical character and chemical complexity of plant matrices. First of all, it requires the application of a proper sample preparation procedure to fully isolate the analyzed substances from the plant matrix. The high-temperature liquid-solid extraction is commonly applied for this purpose. In the light of recently published results, however, the application of high-temperature extraction for phenolics analysis in plants is disputable as it causes their transformation leading to erroneous quantitative estimations of these compounds.

Recently, research work has been focused on sample preparation methods which would limit or even eliminate the degradation/transformation of the analyzed plant constituents. One of such method is the sea sand disruption method (SSDM) combining the homogenization, extraction and purification processes into a single step. There are many examples showing that the effectiveness of this simple, quick and cheap low-temperature method is an alternative not only to the traditional high-temperature solvent extractions (under reflux and in the Soxhlet apparatus) but also to the supported ones (pressurized liquid extraction, supercritical fluid extraction, ultrasound assisted solvent extraction and microwave-assisted solvent extraction).

The report presents the results of research work on the application of SSDM for the evaluation of the true content of quercetin and its derivatives in the following plants: flowers of black elder (*Sambucus nig*ra L.) and hawthorn (*Crataegus* L.); leaves of green tea, nettle (*Urtica dioica* L.) and yerba maté (*Ilex paraguariensis* A.St.-Hil.); the heartsease herb (*Viola tricolor LINN.*), St John's wort (*Hypericum perforatum* L.), and artichoke (*Cynara cardunculus*) flower buds. The results obtained using SSDM are compared to those revealed by the traditional extraction under reflux.

Comparing the results presented in Fig. 2 it can be seen the lower number of the quercetin derivatives in the SSDM extract of green tea in relation to their number in the green tea extract obtained under reflux. It is evident that the high-temperature extraction promotes the formation of the quercetin derivatives, which are not necessarily native plant components. The lack of peaks corresponding with the quercetin and rutin derivatives in Fig. 2 E and F proves that quercetin and rutin do not transform and/or degrade in SSDM and indicates that this sample preparation method can be applied for the analysis of quercetin and its native derivatives in plants.

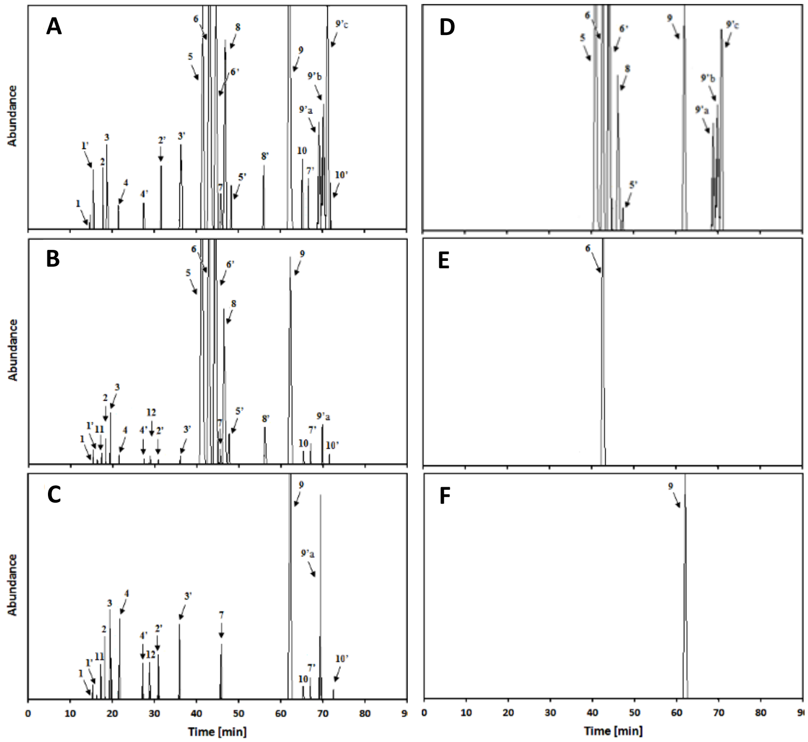

Fig. 2. Exemplary chromatograms of the green tea leaves (A, D), solutions of rutin (B, E) and quercetin (C, F) subjected to the extraction under reflux and the SSDM procedure, respectively

Experiments performed on different plants additionally support the conclusion that the transformation/degradation of quercetin and its glycosides is not induced by the SSDM method and prove the method to be most appropriate for the estimation of quercetin and its derivatives in plants. What is more, the application of SSDM in plant analysis allows the researcher, to determine which quercetin derivatives are native plant components and what is their true concentration. In other word, the application of SSDM in plant analysis eliminates errors in the study of plant metabolism involving quercetin and its derivatives.

Screening of Antibacterial Compounds in Thymus vulgaris L. Tincture using TLC-Direct Bioautography and LC-MS/MS techniques•

Thymus vulgaris L., a perennial herb from the Lamiaceae family, is a popular medicinal plant well-known for its anti-inflammatory, antibacterial, antifungal, antispasmodic, carminative, and antioxidant properties. Although composition and biological properties of thyme, as of many other common herbs, are well described in the literature (especially the composition of essential oils) [3], there is still a need for explaining relations between biological properties and chemical composition of plants. The method of choice is an Effect Directed Analysis (EDA), that is a hyphenation of an analytical technique (e.g. TLC) with a bioassay followed by an identification of biological active substances (e.g. by spectroscopic methods). Thin-layer chromatography – direct bioautography (TLC–DB) followed by LC-MS/MS gives such a possibility [4,5]. Mostly, antibacterial properties of separated compounds are evaluated [6,7]. TLC-DB, in particular, can be used for screening chromatographic and antibacterial properties of plants and their constituents in parallel [7,8]. The developed TLC plate is immersed in a bacterial suspension (bacteria growing in a nutrient broth) and left for incubation. Bacteria grow directly on the surface of the TLC plate except the spots of antibacterial substances. The incubated plates are generally visualized by spraying with tetrazolium salt (a vital dye) which is converted by dehydrogenases of living bacteria into the purple formazan. Finally, pale yellow inhibition zones are observed against the purple surface of the plate. However, using luminescent bacteria the visualization can be performed by the detection of light emission of viable cells with a low-light camera. The structure of active compounds can be found using spectroscopic methods, as liquid chromatography - mass spectrometry (LC-MS). This can be done directly from the plate using TLC-MS Interface or after isolation of active fractions using, for instance, preparative TLC.

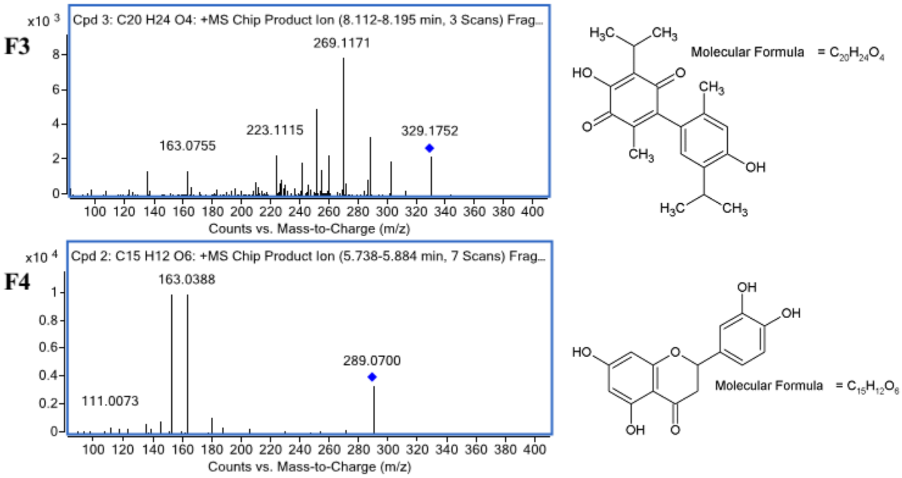

Fig. 3. LC/Q-TOF product spectra of fraction components F3 and F4; collision energy 20 eV.

Thin-layer chromatography–direct bioautography (TLC-DB) was used for guiding the isolation and identification of antibacterial constituents of *Thymus vulgaris* L. ethanol extract. Seven bacterial strains were used as test organisms, both pathogenic and nonpathogenic, including methicillin-resistant *Staphylococcus aureus* as well as luminescent bacteria like *Aliivibrio fischeri*. These were: *M. luteus*, *B. subtilis*, *S. aureus*, MRSA,*S. epidermidis*, *P. syringae* pv. *maculicola*, and *A. fischeri*. Five fractions with the widest antimicrobial spectrum were detected using TLC-DB, isolated by semi-preparative TLC and subjected to LC-MS/MS analyses. Finally, two bioactive components were tentatively identified, basing on their fragmentation pattern, as: eriodictyol and 4,4'-dihydroxy-5,5'-diisopropyl-2,2'-dimethyl-3,6-bifenylodion – see Fig. 3. According to our best knowledge antibacterial properties of 4,4'-dihydroxy-5,5'-diisopropyl-2,2'-dimethyl-3,6-bifenylodion were evaluated for the first time.

Morphology and surface chemistry of kefir grains

Gelatinous, irregularly-shaped kefir grains (KG) are formed by a symbiotic combination of yeasts, acetic acid bacteria and lactic acid bacteria (LAB). KG have gel-like shells consisting of polysaccharides and some other compounds.

Water state and temperature behaviour play an important role in KG. Water located in cells and bacteria and between them (i.e. bulk water) can be in a strongly structured (bound) state. It depends on water content, topology and chemistry of surroundings, presence and content of solutes (salts, small molecules as saccharides, fats, amino acids, etc.) and temperature. Bacteria used in food industry can be stored in freeze-dry state. Therefore, the behaviour of water bound in bioobjects stored at T<273 K is of interest. This is of importance since practically all properties of water are unusual in comparison of them for hydrides of other elements, e.g. SH_2, NH_3, CH_4, etc. In the case of a large part of bulk water in bio-objects, it is difficult to study the properties of bound water. Therefore, the systems with small and controlled content of water are more appropriate to analyze the temperature behaviour of water bound in cells and bacteria. So, it was very interesting to study the morphology and chemistry of surface of kefir grains with various water content [9].

The study was performed using TG-DTA (Derivatograph C, MOM Hungary), SEM (DualBeam Quanta 3D FEG (FEI, USA) and FTIR (Specord M80 (Carl Zeiss, Jena) methods.

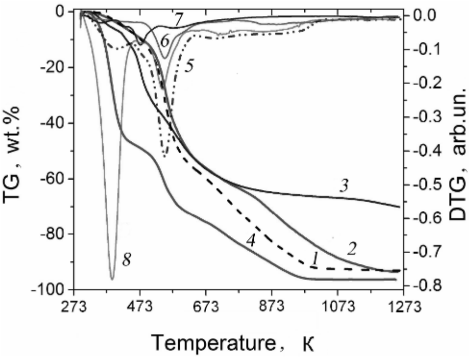

Fig. 4. TG (1–4) and DTG (5–8) curves of initial(1,5), wetted (4,8) (water:dry KG = 1:1), dried kefir grains upon heating in air (2,6) and nitrogen (3, 7) atmosphere

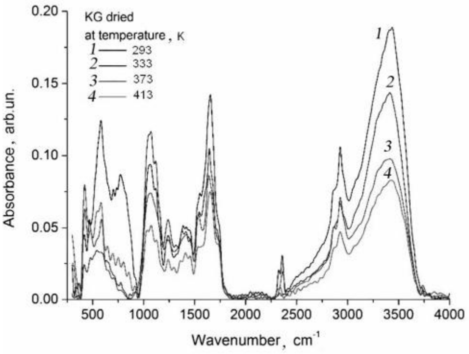

Fig. 5. IR spectra of KG dried at room temperature for 4 days (curve 1) and at 333 (2), 373 (3), and 413 (4) K for 2 h

In Fig. 4 the TG and DTG curves of initial, dried, and hydrated KG recorded upon heating from 293 to 1273 K show several characteristic parts. The first weight loss (Fig.4) from 293 to 398 K corresponds to desorption of bulk or weakly bound water (WBW) and other low-molecular weight compounds (e.g. CO_2, alcohol, etc.). The second range (393–473 K) is due to desorption of structured strongly bound water (SBW) and decomposition of a portion of macromolecules. The third range

(473–673 K) with rapid loss of the weight corresponds to dehydration and decomposition of biomacromolecules (e.g. polysaccharides, etc.). At T>673 K, there is significant difference in the TG/DTG curves recorded in the air and nitrogen atmosphere. For the former (curves 2 and 6), oxidation processes are characteristic in contrast to the latter (curves 3 and 7). Therefore, the weight loss in air is much greater ~93.4 wt. % for dry KG (i.e. ~6 wt. % corresponds to mineral components in dried kefir grains) at 1273 K than that in the nitrogen atmosphere without access of oxygen ~70 wt. %, in which the processes are stopped on the carbonization stage (i.e. formation of char).

The IR spectra (Fig. 5) show that heating of KG results in the loss of water, since intensity of a broad band at 3700–2500 cm^{-1} decreases with increasing preheating temperature. However, even after preheating at 413 K for 2 h the KG keep the main structural features, despite thermal inactivation of bacteria and cells. A broad complex band at 1200–1000 cm^{-1} related to C–O–C and C–O is characteristic for carbohydrates. Bands at 1700–1500 cm^{-1} are linked to the C=O and C=C stretching vibrations and the δ_{CN} bending vibrations and C–H overtones. The bands at 1460 and 1400 cm^{-1} can be assigned to the CH_2 deformation and to vibrations of the amino acid side chains, respectively. A decrease in intensity of all bands observed can be due to desorption of low molecular weight organics (e.g., saccharides) in parallel to desorption of water.

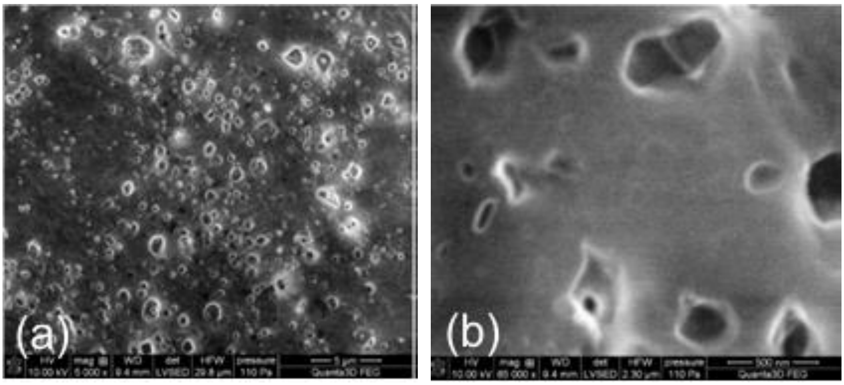

Fig. 6. SEM images of dried kefir grains at magnifications: (a) ×6500 and (b)×65000

Supracellular and cellular structures observed in kefir grains (Fig. 6) show their nonuniform morphology of a great complexity. Deviation of the cellular shapes (Fig.6b) can be caused by drying of cells. This suggests that intracellular and extracellular structures of water can demonstrate complex temperature behaviour, which is typical for cellular objects and can strongly depend on the water content.

DSC and ^{1}H NMR studies of water bound in kefir grains

Kefir grains (KG) are characterized by certain antimicrobial, antioxidant and disease-resistant activities depending on KG composition, amounts and organization of water. Water state and temperature behaviour play an important role in KG. The confined space effects can result in significant changes in the properties of liquids as solvents, since the activity and molecular mobility decreases in comparison with the bulk liquids. The stronger the bonding of interfacial water, the lower the activity of this water as a solvent.

There are several methods which can give useful information on the structure, temperature and interfacial behaviours, and other properties of water in bioobjects. In this regard the aim of the work was to study the characteristics of water bound in kefir grains depending on water content, dispersion media with air or weakly organic solvent $CDCl_3$ and the presence of trifluoroacetic acid F_3CCOOD (TFAA) [9]. The study was performed using low-temperature ^1H NMR and DSC methods.

^1H NMR spectra of static samples with various amounts of water in various dispersion media (air, $CDCl_3$, $CDCl_3$ + F_3CCOOD) were recorded using a Varian 400 Mercury spectrometer. Differential scanning calorimetry (DSC) measurements of interactions of kefir grains with water and n-decane were carried out using a PYRIS Diamond (Perkin Elmer Instruments, USA) differential scanning calorimeter at the constant heating/cooling rate of 10 K/min. Similar to the NMR cryoporometry, the DSC melting thermograms were used in the DSC thermoporometry for structural characterization of the materials.

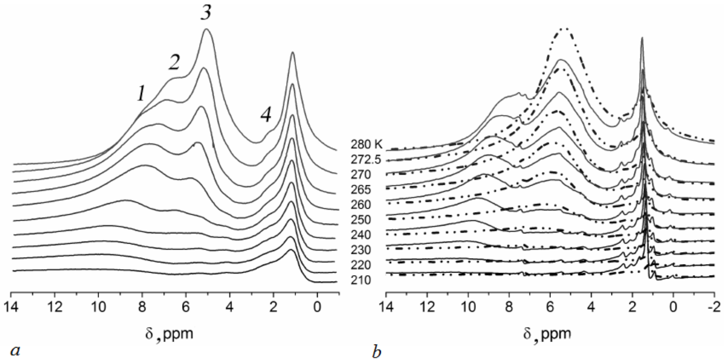

Fig. 7. Exemplary ^1H NMR spectra of water bound in KG recorded at different temperatures and different hydration degree h = (a) 0.3 g/g and (b) 0.8 g/g, in (b) $CDCl_3$ (dotted-dashed lines) and (a, b - solid lines) $CDCl_3$ + TFAA.

Figure 7 presents exemplary ^1H NMR spectra of water bound in KG. On the basis of ^1H NMR results it was shown that the structural and thermodynamic characteristics of intracellular liquids (water and organics) in kefir grains depend strongly on their contents and temperature, especially below freezing points of these liquids. Partially hydrated/dehydrated kefir grains include water structures in a broad range of sizes from small clusters (around 1 nm in size) to large nanodomains 10–50 nm in size. Changes in the hydration degree of kefir grains cause changes in their textural organization. Contributions of weakly (WAW) and strongly (SAW) associated waters and weakly (WBW) and strongly (SBW) bound waters depend on the amounts of water and the type of dispersion medium. The ratios between SAW/WAW and SBW/WBW depend on temperature since the larger the water structure (approaching to bulk water), the higher the freezing/melting temperature (approaching to 273 K). These water clusters and domains are characterized by different ability to dissolve strong acids (e.g. F_3CCOOD). Enhanced cauterization of water bound to kefir grains results in diminution of dissolution of the acid in this water.

Additional information on the temperature behaviour of water bound in KG differently hydrated can be obtained using DSC measurements. DSC investigations show that at a minimal content of water (h = 0.3 g/g), exotherms of freezing of water and some low molecular weight organics (sugars, etc.) are observed between 263 and 273 K (Fig. 8a) in contrast to a melting peak (Fig. 8b).

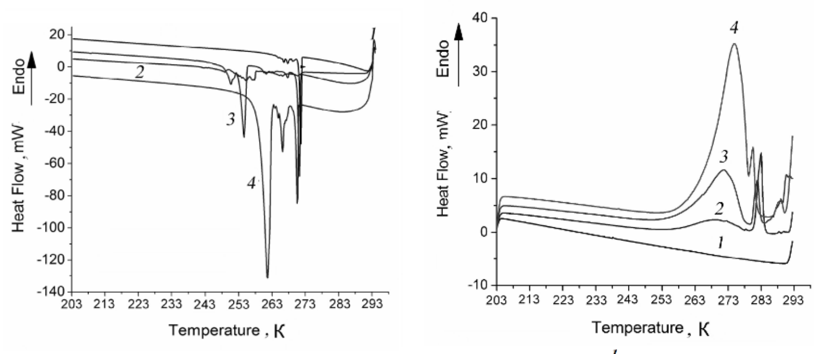

a *b*

Fig. 8**.** (a) Freezing and (b) melting DSC thermograms for KG at different hydration degree h = 0.3 (curve 1), 0.5(2), 0.7(3) and 1 (4) g/g.

An increase in content of water, the shape of both freezing exotherms and melting endotherms becomes more complex. The freezing exotherms shift toward lower temperatures at h = 0.5 and 0.7 g/g but at h = 1 g/g they shift toward higher temperatures. This effect is due to changes in contribution of weakly and strongly bound compounds observed also in NMR measurements and the textural organization of kefir grains at nano and micro-scales. In other words, contribution of WBW increases at h = 1 g/g (Fig. 8a). The endotherm effect value of water melting increases with increasing value of h but it is much lower than that for transformation of hexagonal ice/bulk water (330 J/g). This result can be caused by several reasons: (*) there are many states of bound water frozen at different temperatures (i.e. melting of different ice crystallites or amorphous structures occurs over large temperature range); (**) the energy of interactions of water/water and water/biostructures in KG differs strongly in both directions. Therefore, total changes in phase transition of amorphous ice (bound water can form amorphous ice upon freezing) into bound water needs smaller energy than that for hexagonal ice transforming into bulk water.

The vibrational spectrum of 1,4-dioxane in aqueous solution

Most chemistry and essentially all biochemistry take place in solutions. The solvent, particularly a polar solvent like water, has a significant effect on the solute. Accurate thermodynamic modeling of solvent effects is very time-consuming, and it is often replaced by continuum solvation models or other simplified methods [10-12]. It is important to evaluate the accuracy of such methods. Vibrational spectroscopy offers an excellent test since modern quantum chemical methods can predict vibrational frequencies with remarkable accuracy, and intensities fairly with modest computational effort.

The solvent (water) effect on the vibrational frequencies of dioxane was investigated by two solvation models: the conductor-like screening model (COSMO) [10-12] and by using explicit solvation model (ESM) [13]. The ESM calculations were carried out in the following way. Equilibrium geometries and harmonic vibrational frequencies of dioxane and its hydrogen bonded complexes with water (cf. fig. 9) were determined at the B3LYP level with 6-311++G** basis set. All optimized structures were local minima (all frequencies are real). This step was followed by the potential energy distribution (PED) analysis and ESFF frequency scaling (for the dioxane molecule only) to confirm the bands assignments. The vibrational frequencies of dioxane in aqueous solution were modeled by averaging the frequencies obtained for all clusters. For the COSMO solvation model, we used ε=78.39 for the dielectric constant of the water solvent in all calculations. Note that the calculated shifts refer to harmonic frequencies. The obtained results were compared to shifts obtained by us with the aid of IR and Raman spectroscopy. Shifts corresponding to infinite dilution were shown to correspond to those for 1:28 water:dioxane molar ratio.

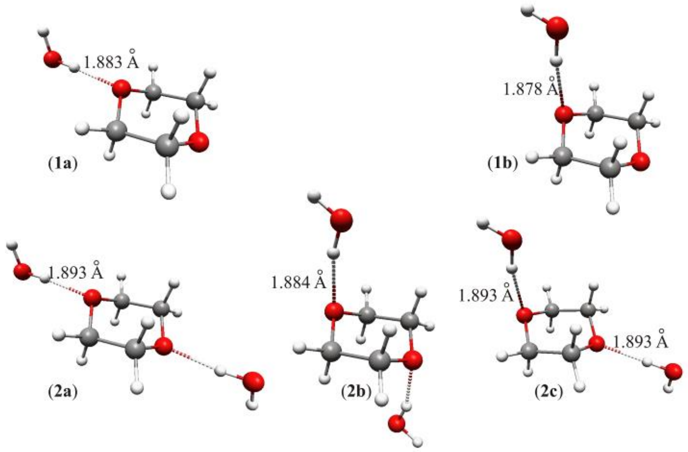

Fig. 9. The optimized structure of 5-CQA

Experimental and calculated frequency shifts (Δ) for dioxane upon dilution in the fingerprint range are gathered in Table 1. As can be seen low frequencies (CC and CO stretching and various types of bending vibrations) are poorly described with the COSMO model. In more than half cases (15 out of 26) the sign of the shift is incorrect and deviations between the calculated and observed shifts are frequently larger than 10 cm^{-1}, up to 16 cm^{-1} in two cases. The RMS difference between the experimental and calculated shifts is close to 9 cm^{-1} for the 26 identified modes in this range. COSMO predicts the correct sign for the CO stretching vibrations (modes 7, 9, 14, and 15) but overestimates the magnitudes. In the case of ESM in all but two cases the sign of the shift is correctly predicted when the specific interactions are explicitly incorporated in the calculations. In addition, the RMS value between the experimental and calculated frequency shifts for the 26 mid-range modes is as low as 1.7 cm^{-1}. Apparently ESM is much more accurate in describing the solvent effect in the fingerprint region when hydrogen bonding occurs. In particular, it is much superior to COSMO for the shifts in the CO stretching vibrations region, giving almost perfect agreement with experiment. However, it should be noted that COSMO slightly outperforms ESM in the CH stretching range.

Table 1. Experimental and calculated frequency shifts (Δ) for dioxane upon dilution in the fingerprint range

B3LYP		Expt			Shifts			
					COSMO	Δ^{COSMO}	ESM	
No	ν	Dx	Dx+28H_2O	Shift			Mean	Δ^{ESM}
3	416.5	425.1	426.0	0.9	2.8	1.9	6.1	5.2
4	440.3	435.3	443.9	8.6	-1.8	-10.4	10.3	1.7
5	490.8	488.7	487.2	-1.5	-2.8	-1.3	-1.1	0.4
6	616.8	613.3	614.3	1.0	-1.3	-2.3	3.1	2.1
7	840.2	837.0	833.0	-4.0	-10.9	-6.9	-4.6	-0.6
8	860.9	854.2	854.6	0.4	-4.7	-5.1	-0.9	-1.3
9	881.9	873.6	869.4	-4.2	-17.5	-13.3	-4.6	-0.4
10	891.8	888.4	892.4	4.0	-1.5	-5.5	4.6	0.6
11	1016.2	1017.4	1017.7	0.3	-7.3	-7.6	-0.8	-1.1
12	1060.9	1048.7	1046.1	-2.6	-7.8	-5.2	-2.6	0.0
13	1102.2	1083.4	1082.0	-1.4	-11.7	-10.3	-1.0	0.4
14	1126.9	1111.1	1099.8	-11.3	-20.5	-9.2	-12.6	-1.3
15	1133.0	1121.2	1118.4	-2.8	-18.9	-16.1	-4.8	-2.0
16	1143.2	1130.2	1133.0	2.8	-5.4	-8.2	2.5	-0.3
17	1238.1	1219.3	1223.2	3.9	-0.6	-4.5	3.3	-0.6
18	1279.4	1254.8	1258.3	3.5	-4.3	-7.8	1.6	-1.9
19	1316.0	1289.1	1295.7	6.6	-2.6	-9.2	4.2	-2.4
20	1326.0	1307.1	1311.8	4.7	-1.5	-6.2	4.2	-0.5
21	1358.1	1337.8	1342.1	4.3	0.7	-3.6	3.9	-0.4
22	1387.2	1366.3	1372.6	6.3	2.9	-3.4	6.7	0.4
23	1405.1	1375.0	1378.7	3.7	-3.6	-7.3	0.7	-3.0
24	1416.5	1398.4	1403.4	5.0	-1.2	-6.2	5.2	0.2
25	1481.1	1446.4	1449.4	3.0	-9.2	-12.2	2.9	-0.1
26	1482.2	1445.0	1445.8	0.8	-9.8	-10.6	4.0	3.2
27	1489.5	1454.9	1456.9	2.0	-11.3	-13.3	3.3	1.3
28	1494.8	1460.5	1464.6	4.1	-12.4	-16.5	3.4	-0.7

References:

[1] A.L. Dawidowicz, M. Dybowski and J. Szewczyk; Modified application of HS-SPME for quality evaluation of essential oil plant materials; *Talanta*, **146** (2016) 195–202;10.1016/j.talanta.2015.08.043

[2] A.L. Dawidowicz, J. Szewczyk and M. P. Dybowski; Modified HS-SPME for determination of quantitative relations between low-molecular oxygen compounds in various matrices, *Analytica Chimica Acta*, **935** (2016) 121-128; 10.1016/j.aca.2016.06.041

[3] M. Soleimani, A.P. Daryasari, A. Ghorbani, O.M. Hejri, R. Mazaheri, *J. Essent. Oil Bear. Pl.*, **17** (2014) 1233−1240.

[4] I.M. Choma, W. Jesionek, Instrumental Thin-Layer Chromatography: Effects-Directed Biological Detection: Bioautography, Elsevier, Amsterdam, 2014.

[5] G.E. Morlock, W. Schwack, *J. Chromatogr. A*, **1217** (2010) 6600−6609.

[6] I.M. Choma, E.M. Grzelak, *J. Chromatogr. A*, **1218** (2011) 2684−2691.

[7] A. Marston, *J. Chromatogr. A*, **1218** (2011) 2676−2683.

[8] Á.M. Móricz, E. Fornal, W. Jesionek, B. Majer-Dziedzic, I.M. Choma, *Chromatographia*, **78** (2015) 707–716

[9] V.M. Gun'ko, V.V. Turov, T.V. Krupska, A.P. Golovan, M.D. Tsapko, J.Skubiszewska-Zięba, B.Charmas, Water state vs. temperature in differently hydrated kefir grains, Chemistry, *Physics and Technology of Surface*, **7, 1** (2016) 86-96

[10] A. Klamt, G. Schüürmann, *J. Chem. Soc., Perkin Trans.*, **2** (1993) 799-805.

[11] J. Andzelm, C. Kölmel, A. Klamt, *J. Chem. Phys.*, **103** (1995) 9312-9320.

[12] A. Klamt, *J. Phys. Chem.*, **99** (1995) 2224-2235.

[13] P. Borowski, W. Gac, P. Pulay, K. Woliński, *New J. Chem.*, **40** (2016) 7663-7670.

THEORETICAL AND EXPERIMENTAL STUDIES ON NEW MATERIALS, ITS STRUCTURE AND PHYSICOCHEMICAL PROPERTIES

Mariusz BARCZAK, Andrzej DĄBROWSKI, Mateusz DRACH,
Leszek ŁAJTAR, Jolanta NARKIEWICZ-MICHAŁEK,
Krzysztof NIESZPOREK, Przemysław PODKOŚCIELNY,
Paweł SZABELSKI, Krzysztof WOLIŃSKI
DEPARTMENT OF THEORETICAL CHEMISTRY

It has been proved that liquid water forms dynamic, labile H-bond networks whose connectivity changes constantly[1]. Such a non-diffusive jump-reorientation mechanism has been also observed between water molecules in the solvation shell of simple ions[2]. Moreover, the addition of ions to liquid water has no influence on the rotational dynamics of water molecules outside the first hydration shell[3].

Sciortino et al.[4] concluded that the bifurcated hydrogen bonds play a fundamental role in the mobility of the molecules in the liquid state due to the lowered energy required to break such a bond. Thus the first hydration shell dynamics can be responsible for many effects observed during chemical and electrochemical reactions in water. The more profound understanding of phenomena can be helpful in designing liquid systems in which the ions mobility plays a crucial role.

Recently[5,6], based on the classical molecular dynamics simulations, we investigated the time evolution of geometric quantities characterizing H-bonds between perchlorate anion and water. As the perchlorate anion includes four oxygen atoms which are H-bond acceptors, besides the classical H-bond the bifurcated and trifurcated H-bonds will be investigated. On the contrary to the classical hydrogen bond, where the hydrogen bond donor interacts with one acceptor, the bifurcated and trifurcated H-bonds are the interactions between one donor and two or three H-bond acceptors.

The time evolution of geometric parameters characterizing the making and breaking of H-bond averaged in relation to the center of the observed angular jump event can provide information about the mechanism of making/breaking of H-bond. The average jump amplitude as well as time evolution of distance characterizing particular H-bonds in the investigated system are shown in Fig. 1.

The simulations indicate a large angular jump mechanism for H-bond exchange in the aqueous perchlorate solution. The rapid change of angular orientation of water during bond making/breaking was clearly visible in all cases of the investigated hydrogen bonds. Before and after the switch event, the angular water orientation remains approximately unchanged. As the angular jump is characteristic of hindering water rotational motion by other hydrogen bonds, it makes it possible to conclude that the multi-centered hydrogen bonds between water and perchlorate anion are of transitional character.

Further investigations showed that initially the water molecule forms with perchlorate the classical H-bond. Next it can turn into the bifurcated or trifurcated hydrogen bridge. In this view, water can slide around the perchlorate anion. Such conclusion confirm PMF profiles, their minima corresponding to the total binding energies of multi-centered hydrogen bonds are located at similar distances from chloride atom.

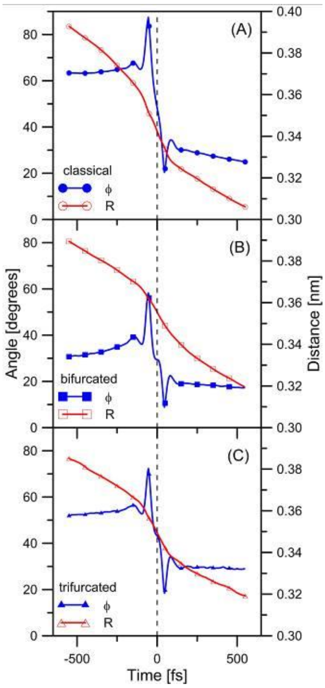

Fig. 1. Time evolution, centered on the H-bond switching event, of the geometric parameters representing the making of classical, bifurcated and trifurcated hydrogen bridge.

When water approaches the perchlorate anion, its rotation helps overcome potential barriers and can cause switching between different hydrogen bridges.

The history-independent correlation functions of the existence of particular hydrogen bridges show that the classical H-bond between the water and perchlorate is a more stable than bifurcated or trifurcated one. Moreover, the reactive flux correlation function for the trifurcated H-bond decays fastest indicating the shortest time necessary to achieve the equilibrium state.

Summing up, the transitional character of water-perchlorate H-bonds is one of the main factors influencing on reorientational dynamics of water located within the perchlorate first shell. This finding can be a contribution to better understanding of the impact of ions on the structure and dynamics of water.

References:

[1] D. Laage, J. T. Hynes, *Science*, **311** (2006) 832.
[2] D. Laage, J. T. Hynes, *PNAS*, **104** (2007) 11167.
[3] A. W. Omta, M. F. Kropman, S. Woutersen, H. J. Bakker, *Science*, **301** (2003) 347.
[4] F. Sciortino F, A. Geiger, H. E. Stanley, *Nature*, **354** (1991) 218.
[5] K. Nieszporek, P. Podkoscielny, J. Nieszporek, *PCCP*, 18 (2016) 5957.

PREPARATION AND INVESTIGATION OF CATALYTIC SYSTEMS IN THE REACTIONS INVOLVING CARBON OXIDES, HYDROCARBONS AND THEIR OXYGEN CONNECTIONS

Tadeusz BOROWIECKI, Marcin CICHY, Wojciech GAC, Magdalena GRELUK, Andrzej MACHOCKI, Sylwia PASIECZNA-PATKOWSKA, Marek ROTKO, Janusz RYCZKOWSKI, Grzegorz SŁOWIK, Witold ZAWADZKI, Bogna BANACH, Adam LESIUK
DEPARTMENT OF CHEMICAL TECHNOLOGY

Preparation and analysis of catalytic materials for the process of removal (oxidation) of soot from Diesel exhaust gases

Investigations associated with the search of a highly active and selective catalytic material for the process of soot oxidation from diesel exhaust gases were continued. It is very important issue because the emission of soot into the atmosphere is highly undesirable. Diesel soot is strongly carcinogenic and contributes to the greenhouse effect.

Catalysts containing different amounts of cobalt and manganese were tested. They were prepared by a co-precipitation method and calcined at 400^{o}C. Their catalytic properties were measured in the "tight contact" using model soot (Printex U) and the reaction mixture containing 10 vol.% of O_2 and inert gases (argon and helium). The studies were conducted in a quartz reactor filled with 50 mg of the catalyst-soot mixture (45 mg of catalyst and 5 mg of soot) and 450 mg of finely ground quartz. The effects of soot oxidation during a temperature-programmed experiment (ramp rate was 10^{o}C/min) were analyzed by a mass spectrometer.

Cobalt-manganese catalysts permit to significantly decrease the temperature of soot oxidation and prevent the formation of carbon monoxide. The highest activity is demonstrated by the catalytic materials containing much more cobalt than manganese. The catalysts containing equal amounts of cobalt and manganese and also those containing more manganese are worse. Further studies will be conducted.

The effect of temperature on activity of cobalt catalysts for ethanol steam reforming

The aim of work was to study the catalytic properties of the supported cobalt catalyst under steam reforming of ethanol conditions.

The reaction of ethanol conversion with water was carried out under atmospheric pressure in a fixed-bed continuous-flow quartz reactor over the catalyst (0.1 g; 0.15-0.3 mm) reduced in situ with hydrogen at 400°C for 1 hour, prior to the reaction. The aqueous solution of ethanol (H_2O/ethanol=12/1) was supplied to an evaporator (150°C) and the reactant vapours, without diluting with any inert gas, and were fed to the reactor at a flow rate of 100 mL×min-1. The catalytic performance was tested in the temperature range of 390-480°C. The analysis of the reaction mixture and the reaction products (all in gas phase) were carried out on-line by means of two gas chromatographs. One of them, Bruker 450-GC was equipped with two columns, the first filled with a porous polymer Poropak Q (for all organics, CO_2 and H_2O vapor) and the other one—capilary column CP-Molsieve 5 Å (for CH_4 and CO analysis). Hellium was used as a carrier gas and a TCD detector was employed. The hydrogen concentration was analyzed by the second gas chromatograph, Bruker 430-GC, using a Molsieve 5 Å, argon as a carrier gas and a TCD detector.

Steam reforming of ethanol (EtOH/H_2O =1/12) over 2 catalyst showed that the temperature of 420°C was the most advantageous for this process. The catalyst indicated the high SRE process selectivity to two most desirable products of reaction, hydrogen and carbon dioxide and amounts of carbon monoxide, methane and acetaldehyde formed in side reactions were much smaller.

Synthesis and characterization of Pd/ZnO-CeO_2 catalysts for the steam reforming of methanol

Steam reforming of methanol (SRM) is one of the most efficient low-temperature hydrogen production methods. The reaction product mixture containing mainly H_2 and CO_2 can be easily handled and utilized in the fuel cell systems for electricity production. The main obstacle of widely studied SRM copper catalysts is low thermal stability. The aim of the recent studies was synthesis and characterization of novel palladium-zinc oxide catalysts modified with ceria. ZnO-CeO_2 supports of different Ce/Zn molar ratio ranging from 0 to 0.5 were prepared by the co-precipitation method. Palladium was introduced by the impregnation method. It was found that modification of the support composition influenced the way of active phase formation and redox properties of catalysts. Partial replacement of ZnO with CeO_2 in the supports led to the slight decrease of the selectivity of catalysts to CO_2 without significant changes of initial activity.

Catalysts

The main objectives of the studies was the preparation and physico-chemical characterization of the unpromoted and potassium-promoted cobalt-based catalysts with ceria support. The Co/CeO_2 catalyst was prepared by impregnation of the commercial nano-dispersed ceria support with a solution of cobalt nitrate and citric acid. The catalyst's precursor was dried and then calcined. The K/Co/CeO_2 was prepared by impregnation of potassium nitrate solution to the Co/CeO_2. The sample was dried, and then calcined , as it was previously described. The Co/K/CeO_2 was prepared similarly, however, firstly dried nano-ceria support was impregnated with potassium nitrate solution and then subsequently with a solution of cobalt nitrate and citric acid. For all samples, the amounts of cobalt and potassium introduced were 10 and 2 wt.%. The catalysts were characterized by nitrogen adsorption, hydrogen chemisorption, XRF, XRD and TPR methods. The studies have shown that the order of potassium addition (to the support or onto Co/CeO_2) does not significantly change the physico-chemical properties of the catalyst. In the further studies the obtained catalysts will be characterized by the XPS technique.

Additionally the gravimetric studies over zirconia-supported catalysts for EtOH/H_2O equal 1/3, 1/9 and 1/12 were performed in order to supplement the data presented in the PhD thesis (S. Turczyniak).

INVESTIGATION OF ADSORPTION OF INORGANIC AND ORGANIC SUBSTANCES IN MICELLAR, OXIDE AND ENVIRONMENTAL DISPERSE SYSTEMS

Marta SZYMULA, Stanisław CHIBOWSKI, Elżbieta GRZĄDKA,
Jerzy JABŁOŃSKI†, Władysław JANUSZ, Andrzej KOMOSA,
Adam W. MARCZEWSKI, Jolanta ORZEŁ, Małgorzata PASZKIEWICZ,
Jacek PATKOWSKI, Marek RESZKA, Ewa SKWAREK, Teresa URBAN,
Małgorzata WIŚNIEWSKA
DEPARTMENT OF RADIOCHEMISTRY AND COLLOID CHEMISTRY

One of the most important characteristics of micelles is their ability to take up all kinds of substances. Binding of these compounds to micelles, co-called solubilization, is generally driven by hydrophobic and electrostatic interactions. Solubilisation is usually treated in terms of the pseudophase model, in which the bulk aqueous phase is regarded as one phase and the micellar pseudophase as another. The micelles catalytic effect on unimolecular reactions can be attributed exclusively to the local medium effect. For more complicated bimolecular or higher-order reactions, the rate of reaction is affected by an additional parameter: the local concentration of the reacting species in or at the micelle [1].

In this report the results of our investigations of the reactivity of diphenylpicryl hydracil radicals (DPPH) towards phenolic acids in the Triton X-100 micellar solution are presented. We used this micellar solution as a simple model of food system.

Phenolic compounds are a complex group of substances that have attracted a considerable attention due to their role in maintenance of flavour and colour characteristics of food as well as in protecting human health. Many of the benefits of phenolic-rich foods consumption are due to their antioxidant activities. The efficiency of a phenolic antioxidant will depend upon the reactivity of its phenolic groups and locations of the radical and the antioxidant in the microheterogeneous food system. The rate of the reaction between an antioxidant and a radical totally incorporated within a microphase will be determined by the antioxidant hydrophobicity. The hydrophobicity will strongly influence its distribution between the microphase and the external medium as well as its location inside the microphase.

To address these two aspects, the reactivity of DPPH towards cumaric (CA), ferulic (FA) and caffeic (CAA) acids was investigated in the Triton X-100 micellar solution of various concentrations (0.001M, 0.003M and 0.005M) and at different temperatures.

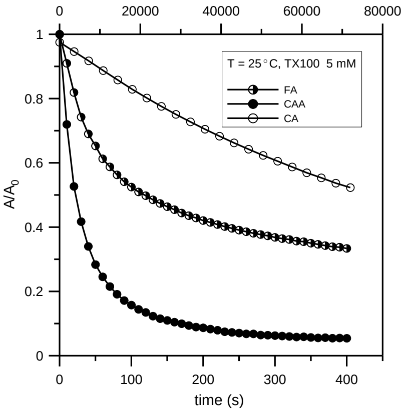

Fig. 1. Effect of phenolic acid molecular structure on the reaction rate with DPPH in the micellar solution.

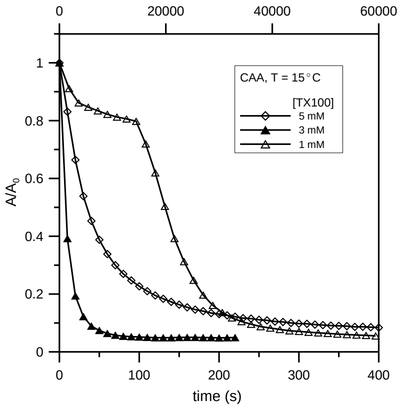

Fig. 2. Effect of TX-100 conentration on the reaction rate of phenolic acid with DPPH.

Using the relationship A(t) the rate constant k_{obs} of CA+DPPH reaction at various temperatures was determined. The activation energies of these reactions from the realationship $\ln k_{obs}(T^{-1})$ were found.

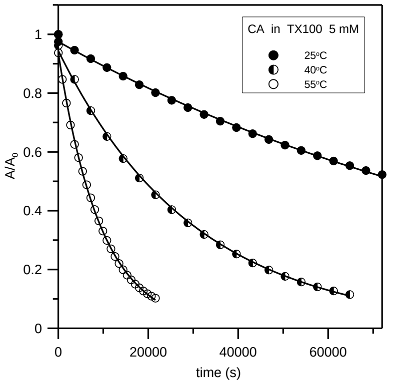

Fig. 3. Effect of temperature on the reaction rate of phenolic acid with DPPH.

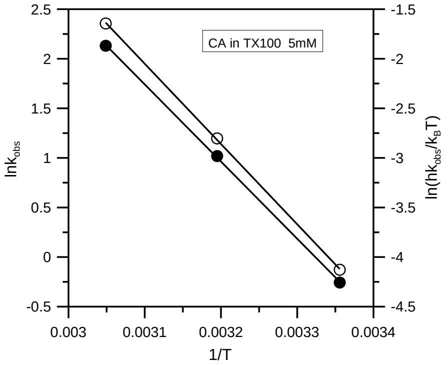

Fig. 4. Temperature dependence of CA and DPPH reaction rate constant.

The main factors influencing the reaction of phenolic acids with DPPH in the TX-100 micellar system are the acid molecular structure and reagents localisation in micelles. Cumaric acid is the least active radical scavenger. Ferulic and caffeic acids exhibit similar antioxidant activities.

In the most concentrated TX-100 solution the reaction between the phenolic acid and DPPH proceeds according to the pseudo-first order mechanism.

The method with DPPH is very suitable for determination of antioxidant activity of phenolic acids in the micellar systems.

References:

[1] M. Niyaz Khan, Micellar Catalysis, Surfactant Science Series vol. 133, Taylor & Francis Group, A CRC PRESS BOOK, 2006.

SYNTHESIS AND INVESTIGATIONS OF NEW COORDINATION COMPOUNDS AND SUPRAMOLECULAR COMPLEXES

Agata BARTYZEL, Beata CRISTÓVÃO, Wiesława FERENC, Halina GŁUCHOWSKA, Renata ŁYSZCZEK, Liliana MAZUR, Agnieszka OSTASZ, Dariusz OSYPIUK, Iwona RUSINEK, Zofia RZĄCZYŃSKA, Justyna SIENKIEWICZ-GROMIUK
DEPARTMENT OF GENERAL AND COORDINATION CHEMISTRY

Novel molecular and supramolecular complexes, coordination polymers of: acylamidrazones, Schiff bases, mono- and dicarboxylic acids with d- and f-metals were synthesized and investigated. These compounds have attracted great attention as new functional materials in a number of fields (catalysis, optoelectronics, pharmacy etc.). In order to characterization these compounds: X-ray single crystal and powder diffraction techniques, photoluminescence, CHN, TG-DSC, TG-FTIR, FT-IR, Raman, UV-VIS, XANES, XPS, biological, magnetic methods were applied and the quantum chemical calculations were performed.

The complexes of 4,4'-{(1,3-propanediyl)bis[nitrilophenylmethylidene]}di(1,3-benzenodiol) with Mn(III), Co(II), Ni(II), Cu(II) and Zn(II) ions were synthesized from the direct reaction of symmetrical Schiff base with M(II) acetates. The Ni(II) complex crystallizes as a methanol solvate in the monoclinic space group $P2_1/c$. The N_2O_2 coordination geometry around the metal centre is slightly tetrahedrally distorted from square-planar. During heating, at first complexes lose solvent molecules (water or methanol), after that the organic part undergoes defragmentation and combustion. The magnetic studies of paramagnetic complexes exhibit the existence of weak antiferromagnetic (for Mn(III) and Co(II) complexes) and weak ferromagnetic (for Cu(II)) interactions.

3,4-dimethoxyphenylacetates of Mn(II), Co(II), Ni(II), Cu(II), Zn(II) were obtained with the formula $ML_2 \cdot nH_2O$, where: $L=C_{10}H_{11}O_4$, and n=1-4). The compounds crystallize in monoclinic or triclinic systems. The carboxylate groups form bidentate chelating or bridging ligands. On heating in air they decompose in three steps. The magnetic moments determined for the complexes confirm that they follow the Curie–Weiss law. The Mn(II) and Ni(II) compounds are high-spin complexes with octahedral structures while that of Co(II) with tetrahedral one. The new complexes of 4-oxo-4-[(4-fluorophenyl)amino]but-2-enoic acid with Mn(II), Co(II), Ni(II), Cu(II), Zn(II), Nd(III), Gd(III) and Er(III) ions were synthesized of the formulae: $MnL_2 \cdot 2H_2O$, $CoL_2 \cdot H_2O$, $NiL_2 \cdot H_2O$, $CuL_2 \cdot 4H_2O$, $NdL_3 \cdot 2H_2O$, $GdL_3 \cdot 3H_2O$ and ErL_3, where: $L^- = C_{10}H_7O_3FN$. The Co(II) and Cu(II) complexes crystallize in the monoclinic system whereas those of Mn(II), Ni(II), Nd(II), Gd(III) and Er(III) in the triclinic one. Heated in air they decompose in three steps (except the Er(III) complex). The magnetic measurement data indicate all complexes to obey the Curie–Weiss law and to show the paramagnetic properties with the ferromagnetic interactions between molecular centres.

Novel heterotrinuclear complexes Cu(II)-Ln(III)-Cu(II) (Ln = La, Pr, Nd, Ho, Er, Tm, Yb) were obtained in the reaction of *N,N'*-bis(2,3-

dihydroxybenzylidene)2,2-dimethyl-1,3-diaminopropane ($H_4L = C_{19}H_{22}N_2O_4$) with the respective salts of Ln(III) and Cu(II). The temperature dependence of the magnetic susceptibility and the field-dependent magnetization indicate that the interactions between Cu(II) and Ln(III) ions are antiferromagnetic for Ln = Pr and Nd, whereas in the Cu(II)–Ln(III) pairs (Ln = Ho, Er, Tm, Yb) the weak ferromagnetic interaction between the paramagnetic centers is observed.

The disubstituted *N*-acylamidrazones crystallize in the monoclinic space group $P2_1/n$, with one molecule in the asymmetric unit of the crystal. The complexes of amidrazones with Cu(II) crystallize in the centrosymmetric space groups: *P*-1, $P2_1/c$ or *C*2/*c*. Reaction with copper(II) acetate results in double deprotonation of the ligands and leads to centrosymmetric binuclear species with CN = 4. The reaction of the studied amidrazones with $CuCl_2$ leads to mononuclear species with CN = 5. The carboxylic group of the ligand is not deprotonated and the charge of the central ion is compensated by Cl^- ion. Uncoordinated COOH group is involved in intramolecular hydrogen-bonding. The obtained complexes are air-stable and they do not disintegrate in DMSO, ethanol or water. In *in vitro* cytotoxicity research some of them exhibited moderate cytostatic activity against HL-60, MCF-7 and HT-29 cancer cell lines.

Trimethoprim(TMP) and *p*-xylylene-bis(thioacetic) acid (*p*-XBTA) form three forms of salts. Crystal structure of salt s1 belongs to the monoclinic $P2_1/c$ space group while salts s2 and s3 crystallize in triclinic P-1 space group. The trimethoprim is a protonated at atom N of the pyrimidine moiety. The crystal packing of all three forms of salts is characterized by the extended network of hydrogen bonds containing related trimethoprim homodimers formed by a pair of N-H···N hydrogen bonds. The melting point of salt was distinct from that of the individual components confirming the formation of new phases.

The series of lanthanide coordination polymers of biphenyl-4,4'-dioxydiacetic acid (H_2bpoda) of the general formula $Ln_3(bpoda)_3{\cdot}x solv$ (where Ln= from La(III) to Lu(III); solv=DMF or water and bpoda=$(C_6H_4)_2(OCH_2COO)_2^{2-}$) were obtained under the solvothermal conditions with microwave heating. Coordination of Ln(III) ions occurs through both the deprotonated carboxylate groups and covalently bonded DMF or water molecules. The Eu and Tb complexes display intensive red and green luminescence. Polycrystalline lanathnide complexes of 1,2- and 1,3-phenylenediacetic acids (H_2pda) of the formula $Ln_2(pda)_3{\cdot}nH_2O$ (Ln=from La(III) to Lu(III); pda= $C_6H_4(CH_2COO)_2^{2-}$) obtained in the classical method exhibit perfect thermal stability. They dehydrate in one or two steps forming metal-organic frameworks stable up to 400°C.

The quantum chemical calculations for benzylthioacetic acid (*Hbta*) were been performed. In the case of optimized dimeric structure, the molecules of acid form the eight-membered hydrogen-bonded (HB) ring system similarly to that in the crystal structure. The appearance of two equivalent stable hydrogen-bonded O–H···O intermolecular contacts results in the increased stabilization of the theoretical model of the dimeric structure in comparison to monomeric one. The optimized model of the dimeric structure significantly improves the convergence of carboxylic geometrical parameters in relation to the experimental data.

SYNTHESIS AND PROPERTIES OF POLYMERS

Barbara GAWDZIK, Andrzej BARTNICKI, Marta GROCHOWICZ,
Jerzy KSIĘŻOPOLSKI, Anna KULTYS, Małgorzata MACIEJEWSKA,
Janina NOWAK,
Joanna OSYPIUK-TOMASIK, Beata PODKOŚCIELNA,
Maciej PODGÓRSKI,
Andrzej PUSZKA, Magdalena ROGULSKA, Łukasz SZAJNECKI,
Magdalena SOBIESIAK, Marta WORZAKOWSKA
DEPARTMENT OF POLYMER CHEMISTRY

Polyurethanes, owing the variety of their uses, have an important place in the world production of polymeric materials. They can be either thermoplastic or thermosetting. Thermoplastic polyurethanes (TPUs) are usually produced by the reaction of diisocyanates with both oligomeric and short-chain diols, resulting in block copolymers of the $(A\text{-}B)_n$ type. One block of the polymer chain, called the soft segment, is constituted by oligomeric diol, while the second block, referred to the hard segment, is built of a diisocyanate and short-chain diol. The soft segments confer the polyurethanes with their softness, elasticity, long elongation at break and low-temperature resistance, whereas the hard segments particularly affect the modulus of elasticity, hardness and tear strength. Oligoester, oligoether and oligocarbonate diols are the most used oligomeric diols to synthesize conventional TPUs. The polymers based on the latter diols, which are relatively new, have at the same time a high resistance to heat, hydrolysis and oxidation in comparison with ones derived from oligoether and oligoester diols [1,2]. The best mechanical properties give these polymers the hard segments formed by 1,1'-methanediylbis(4-isocyanatobenzene) (MDI) and butane-1,4-diol (BD). In special cases, e.g. to obtain polymers with higher modulus of elasticity and hardness, enhanced thermal stability or liquid-crystalline properties, BD is replaced by nonconventional chain extenders.

The studies undertaken by us are a part of an on-going investigation concerning new TPUs obtained from nonconventional aliphatic-aromatic sulfur-containing chain extenders, derivatives of, among others, diphenylmethane, diphenylethane, benzophenone, diphenyl ether and diphenyl sulfide, commercial aliphatic and aromatic diisocyanates and oligoester, oligoether and oligocarbonate diols. On the basis of the studies conducted for selected polymers it was stated that the introduction of sulfur atoms to the polymer chain improved their adhesive strength [3-6] and refractive index [5,6] in relation to conventional ones. Polymer antimicrobial activity against Gram-positive bacteria was also discovered [6].

The aim of these studies [7-9] was to synthesize and determine the structure and some properties of new TPUs based on chain extenders with different content of sulfur atoms, i.e. 2,2′-[sulfanediylbis(benzene-1,4-diyloxy)]diethanol (diol OSOE), 2,2′-[oxybis(benzene-1,4-diylsulfanediyl)]diethanol (diol SOSE) or 2,2′-

[sulfanediylbis(benzene-1,4-diylsulfanediyl)]diethanol (diol SSSE), MDI, 1,1'-methanediylbis(4-isocyanatocyclohexane) (HMDI) or 1,6-diisocyanatohexane (HDI) and 30–60 mol% poly(hexane-1,6-diyl carbonate) diol of $M_n = 860$ (PHCD-860) or 2000 g/mol (PHCD-2000).

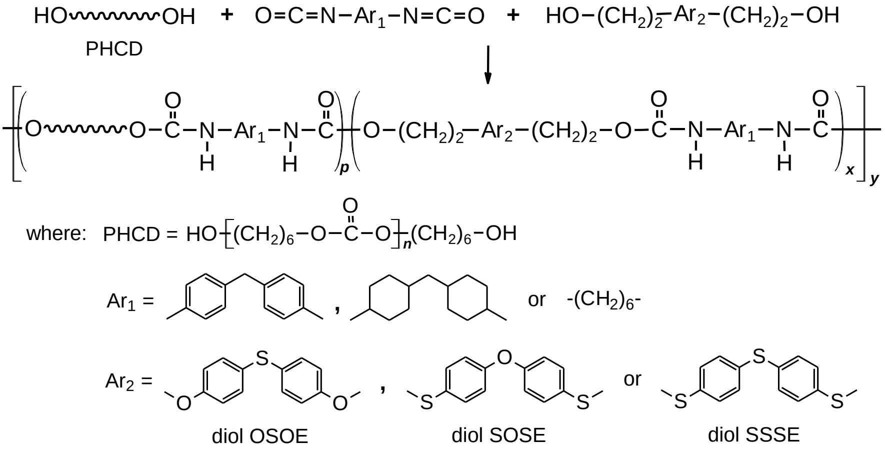

The structures of the TPUs were examined by FTIR, X-ray diffraction analysis and atomic force microscopy. Their thermal behavior was investigated by means of differential scanning calorimetry and thermogravimetry (TG). For the selected polymers the gaseous products evolved during the decomposition process were analyzed by TG-FTIR. Moreover, their physicochemical, optical, tensile and adhesive properties as well as Shore A/D hardness were determined.

The obtained TPUs were transparent or opaque high-molar-mass materials, showing amorphous or partially crystalline structures. The polymers based on PHCD-2000 exhibited lower glass-transition temperatures than those based on PHCD-860 (–35–20°C vs. 10–46°C) as well as a higher degree of microphase separation.

On the basis of TG data it was found that thermal stability of the TPUs was relatively good and slightly depended on the kind of the chain extender used and the length and content of the soft segment, but was more dependent on the kind of the diisocyante applied. The temperatures of 1% mass loss were contained in the range of 262-265°C (from HMDI), 266-272°C (from HDI) and 280-290°C (from MDI). The polymers decomposed in two or three stages. The main volatile products of the hard-segment decomposition were carbon dioxide, water and carbonyl sulfide, while aliphatic ethers, aldehydes and unsaturated alcohols, as well as carbon dioxide, originated from the soft-segment decomposition.

The synthesized TPUs were characterized by very good or good tensile strength, ranged from 28.5-51.9 MPa, with elongation at break in the range of 200-600%. The best tensile strength (49.7–51.9 MPa) was revealed by the polymers derived from diol OSOE, MDI and PHCD-860.

The TPUs based on PHCD-860 showed middle or high refractive index values (1.573–1.602), whereas those based on PHCD-2000 exhibited rather low these values (1.494-1.533). All the TPUs were characterized by improved adhesion to copper in comparison with those of conventional ones. It was also shown that both these parameters increased with an increase of the content of sulfur atoms in the polymer chain.

Such materials can be attractive for numerous medical applications like blood tubing, catheters, cannulae, pacemakers, neurostimulators and orthopedic nail encapsulation [2,10], as well as for optical applications like ophtalmic lenses, fiber optics and non-linear optics, and so on [11]. They can also be applied as interlayers or inner layers for automobile laminated windscreens [12]. Moreover, in view of good adhesion to copper they can be considered as materials used in the production of printed wiring boards [13].

References:

[1] M. F. Sonnenschein, "*Polyurethanes: Science, Technology, Markets, and Trends*", New Jersey, Wiley 2014.
[2] I. Resiak and G. Rokicki, *Polimery/Polymers,* **45** (2000) 592.
[3] M. Rogulska, A. Kultys and J. Lubczak, *Journal of Thermal Analysis and Calorimetry,* **121** (2015) 397.
[4] M. Rogulska, A. Kultys and E. Olszewska, *Journal of Thermal Analysis and Calorimetry,* **114** (2013) 903.
[5] A. Kultys and A. Puszka, *Polish Journal of Chemical Technology,* **15** (2013) 1.
[6] A. Kultys and A. Puszka, *Journal of Thermal Analysis and Calorimetry,* **117** (2014) 427.
[7] M. Rogulska and A. Kultys, *Journal of Thermal Analysis and Calorimetry,* **126** (2016) 225.
[8] M. Rogulska, A. Kultys and S. Pikus, *Journal of Thermal Analysis and Calorimetry,* (2016) DOI: 10.1007/s10973-016-5756-4.
[9] M. Rogulska, A. Kultys and A. Puszka, *Chemical Papers*, (2016) DOI: 10.1007/s11696-016-0112-5.
[10] T. Choi, J. Weksler, A. Padsalgikar and J. Runt, *Journal of Biomaterials Science, Polymer Edition,* **22** (2011) 973.
[11] G. S. Jha, G. Seshadri, A. Mohan and R. K. Khandal, *e-Polymers,* (2008) 035.
[12] C. Hepburn, *Iranian Journal of Polymer Science and Technology,* **1** (1992) 84.
[13] H. Hirano, J. Kadota, Y. Agari, T. Harada, M. Tanaka and K. Hasegawa, *Polymer Engineering & Science* **47** (2007) 262.

SYNTHESIS OF NEW HYBRID SILICA MATERIALS WITH CONTROLLED QUANTITIES OF MESO AND MICROPORES

Stanisław PIKUS, Małgorzata SKIBIŃSKA, Marek STANKEVIC,
Piotr BABUT, Aleksander PADEWSKI
DEPARTMENT OF CRYSTALLOGRAPHY

This work aims is presenting the properties of new materials – palladium nanoparticles deposited on mesostructural cellular foam (MCF) synthesized by using of Nay zeolite. The NaY zeolite was chosen as a microporous aluminosilicate source.

Palladium exhibit a strong catalytic activity for important chemical reactions such as: hydrogenation, dehydrogenation and palladium catalyzed coupling reactions. Industrial palladium catalysts are often in the form of metal supported on solid substrates such as porous silica because of their high surface area and pores structure.

The synthesis of MCF was carried out by conventional method and using the appropriate amounts of the copolymer (Pluronic P123), TEOS, TMB and various amounts of zeolite NaY. As result, a series of MCF samples having different amounts of meso and micropores was obtained. Fig.1. shows an MCF image obtained by TEM method.

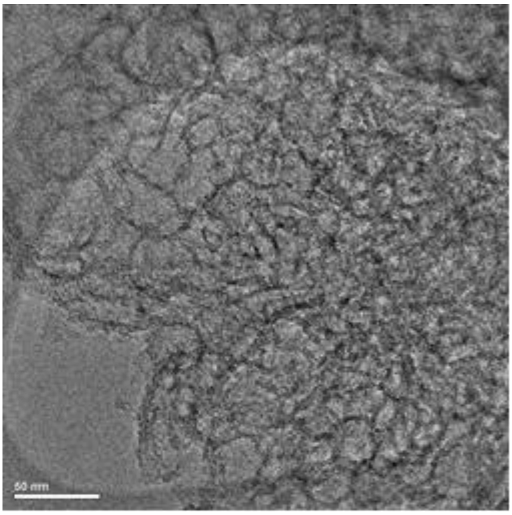

Fig.1. TEM images of MCF prepared by using 3g of Pluronic, 3,47 cm^3 of TMB , 7 cm^3 of TEOS and 2.25g of NaY zeolite.

In this work MCF materials containing palladium species were prepared by using of tetraammine palladium chloride ($[Pd(NH_3)_4]Cl_2$) complex as a palladium source. This complex was adsorbed on MCF samples in an amount such that the content of palladium was 1%, 2% or 3%. Then the complex to be reduced to palladium metal using ascorbic acid. Fig. 2 shows the XRD pattern for the selected system Pd^o /MCF.

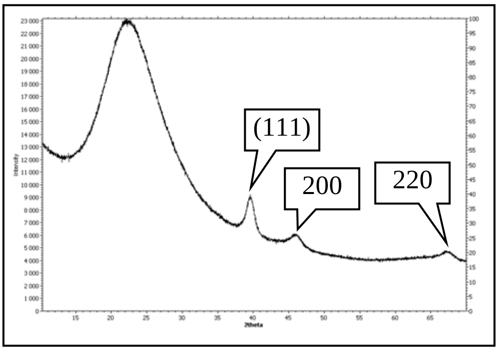

Fig.2. XRD pattern for3% Pd^o/MCF prepared by using 3g of Pluronic 1,74 cm^3 of TMB , 7 cm^3 of TEOS and 2.25g of NaY zeolite.

As seen in Figure 2. XRD pattern shows a high broad peak characteristic of amorphous materials, and 3 smaller peaks that have been identified as originating from the palladium metal (peaks 111, 200, 220). High broad peak undoubtedly comes from the amorphous structure of the MCF. Using the Scherrer formula the average crystallite size of palladium metal was calculated. The values obtained for the different samples are very small - the size of crystallites is in the range of 5.7 to 7.8 nm.

Thus, obtained Pd^o/MCF samples have been checked in Suzuki-Miyaura coupling between o-tolylboronic acid and different phenyl halides. With phenyl iodide all tested catalysts effectively promoted coupling with boronic acid in water as a solvent under standard reaction conditions (110°C, 24h). With phenyl bromide, the reaction performed in water failed to produce the corresponding biphenyl. Fortunately, the analogous reactions performed in toluene as a solvent afforded cleanly the desired product with high yields for each catalyst. With phenyl chloride the reaction was the least selective. Here, the formation of 1,3,5-triarylboroxine was observed. For the sample (3g of Pluronic 3.47 cm^3 of TMB, 7 cm^3 of TEOS and 0.75g of NaY zeolite, 3% Pd^o) this compound was be only isolated from the reaction mixture. For two other catalysts, (3g of Pluronic 3.47 cm^3 of TMB , 7 cm^3 of TEOS and 1.5g of NaY zeolite, 3% Pd^o) and (3g of Pluronic 1.74 cm^3 of TMB , 7 cm^3 of TEOS and 1.5g of NaY zeolite, 1% Pd^o) the formation of both biphenyl and 1,3,5-triarylboroxine was observed.

In conclusion, the synthesized Pd/MCF system exhibit a well-shaped porous structure, palladium crystallites are very small; the whole system has a high catalytic activity.

STEREOCHEMISTY OF HETEROCYCLIC COMPOUNDS POSSESSING BIOLOGICAL ACTIVITY

Izabela DYBAŁA, Anna KOZIOŁ, Irena WAWRZYCKA-GORCZYCA
DEPARTMENT OF CRYSTALLOGRAPHY
Krzysztof SZTANKE[*]
[*]MEDICAL UNIVERSITY, LUBLIN

A number of hexahydroimidazo[2,1-*c*][1,2,4]triazin-4-ones differently substituted at the *N*-8 position, with an additional acetic acid moiety or different ester functionalities, have been designed and prepared mostly as antiproliferative [1], antibacterial [2,3] and antiviral [3] agents.

The new compound **1** (Fig. 1) have both antiproliferative and antibacterial activities [1,3]. Structural studies of **1** showed that molecule is planar, the conformer is stabilized by the intramolecular N–H···O hydrogen bond. Molecules form layers connected *via* weak C–H···O and C–H···Cl interactions only, while weak C–H···N and C–H···π interactions occur between layers.

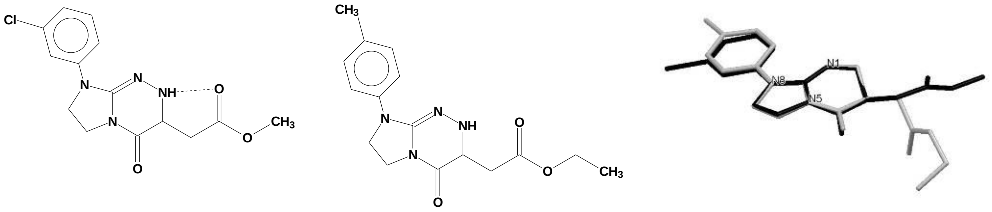

1 **2** **1 *vs* 2**

Fig. 1. Molecular formulae of compounds **1** and **2**, and fitting of conformers

The hexahydroimidazo[2,1-*c*][1,2,4]triazin-4-one system was not studied so far. The only derivatives of this moiety are compounds **1** [4] and **2 [**1]. They have different aryl substituents and ester groups. As a result, a different conformation of molecules as well as intermolecular bonding pattern is observed.

Within the molecule of **2** no intramolecular hydrogen bond is formed. Instead strong intermolecular hydrogen bonds N–H···N result in the formation of cyclic hexamers. Such differences are possible due to the significant conformational freedom of the ester moiety which is *E*-oriented in **2**, while in **1** it adopts *Z* orientation.

Moreover, the geometry of the minimum energy conformers of **1** and **2** in the gas phase were calculated by B3LYP/6-311+G methods. It was find out that in the solid state molecule **1** adopts the lowest energy while **2** has the higher (by about 2.5 kcal/mol) energy conformation.

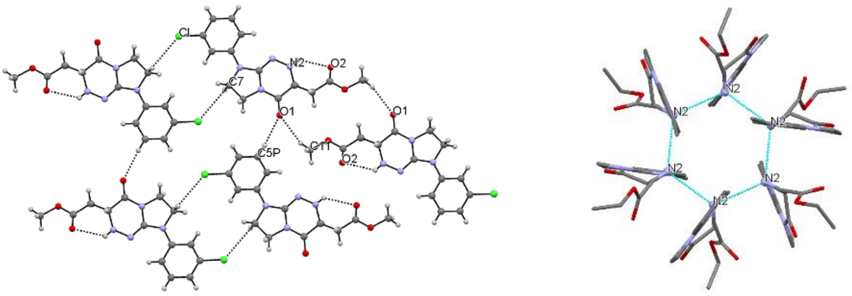

1

2

Fig. 2. Molecular association in crystal structure

References:
[1] K. Sztanke, J. Rzymowska, M. Niemczyk, I. Dybała, A.E. Kozioł, *Eur. J. Med. Chem.*, **41** (2006) 1373-1384.
[2] K. Sztanke, A. Sidor-Wójtowicz, J. Truchlińska, K .Pasternak, M. Sztanke, *Ann. UMCS, Sect. D*, **59** (2004) 96-99.
[3] K. Sztanke, K. Pasternak, B. Rajtar, Sztanke, M. Majek, M. Polz-Dacewicz, *Bioorg. Med. Chem.*, **15** (2007) 5480-5486.
[4] I. Dybała, K. Sztanke, *J. Mol. Struct.*, **1119** (2016), 78–85.

FUNCTION OF TRIFLUOROMETHYL GROUP IN SUPRAMOLECULAR SYSTEMS

Anna E. KOZIOŁ, Ilona MATEREK, Oleksandra SAVCHENKO
DEPARTMENT OF CRYSTALLOGRAPHY

The fluoro-organic compounds are very scarce in nature. Fluorine has been identified as a component of only 13 secondary metabolites [1]. Hovewer, the population of fluorine substituted xenobiotics, used as biologically active compounds in commercial pharmaceuticals and agrochemicals, could be estimated at 20–25% [2].

The introduction of fluorine into a molecule of drug allows modification of electronic, lipophilic and steric parameters. Changes of these parameters can critically influence both the pharmacokinetic and pharmacodynamic properties of compounds [3]. Fluorine and fluorine containing moieties may be used for incorporation of a group capable of reinforcing drug–receptor interactions, e.g. the $–CH_3$ or –OH groups could be bioisosterically substituted by $–CF_3$ (Fig. 1).

van der Waals' radii:

F	1.47 Å
O	1.52
C	1.70
H	1.20

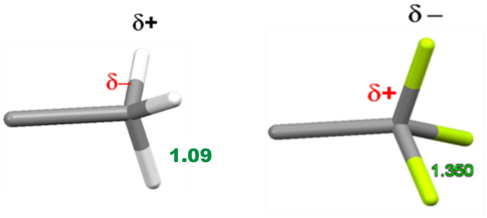

Fig. 1. Comparison of geometric parameters of methyl and trifluoromethyl groups

Such activity results from non-covalent intermolecular interactions, thus, the association patterns formed by small organic molecules in crystalline solids can be considered as model.

Analysis of structural database CSD [4] indicated more than 7,000 crystals formed by organic molecules substituted with $–CF_3$ group. These groups are not involved in 'classic' hydrogen-bonding, but promote formation of molecular layers, stabilize π-stacking and, in many cases, introduce disorder.

References:

[1] D. O'Hagan, D.B. Harper, *J. Fluorine Chem.*, **100** (1999) 127-133.
[2] C. Isanbor, D. O'Hagan, *J. Fluorine Chem.*, **127** (2006) 303-319.
[3] B.E. Smart; *J. Fluorine Chem.*, 109 (2001) 3-11.
[4] F.H. Allen; *Acta Cryst.*, **B58** (2002) 380-388.

STEREOCHEMISTY OF HETEROCYCLIC COMPOUNDS POSSESSING BIOLOGICAL ACTIVITY

Barbara MIROSŁAW
DEPARTMENT OF CRYSTALLOGRAPHY

The 1-pyridinecarbonyl-4-substituted thiosemicarbazide derivatives (**1**–**10**) were prepared by the reactions of 2-, 3- or 4-pyridine carboxylic acid hydrazide with isothiocyanates (Fig. 1) [1].

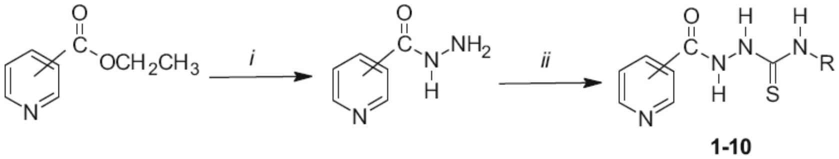

1-10

Fig. 1. Scheme of synthesis

In this study [1], the antibacterial, cytotoxic and antiproliferative activities of novel thiosemicarbazide derivatives were assessed. Our results demonstrated that some of the novel compounds possess good antibacterial properties against *Staphylococcus epidermidis*, *Streptococcus mutans* and *Streptococcus sanguinis,* and are only slightly cytotoxic; thus, they exhibit an excellent therapeutic index, which is higher than that of ethacridine lactate. Moreover, data showed that compounds **2** (Fig. 2) and **4** have an antiproliferative activity against human breast adenocarcinoma and human hepatocellular carcinoma cell lines. The prominent antibacterial and antiproliferative effect of compounds **2** and **4** may be due to changing the number of chlorine atoms in the phenyl ring. Thus, it is worth underlying that 4-(2-chloro/2,4-dichlorophenyl)-1-(pyridine-2yl) carbonylthiosemicarbazide derivatives will be auspicious as potential agents for caries. We expect that the novel thiosemicarbazide derivatives can be used as agents for treatment of dental caries and also for chemotherapy support.

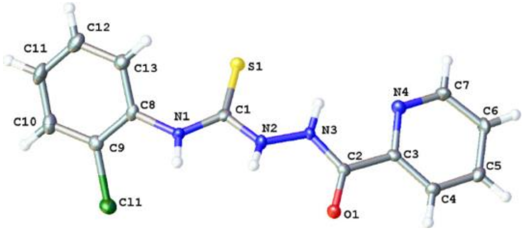

Fig. 2. Molecular structure of compound **2**

References:

[1] M. Pitucha, M. Wos, M. Miazga-Karska, K. Klimek, B. Mirosław, A. Pachuta-Stec, A. Gładysz, G. Ginalska, Synthesis, antibacterial and antiproliferative potential of some new 1-pyridinecarbonyl-4-substituted thiosemicarbazide derivatives, *Medicinal Chemistry Research,* **25** (2016) 1666–1677.

STUDIES ON FACTORS AFFECTING THE PROCESS OF CHEMICAL EDUCATION AND ITS RESULTS

Ryszard M. JANIUK, Agnieszka KAMIŃSKA-OSTĘP
DEPARTMENT OF CHEMICAL EDUCATION

For several years there have been observed decreasing interest in studies of chemical subjects in many countries. In Poland it is additionally associated with the number of pupils finishing secondary schools diminishing every year. The example can be the Faculty of Chemistry, Maria Curie-Skłodowska University at which the number students is twice smaller than 10 year ago. This requires searching for new forms encouraging pupils to enrol for such studies as those existing so far do not give satisfactory results.

One of such forms was organizing piloting classes for the secondary school pupils at the Faculty of Chemistry, Maria Curie-Skłodowska University at the end of June. They aimed at developing interests in chemistry and showing prospects connected with studies of chemistry. Evaluation of the classes assumptions, their program and course was made using the questionnaire which was sent electronically to the pupils participating in them after they were over. The results of the questionnaire confirmed the need for their organization, particularly in the case of pupils from the schools situated out of Lublin. [1].

Over the past few years several changes have taken place in the Polish education system which may have had negative influence on the interest of university students in becoming teachers. Some of these changes have had to do with the educational reform in secondary schools which has caused a reduction in teaching hours in natural science subjects and with the fact that as a result some teachers have been made redundant. Another factor which may have had a negative impact on students' perceptions of the teaching profession are constant changes in the regulations concerning teacher education, including a provision which has made it necessary for future teachers to pay for attending classes which offer teaching qualifications.

The survey was conducted in order to collect information on the current attitude of the third year students at the Faculty of Chemistry at Maria Curie-Skłodowska University (group I) towards the profession of chemistry teacher and their plans regarding their potential enrolment for classes which would offer qualifications in teaching chemistry. A similar survey was carried out among the post-graduate students (group II) who were attending such classes [2].

Over 70% students of group I express the wish to do the course giving teaching qualifications. Such wish is expressed more often by women than by men. Their justification is having some possibility in case they do not find another job. Students' opinions indicate that they possess quite good and objective knowledge about strength and weaknesses of teacher's job. However, only several percent declares clearly that they want to work as the teacher after being graduated. The similar situation was in group II but relatively more students are interested in working as the teacher.

Stimulating students' interest in chemistry is a key issue for teacher's success. This success manifests itself in students' achievements as far as acquisition of chemical knowledge is concerned as well as in the fact that students find chemistry as an interesting subject and learn it willingly. The studies were conducted which the main aim was to determine the factors influencing effective learning of chemistry by junior secondary school students. Of special importance was to study the factors affecting students' motivation for learning chemistry which is connected with the teacher – its characteristics and skills. The studies included 384 students of whom 229 were from municipal schools and 155 from rural schools.

The results of studies showed that the teacher affects significantly students' approach to the subject and will to learn. Being friendly and just for the students is the most important for them. The studies show favorable effects of motivation and praise even for minor achievements on students' attitude to learning [3].

Getting to know which factors affect pupils' motivations to learn chemistry the study was undertaken where 384 pupils from junior secondary schools, of whom 229 were from urban schools and 155 from rural schools, took part. The investigation results show that pupils from junior secondary schools have positive approach to the subject of chemistry. They are willing to undertake extra activities which can affect the growth of interest in chemistry, such as participation in after school forms of education and performing chemical experiments. However, they do not take interest in participation in competitions and subject contest developing knowledge. The research also showed that the junior secondary school pupils are not keen on working in groups. They prefer individual work during which they often make use of the Internet, make notes, learn formulae and definitions but rarely solve tasks [4].

References:

[1] R. M. Janiuk, Poszukiwanie nowych form zwiększenia zainteresowania uczniów studiami chemicznymi, in: *Materiały 59 Zjazdu Polskiego Towarzystwa Chemicznego.* Poznań 2016, 347.

[2] R. M. Janiuk, Chemistry students' perceptions of the teaching profession, in: *Abstracts of 7th International Conference on Research in Didactics of the Science,* Kraków, 2016, 42.

[3] A. Kamińska-Ostęp, Teacher's Influence Compared to Students' Attitude Towards Learning Chemistry in Gymnasium Age Group in: *Proceedings of 7th International Conference Research in Didactics of the Sciences,* Pedagogical University of Cracow, Kraków 2016, p. 58-60.

[4] A. Kamińska-Ostęp, Opinions of Junior Secondary School Pupils on Factors Affecting Effective Learning of Chemistry, in: *Abstracts of 7th International Conference Research in Didactics of the Sciences,* Pedagogical University of Cracow, Kraków 2016, p. 43.

DEVELOPMENT OF MICROSTRUCTURED OPTICAL FIBERS TECHNOLOGY

Krzysztof POTURAJ, Grzegorz WÓJCIK, Małgorzata GIL,
Lidia CZYŻEWSKA, Janusz PĘDZISZ, Aleksander WALEWSKI,
Jarosław KOPEĆ, Wiesław PODKOŚCIELNY, Paweł MERGO
LABORATORY OF OPTICAL FIBERS TECHNOLOGY

Among other rare earth ions trivalent thulium is one of the most attractive due to relatively simple energy levels' scheme with several metastable levels offering optical transitions spanning the ultraviolet, visible, near- and mid-infrared spectral range. These features enable application of thulium doped active materials in different type of lasers and optical amplifiers.

Specifically, in the long-wavelength domain $^3F_4 \rightarrow {}^3H_6$ transition in the range of 1,7-2,06 μm has been demonstrated in many different crystalline and glassy matrices. This generation range is extremely interesting mainly for high power fiber lasers with commercially available maximum CW output powers up to several kW.

In this work we report the first results on development of thulium doped active SiO_2 fibers manufactured at Maria Curie-Skłodowska University.

Active silica glass with two different doping levels (1300ppm and 6000ppm Tm^{3+}) has been fabricated with MCVD method complemented by a modified impregnation from liquid phase method. Figure 1 presents refractive index profiles of fabricated preforms. Figure 2 presents the absorption and emission spectra of fabricated active glass.

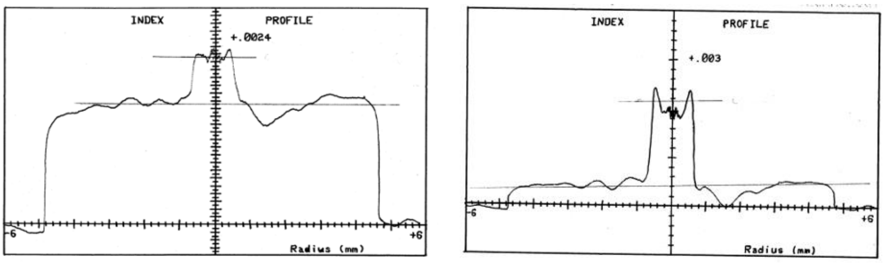

Fig. 1. Refractive index profiles of the fabricated preforms (1300ppm – left, 6000ppm – right)

From the manufactured preforms three different kinds of optical fibers with different cross-sections (standard single mode, circular shape double-clad, stadium shape double-clad) have been drawn. Figure 3 presents the electron microscope photos of manufactured fibers.

Absorption, transmission and Raman characteristics have been recorded, allowing assessment of optical quality of developed glasses, as well as maximum phonon energies.

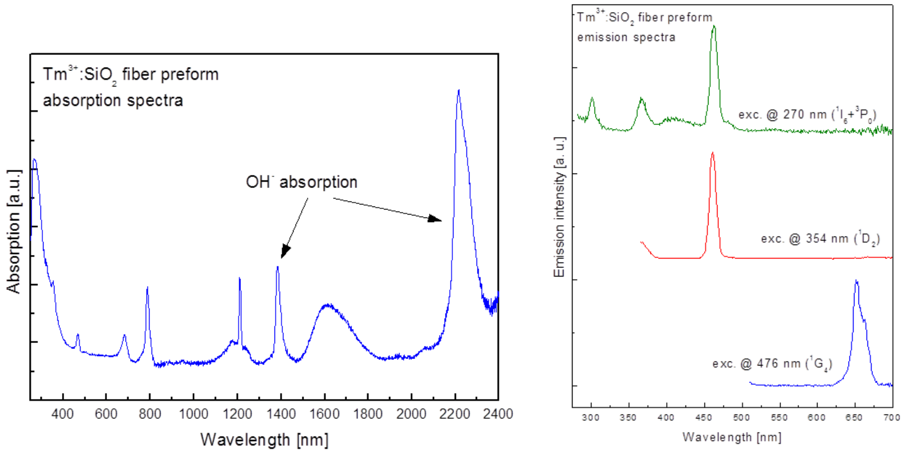

Fig. 2. Absorption (left) and emission (right) spectra of Tm3+:SiO_2 fiber preform.

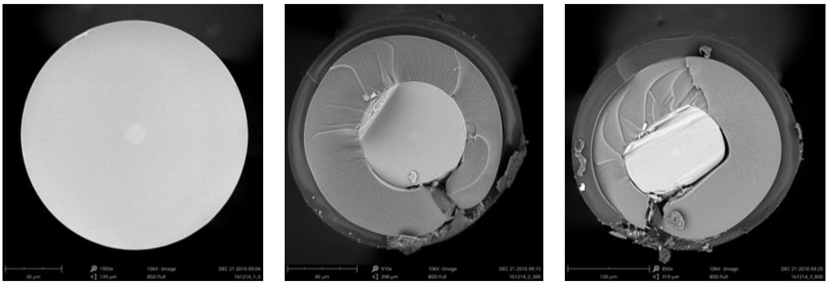

Fig. 3. Photos of cross-sections of fabricated fibers

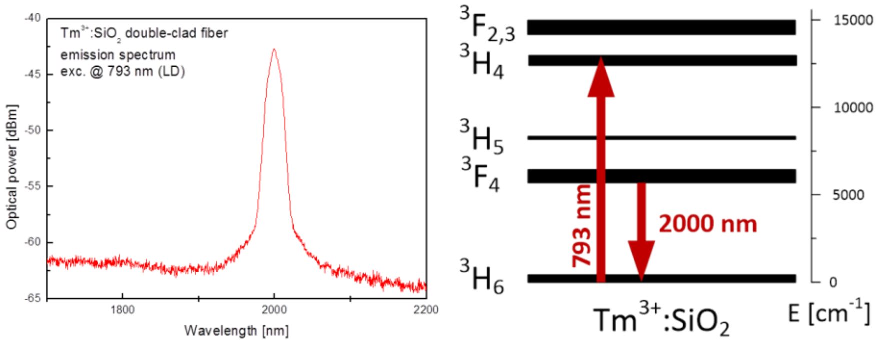

Fig. 4. Emission spectrum under 793 nm laser diode excitation (transition $^3F_4$ -> $^3H_6$ is visible)

Measurements of emission characteristics and fluorescence dynamics profiles have proved the presence of thulium ions and confirmed acceptable luminescent properties of both preforms and drawn fibers. Performed characterization provided also important feedback for technological team enabling further optimization of both bulk glasses and optical fibers.

THE ENVIRONEMNTAL EFFECT OF NANOMATERIALS ANTHROPOGENIC ORIGIN

Bożena CZECH, Patryk OLESZCZUK, Wiesława ĆWIKŁA-BUNDYRA
DEPARTMENT OF ENVIRONMENTAL CHEMISTRY

The treatment of wastewater containing functionalized -OH or -COOH carbon nanotubes (CNT-OHs or CNT-COOHs) will definitely affect the surface properties of CNT. After realizing to the environment, changed CNT, will react with various elements. Fulvic acids (FA) are ubiquitous water components, which has been shown [1] affect pristine CNT behavior. The aim of the presented studies was the determination of the kinetics and mechanisms of sorption of FA onto H_2O_2 and/or UV treated CNTOHs and CNTCOOHs.

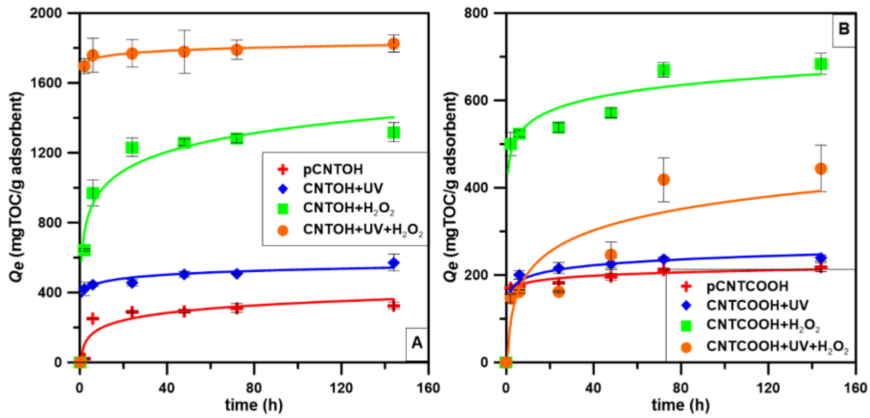

Fig. 1. Kinetics of FA (10 mg·L^{-1}) sorption onto (a) treated CNTOHs (2 mg); (b) treated CNTCOOHs (2 mg).

H_2O_2 and/or UV treatment reduced adsorption of FA by CNT-OHs (Fig. 1) but increased adsorption of FA by CNT-COOHs. Pseudo-second order regime described the sorption of FA onto CNTOHs and CNT-COOHs indicating for chemical sorption as the rate-limiting step.

The literature studies of sorption of organic matter onto pristine or as-produced CNT described the adsorption according to Freundlich model and π-π interactions with hydrogen bond. Our results indicated that UV and/or H_2O_2 treated CNT-OHs and CNT-COOHs behaved completely different comparing to pristine or as-produced CNT.

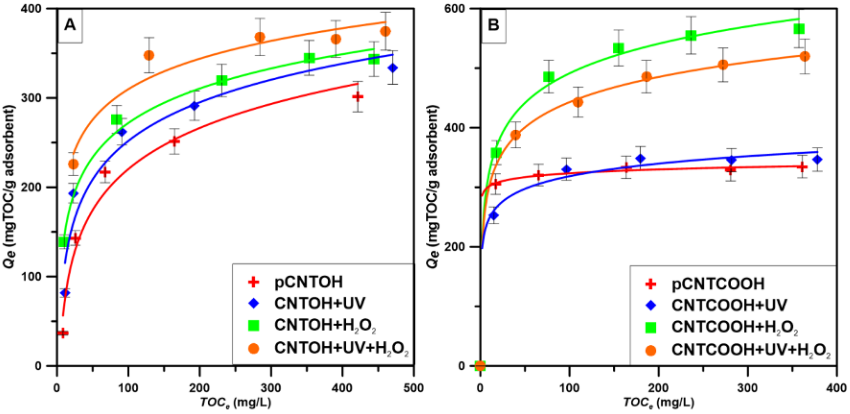

Fig. 2. Initial runs of adsorption isotherms of FA sorption (1-200 mg.L^{-1}) over (a) CNTOHs (2 mg) and (b) CNTCOOHs (2 mg).

Both the models of sorption (Fig. 2, Langmuir – for CNTOH-H_2O_2 and CNT-COOHs, Temkin – CNT-COOH-UV+H_2O_2, and Dubinin-Radushkevich – CNT-OHs, CNT-COOH-UV) and sorption mechanism were different. The adsorption of natural FA onto CNTOHs was governed by π-π, heterogeneous and electrostatic interactions. The π-π and electrostatic interactions can the mostly described FA adsorption onto CNTCOOHs. H-bonding mechanism was excluded. The parameters affecting FA sorption were combination of porosity and dispersity of CNT.

Although the presence of DOM (such as TA as the representative) was proven to increase the stabilization of pristine and functionalized CNT (throughout the introduction of hydroxyl groups) [1] our studies indicated that CNTOH-H_2O_2 and CNTCOOH-H_2O_2 in the presence of tannic acid revealed a slightly reduced stability [2]. Aggregation may reduce the surface area [3] affecting adsorption of other water contaminants and toxicity. Additionally, strong interactions with DOM affect the mobility (dispersed CNT and FA- coated CNT can readily move in environment) and environmental risk of organic chemicals present in water (CNT's high adsorption capacity) [1,4]. Though there is not possible to predict the environmental impact of CNT basing only on previously published results [5].

References:

[1] X. Zhang, M. Liu, X. Zhang, F. Deng, C. Zhou, J. Hui, W. Liu, Y. Wei, *Toxicol Res.*, **4** (2015) 160–168.
[2] B. Czech, P. Oleszczuk, A. Wiącek, *Environ. Pollut.*, **200** (2015) 161–167.
[3] V.K.K. Upadhyayula, S. Deng, M.C. Mitchell, G.B. Smith, *Sci. Total Environ.*, **408** (2009) 1–13.
[4] B. Pan, B. Xing, *Environ. Sci. Technol.*, **42** (2008) 9005–9013.
[5] O.G. Apul, T. Karanfil, *Water Res.*, **68** (2015) 34–55.

ECOTOXICOLOGICAL AND CHEMICAL EVALUATION OF ENVIRONMENT AS THE SUBJECT TO ANTHROPOGENIC PRESSURE

Marcin KUŚMIERZ, Agnieszka MARCEWICZ-KUBA
DEPARTMENT OF ENVIRONMENTAL CHEMISTRY

The application of biochars for soil amendment or remediation has recently gained a lot of interest. Literature data indicate that biochars have a positive effect on many physical, chemical and biological properties of soils. Moreover, the methods of biochar production are simple, well known and can be exploited without use of advanced technologies.

Unfortunately their production and use may pose significant risk to ecosystems and to human health. The process of pyrolysis used for it increases the concentration of metals and metalloids in biochars. At the same time compounds such as furans, dioxins and polycyclic aromatic hydrocarbons (PAHs) can be formed. As aresult those carbonaceous materials usually contain significant amounts of aforementioned toxic chemicals, especially polycyclic aromatic hydrocarbons (PAHs), which are also carcinogenic.

There are many ways of environmental evaluation described in the literature data, but it is a known fact that the simplest of them, based on the total content of toxic compounds often result in overestimation of hazards [1]. In this study three lines of evidence (LoE): chemical, toxicological and ecological, were exploited to to assess the risks posed to the environment by traditional biochar kilns (so called Triad approach) placed in 11 locations (w1a to w5b) throughout Bieszczady National Park (south-eastern Poland) [2,3].

For the purposes of the research the following parameters were determined: total and bioavailable concentrations of PAHs in soils, PAHs concentrations in soil pore water and basic physico-chemical properties of the soils. Te activity of soil enzymes, bacteria counts, fungi counts and toxicological tests were also conducted (germination test, D. Magna, V. fisheri, MARA® Test).

Figure 1 presents risk numbers (RN) calculated without taking into account toxic equivalence factors (TEF), which differentiate PAHs for their toxicity. This lack of the weighting leads to overestimation of risk numbers and the inconsistency within the triad, what undermines a realiability of model. Figure 2 shows the comparison of raw and weighted integrated risk number for each site. It can be clearly concluded, that if a large number of chemical substances are under consideration, even the Triad based approach leads to very high risk numbers (integrated risk number IRN $\approx$ 1.00). It has been succesfully demonstrated, that weighting PAHs concentrations based on toxicity equivalence factors leads to more reasonable, balanced risk levels (IRN $\approx$ 0.18÷0.57) and, especially, consistency within the three lines of evidence, what is the primary condition of evaluation's realiability.

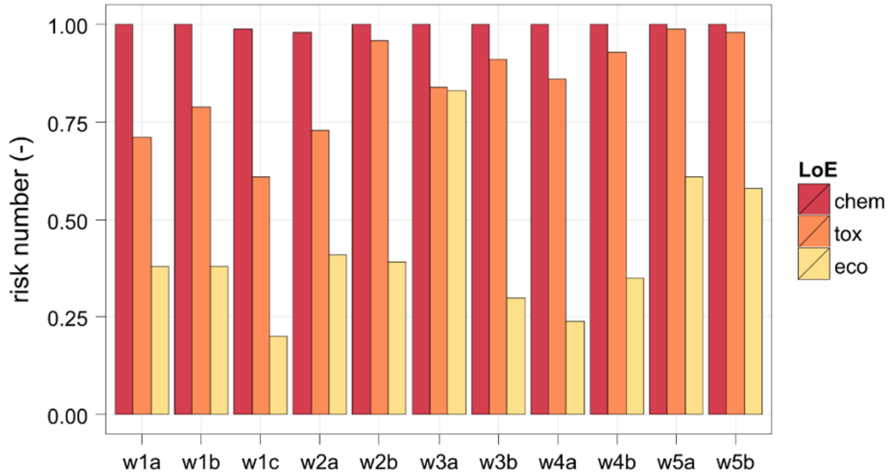

Fig. 1. The results of RN evaluation for chemical, toxicological and ecological line of evidence (LoE) without weighting the results.

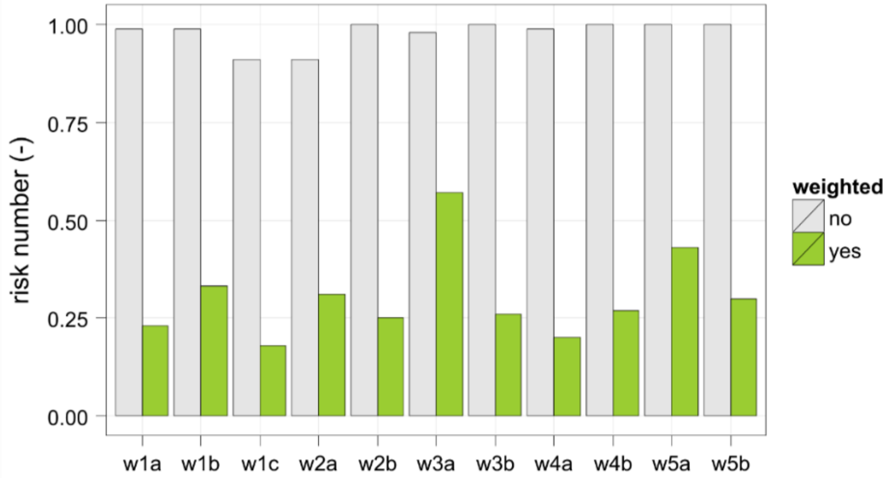

Fig. 2. Comparison of IRNs calculated with and without weighting the raw results.

References:

[1] M. Kuśmierz, P. Oleszczuk, *Environ. Sci. Pollut. Res.*, **21** (5) (2014) 3646.

[2] J. Jensen, M. Mesman, Ecological Risk Assessment of Contaminated Land: Decision support for site specific investigations, 711701047 RIVM (2006) 136.

[3] Verbruggen, E. Environmental risk limits for polycyclic aromatic hydrocarbons (PAHs) : For direct aquatic, benthic, and terrestrial toxicity; 607711007; National Institute of Public Health, Bilthoven, The Nederlands, 2012.

THE SYNTHESIS OF NEW CHIRAL ORGANOPHOSPHORUS FRAMEWORKS FOR ASYMMETRIC CATALYSIS

Kamil DZIUBA, K. Michał PIETRUSIEWICZ, Oleh M. DEMCHUK, Katarzyna SZWACZKO, Sylwia SOWA, Sławomir FRYNAS, Elżbieta ŁASTAWIECKA, Anna FLIS, Anna SZMIGIELSKA, Adam WŁODARCZYK, Marek STANKEVIČ
DEPARTMENT OF ORGANIC CHEMISTRY

The synthesis of new organophosphorus systems is still an important part of organic chemistry mainly due to the application of these compounds as reagents in organic synthesis and as ligands in transition metal-catalyzed transformations. In the last year four different topics have been developed in the frames of statutory tasks.

The first topic was devoted towards the application of six-membered phosphorinanone derivatives as substrates for the synthesis of policyclic compounds incorporating phosphorus atom (Scheme 1).

Scheme 1

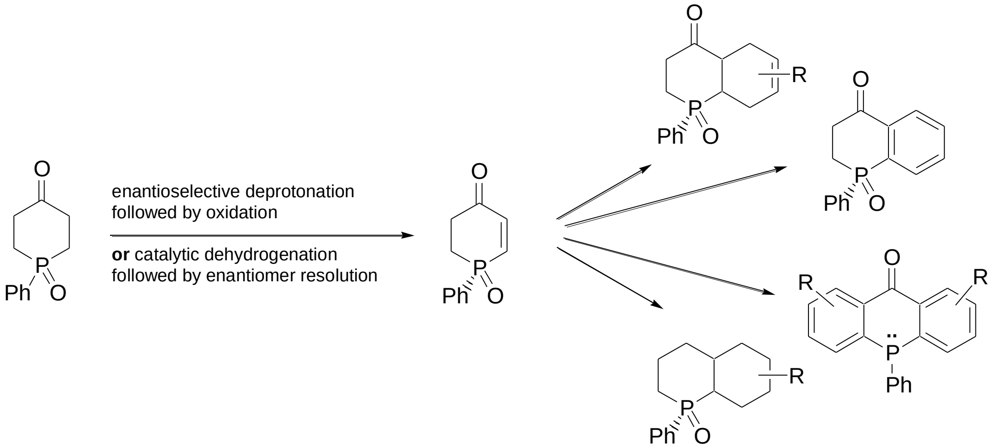

The second topic was based on the development of catalytic Wittig reaction using phosphetane oxides as catalysts in the presence of a reducing agent (Scheme 2).

Scheme 2

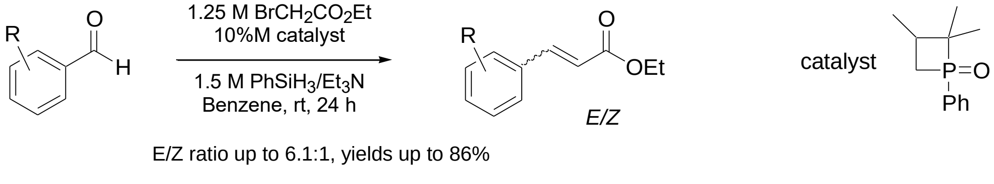

E/Z ratio up to 6.1:1, yields up to 86%

The third topic was devoted to the development of new applications for well-known metathesis catalysts in non-metathetic reactions. The main emphasis has been put towards the studies on cycloisomerization reactions (Scheme 3).

Scheme 3

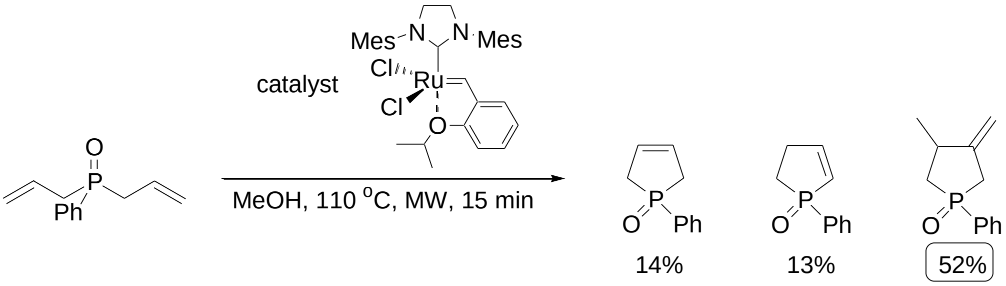

The fourth topic was the development of a new and efficient transition metal and hydrogen-free method of transformation of arylphosphine derivatives into corresponding cycloalkylphosphine derivatives. It appeared that under modified Bouveault-Blanc conditions (alkali metal in the presence of an alcohol) arylphosphine oxides undergo formal exhaustive or partial hydrogenation of arene fragment (Scheme 4).

Scheme 4

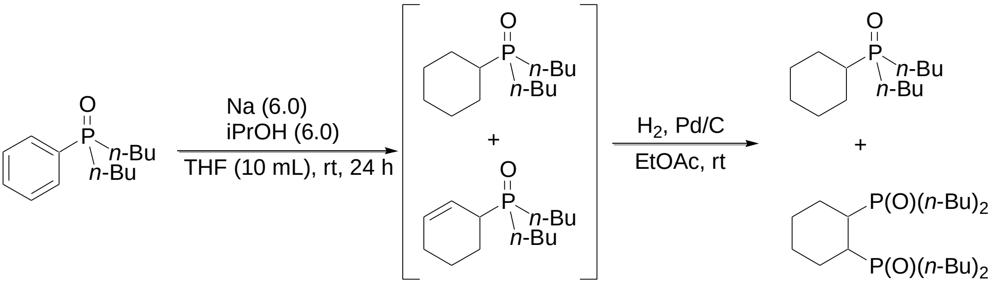

The further development of the presented topics is still continued in the laboratory.

STUDY OF THE THERMODYNAMIC PROPERTIES AND STRUCTURE OF THE SELECTED SURFACE SYSTEMS

Małgorzata BORÓWKO, Paweł BRYK, Andrzej PATRYKIEJEW,
Wojciech RŻYSKO, Stefan SOKOŁOWSKI, Tomasz STASZEWSKI
DEPARTMENT FOR THE MODELLING OF
PHYSICO-CHEMICAL PROCESSES

ORDERING PHENOMENA IN THE (1× 1) MONOLAYER CHEMISORBED ON THE (111) FACE OF AN FCC CRYSTAL

Order-disorder phenomena in strongly adsorbed and chemisorbed monolayers have been a subject of active research for many years now [1,2,3] and those studies have vastly relied on Monte Carlo simulations carried out in a general framework of lattice gas models [2,3].

We assumed that the adsorbate atoms interact via the Stillinger-Weber potential [6].

$$u(r) = \begin{cases} 4\varepsilon\left[(\sigma/r)^{12} - (\sigma/r)^{6}\right]\exp\left[-\sigma/(r - r_C)\right], & r < R_C \\ 0, & r \geq R_C \end{cases}$$

with R_C being the parameter determining the range of interaction.

All adsorbed atoms are bonded to adsorption centers, which form a two-dimensional triangular lattice. It is assumed that $\sigma < a$ so that all lattice sites are accessible to adsorption. In this work, we are not interested in the adsorption process but only in the structure and properties of films in which all sites are occupied by the adsorbed atoms. The bonds between adatoms and surface sites have been assumed to be allowed to undergo harmonic deformations, and the adatom energy changes with the displacement from the lattice site, $\boldsymbol{u} = \boldsymbol{r} - \boldsymbol{r}_{o,i}$ as

$$u_{har}(\boldsymbol{u}) = \frac{1}{2} f\boldsymbol{u}^2$$

where f is the force constant of the harmonic potential.

The model has been studied using Monte Carlo method in the canonical ensemble.

It has been demonstrated that the film may form different ordered phases (see insets to Fig. 1). The ordering depends on the elasticity of the bonds. When the bonds are very stiff the film orders into a simple (1×1) phase. Upon the decrease of bond stiffness, the adatoms exhibit a gradually increasing tendency to displace from surface sites. Since the pair potential is attractive at small distances, the adatoms tend to form small clusters. In the ground state, we have found the ordered states in which such clusters consist of three (T), four (R) and seven (S) atoms (R).

The structures T and R are stable only in the ground state, however. On the other hand, the structure S has been found to be stable at finite temperatures.

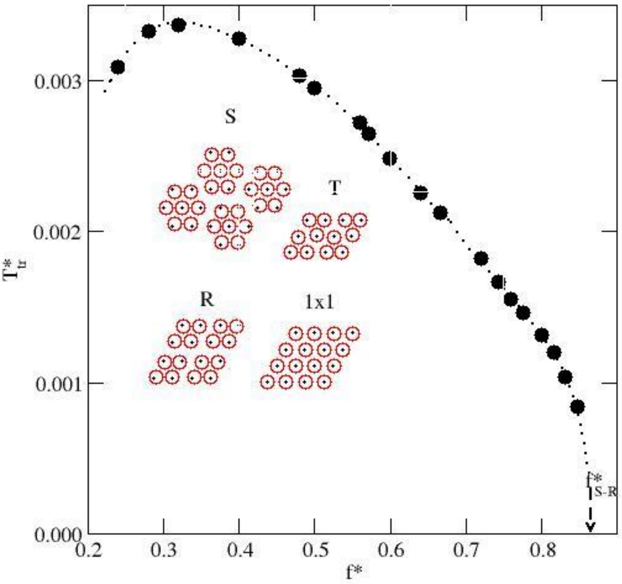

Fig.1. The main figure shows the changes of the transition temperature for the S structure versus f^* obtained for the systems with $\sigma^* = 0.8$ and $R_C^* = 1.05$. The insets shows different ordered structures stable in the ground state.

Our Monte Carlo simulation results, supported by finite-size scaling analysis, have shown that the S phase disorders via the first-order transition. The transition temperature depends on the bond elasticity. This is demonstrated by the results given in Fig. 1.

For sufficiently low values of the harmonic potential force constant, the adatoms enjoy a rather large freedom to displace from adsorption sites and tend to form still larger clusters than those appearing in the S structure.

Although the model considered here is very simple, nevertheless it exhibits interesting physics, novel phase behavior and new types of ordering. In this work, we have considered only the case of fully filled triangular lattice, but the model can be also used to study orderings on surfaces of different symmetry of adsorption sites. It can be also readily extended to take into account three body forces [6] and orientation-dependent interactions [7].

References:

[5] J.G. Dash and R. Ruvalds (Eds.), Phase Transitions in Surface Films, Plenum, New York, 1980.
[6] A. Patrykiejew, S. Sokołowski and K. Binder, *Surf. Sci. Rep.*, **37** (2000) 207.
[7] R. Chakarova, D.E. Oner, I. Zoric. and B. Kasemo, *Surf. Sci.*, **472** (2001) 63.
[8] F.H. Stillinger and T.A. Weber, *Phys. Rev. B*, **31** (1985) 5262.
[9] A.M. Dongare , M. Neurock and V. Zhigilei, *Phys. Rev. B*, **80 (**2009) 184106.

SYNTHESIS OF SILICA AND POLYMER-SILICA CARRIERS OF BIOACTIVE SUBSTANCES

Jacek GOWOREK, Agnieszka KIERYS, Patrycja KRASUCKA,
Andrzej SIENKIEWICZ, Wojciech STEFANIAK
DEPARTMENT OF ADSORPTION

Porous polymers are attending a significant interest during last decade due to their potential applications in separation science and nanotechnology. Many efforts are devoted to property improvements directed to enhancing their mechanical and thermal stability. Both aforementioned features may be modified by introduction into polymer various inorganic additives e.g. silica dioxide [1]. During last five years a new synthesis method is intensively developed which consists in the porous polymer swelling in silica precursor followed by its transformation into silica gel within polymer matrix. A crosslinked resins of the Amberlite family were used as a polymer support and tetraalkoxysilanes served as a source of silica species. Composite materials obtained this way appear as a promising supports for bioactive substances such as drugs in controlled release systems [2]. Release process depends essentially on structural arrangement of polymer and silica component. Thus, any modifications of their preparation are noteworthy.

In the present paper Amberlite XAD7HP was initially saturated with TEOS (tetraethoxysilane). After its transformation in water solution of desired pH the spherically shaped particles of polymer-silica composite were obtained. Two series of composite samples were prepared. First one was prepared conventionally by wetting polymer particles by water solution of desired pH and the second was prior condensation of silica precursor washed with ethanol. Hence, the external part of precursor was removed. Composite samples were additionally calcined to obtain pure silica component.

Table 1 contains numerical values of parameters characterizing the porosity of investigated samples. As is seen in composites specific surface areas and total pore volumes are reduced as compared to the initial polymer. However, for pure silica component one can observe the substantial increase of both these parameters. Different structural parameters for samples washed with ethanol and samples without washing suggest different dispersion of silica component within polymer matrix. The same samples were tested additionally in respect to their mechanical durability. The results of appropriate tests are shown in Fig. 1 and Table 2. For each sample the particles were placed between two discs and pressed up to the moment of their crash at a speed of 5 cm/min.

Table 1. Parameters characterizing the porosity of the received samples obtained from nitrogen adsorption/desorption isotherms at 77 K: S_{BET} – specific surface are, V_p – total pore volume, D_{PSD} – pore diameter at the peak of PSD [3].

Sample	**S_{BET} [m^2/g]**	**V_p [cm^3/g]**	**$D_{PSD\ 1;2}$ [nm]**
XAD7	458	0.56	3.8; 9.4
X7-Si	430	0.26	3.8
SiO2	756	1.27	9.5; 15
X7-SiE	352	0.29	3.8
SiO2E	960	0.91	3.8; 4.8

Table 2. Breaking force describing the mechanical resistance of pure XAD7 polymer and composite samples. Standard deviation σ was estimated from n measurements.

	XAD7	**X7-Si**		**X7-SiE**
Force [N]	4.95	12.33	26.55	16.16
σ	±0.53(n=4)	±0.57(n=6)	±5.95(n=4)	±1.40(n=3)

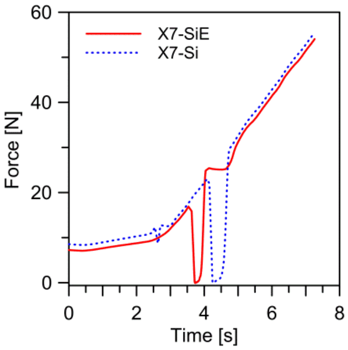

Fig. 1. Force vs. time for X7-Si (dotted line) and X7-SiE (solid line) composite samples [3].

As is seen modification of the composite sample by an ethanol washing makes it less resistant for mechanical stress. The dependence force vs. time shows in this case one minimum. Different effect is registered for sample without ethanol pretreatment. There are two clearly visible steps corresponding to different mechanical stress. It means that in this case the structure of the composite particles is of core-shell type. It is worth to note that mechanical resistance of composites is much higher than for pure polymer and may be tuned by the changes of silica contamination.

References :

[1] K. Rezwan, Q.Z. Chen, J.J. Blaker, A.R. Boccaccini, *Biomaterials*, **27** (2006) 3413-3431.

[2] A. Kierys, R. Kasperek, P. Krasucka, Ł. Zimmer, E. Poleszak, J. Goworek, *RSC Adv*., **5** (2015) 94067–94076

[3] P. Krasucka, R. Zaleski, K. Skrzypiec, J. Goworek, *Micropor. Mesopor. Mat*., **237** (2017) 210-221.

SYNTHESIS, MODYFICATIONS AND STUDIES OF PROPERTIES OF MATERIALS WITH DIFFERENTIATED STRUCTURAL AND SURFACE CHARACTERISTICS WITH REGARD TO APPLICATIONS IN SORPTION PROCESSES

Anna DERYŁO-MARCZEWSKA, Małgorzata ZIENKIEWICZ-STRZAŁKA, Magdalena BŁACHNIO, Dariusz STERNIK,
Agnieszka CHRZANOWSKA, Małgorzata SĘCZKOWSKA
DEPARTMENT OF PHYSICOCHEMISTRY OF SOLID SURFACE

Silver based nanomaterials and composites are important components in materials science and engineering due to the reactivity of silver nanophase which mainly involve surface effects. In the paper the Ag-doped SiO_2 nanocomposites were synthesized by wet impregnation procedure of aminopropyl-functionalized silica materials with submicrometer structure. Aminopropyl-functionalized fumed silicates with amount of amino groups established as half and close to full monolayer were used for immobilization of the nanosilver phase starting from ammoniacal silver complex as a noble metal precursor. Fumed silica as an inexpensive nanostructured material with useful properties including adsorptive affinity for noble metal ions and organic macromolecules was applied as a support first for diamminesilver(I) ions and subsequently for silver nanoparticles. In the present study the effect of amine functionalization and silver nanoparticles deposition was monitored by investigation of the textural properties and thermal stability of obtained nanocomposites. The size and structure of the nanocomposites were investigated by transmission electron microscopy (TEM), nitrogen adsorption-desorption isotherms and thermal analysis (TG/DSC).

Silver nanoparticles deposited on fumed silica surface create homogeneous phase without aggregation to dysfunctional component. Such behavior of silver phase can be related to the presence of 3-ammoniatriethoxysilane groups which can be responsible for homogeneous distribution due to their affinity to noble metal nanoclusters. The presence of silver nanoclusters on the fumed silica surface generates changes over the textural properties reducing the specific surface area and available adsorption sites, however does not block them entirely making the material still useful as a potential sorption agent.

To perform measurement of the particle size, both primary particles of fumed silica and silver nanostructures, transmission electron microscopy was applied. Fig. 1 shows spherical structure of the support and well defined deposited silver nanocrystalites. The TEM images show that the visible aggregates consist of primary particles of silica formed during flame process. The silica particles create merging zones with amorphous structure where SiO_2 tetrahedrons exhibit an irregular arrangement. This organization of tetrahedrons is faintly visible in the amorphous area of composites (inset of Fig. 1C). Silver nanoparticles are visible as dark objects on the pyrogenic silica surface. The distribution of silver phase is uniform but the size of silver crystallites can be differentiated depending on the investigated area. Silver phase exists mostly as small, crystallites with size below 5 nm. HRTEM images confirmed that diamminesilver(I) complex as silver precursor in combination with hydrophilic fumed silica ensure the creation of composites where silver phase forms well defined crystallites with well singled lattice planes without clear marked internal distortion.

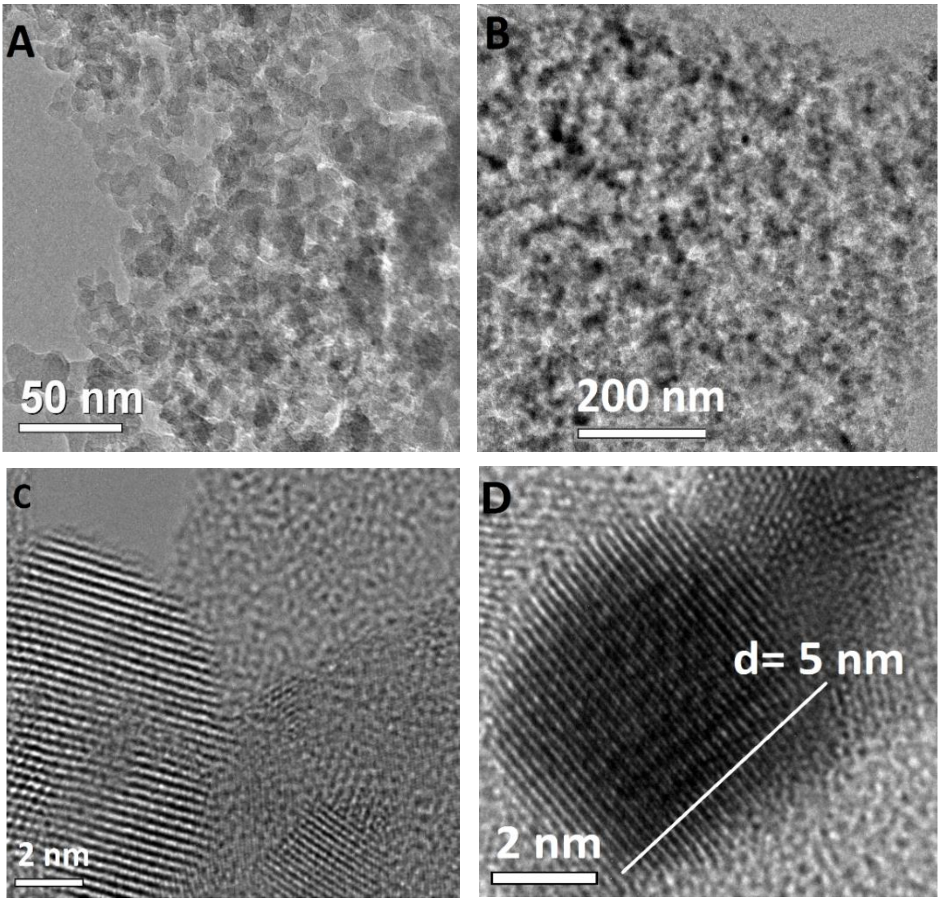

Fig. 1. (A, B) TEM images of fumed silica aggregates modified by silver nanoparticles, (C, D) TEM images with high magnification (HRTEM) of silver nanoparticles deposited on silica surface.

Thermal stability of investigated samples was evaluated by thermogravimetric (TG) analysis before and after silver nanoparticles incorporation. The weight loss starting around 300°C is related to decomposition of ammine groups on the surface. The total weight loss at 950°C was estimated as 9% and 5.5% respectively. The presence of silver ions had no significant effect on thermal stability of the composites.

APPLICATION OF CHROMATOGRAPHIC METHODS FOR INVESTIGATION ON BIOLOGICAL ACTIVE COMPOUNDS.

Małgorzata JANICKA, Katarzyna STĘPNIK,
Irena MALINOWSKA, Marek STUDZIŃSKI
DEPARTMENT OF PLANAR CHROMATOGRAPHY

The investigations of physicochemical properties of coordination compounds, not only as solids, but also in liquid state seem to be very important. The activities of these complexes being changed depending on the environments around the central ion may create various possibilities of their practical applications resulting from the potential sites of their biological action. During recent years coordination compounds of biologically active ligands have received much attention.

The new 19 complexes of carboxylates with transition and rare elements as a central ions and theirs ligands were characterized by chromatographic analyses. The parameter of relative lipophilicity (R_{M0}) of the tested compounds were determined experimentally by reversed-phase high-performance thin layer chromatography method with mixtures of various organic modifier (ACN, acetone, dioxane) and water as a mobile phase. Extrapolated R_{M0} values were compared with *logP* values calculated from molecular structures of solutes tested.

In the work discussed in this paper the effect of a magnetic field on the retention and lipophilicity of new complexes of carboxylates with transition metals or rare earth elements and their ligands was investigated, because the compounds were synthesized as potential anticancer drugs. In other hand the complexes (especially complexed of f-electron elements) have paramagnetic properties, so thy can be cumulated in the ill tissue by specially configured magnetic field.

Thin layer chromatography combined with magnetic field has been proposed as complementary method for determination of lipophilicity of investigated compounds. The chromatograms in the field and outside it were developed simultaneously in two identical chromatographic chambers. One of them was placed in external magnetic field of 0.4 T inductivity.

Fig.1 shows differences between retardation factors of solutes chromatographed absence (R) of the of the magnetic field and in the presence (R_M) expressed by percentages.

$$\%R = \frac{R(\text{outside magnetic field}) - R_M(\text{inside magnetic field})}{R(\text{outside magnetic field})} \cdot 100\% \qquad (1)$$

Data presented in Fig. 1 show that magnetic field can change lipophilicity of the the substances it means that magnetic field can change bioavalibility of the complexes.

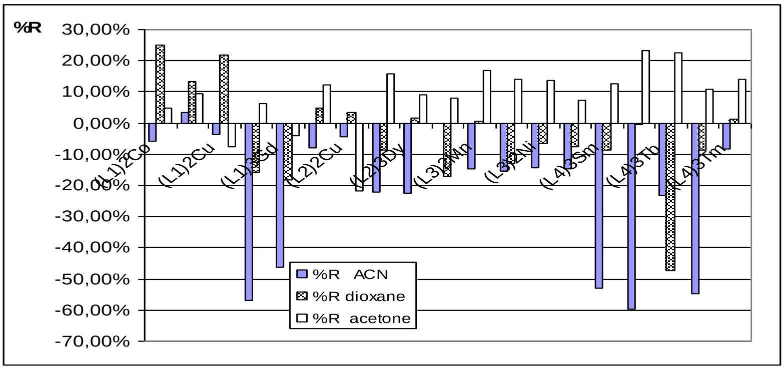

Fig. 1. The relative %R values obtained for all chromatographic complexes in various mobile phases. Relative ΔR_F values were calculated using equation 1.

In order to establish the relationships between different variables in and out external magnetic field, the principal components analysis (PCA) for coordination compound has been done (Minitab 16 software).Similarities between lipophilicity indices were analyses by PCA and linear regression (Fig. 2)

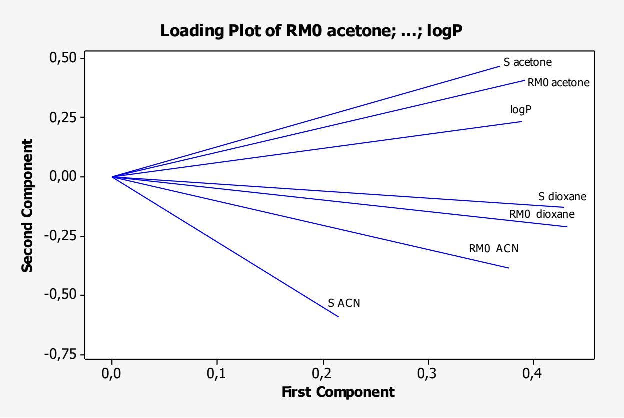

Fig. 2. Loading plot of R_{M0} (acetone, dioxane, acetonitrile), S (acetone, dioxane, acetonitrile) in and without external magnetic field and theoretically calculated logP.

Chelation causes drastic change lipophilicity of compound, but all complexes have not shown enhanced activity as compared to parent ligand. The difference in activity among the tested compounds may be attributed to the electrostatic nature of ligand and central metal ion and the steric factors.

It should be noted, that the software does not take into account all possible interactions that may affect the lipophilicity of the compounds. The correlation value R_{M0} determined experimentally and theoretical values of log P (chemicalize.org $r^2 > 0.98$). Standard programs for logP calculation - provide poor predictions for coordination compounds. Others commonly used programs for logP estimation are not suitable for complex compounds simply because the appropriate input of the central metal atom is usually missing.

SPECIAL PURPOSE SUBSIDY TO CONDUCT RESEARCH AIMED AT DEVELOPING YOUNG SCIENTISTS AND DOCTORAL STUDENTS

LUMINESCENCE PROPERTIES OF POLYCYCLIC AROMATIC HYDROCARBONS (PAHs) ADSORBED ON ALUMINOSILICATES

Agnieszka LIPKE
DEPARTMENT OF INORGANIC CHEMISTRY

Polycyclic aromatic hydrocarbons belong to the main chemicals responsible for the pollution of the environment. The most important representatives are pyrene, benzopyrene, chrysene, anthracene or naphthalene. PAHs are constituents of minerals, so their presence in the environment results from the combustion of different types of fuels, home heating and food preparation. Many industrial processes as well as natural agents (volcanic eruptions, large forest fires) also play a very important role in their formation. All these factors clearly indicate the ubiquity of PAHs in the human environment, which combined with their ability to induce cancerous changes has an impact on human and animal organisms.

Aromatic hydrocarbons are poorly soluble in water, much better in organic solvents. The presence of detergents in sewages improves their solubility. Then they get into the ground water and are deposited on various components of the soil, including aluminosilicate minerals. Many of these compounds exhibit the phenomenon of fluorescence, which is used in their quantitative determination [1,2].

The aim of presented studies was the comparison of modified aluminosilicates in the sorption of polycyclic aromatic hydrocarbons, particularly naphthalene as an example. The modification of red clay and halloysite by two commercial surfactants (phenyltrimethylammonium bromide, *PTMA*-Br; benzyltrimethylammonium chloride, *BTMA*-Cl) and a new non-commercial one (chemical formula: $C_{10}H_6CH_2NH(CH_3)_2Cl$) was conducted for the purpose of sorption enhancement.

A full characterization of sorption process was prepared. Evidently better naphthalene sorption on halloysite comparing to red clay was noticed. This probably results from the adsorbate interactions with the mineral both on the surface and in the interior. The adsorption energy calculated on the basis of the Dubinin-Radushkevich isotherm model indicates the physical character of the reaction. Kinetic evaluation of the equilibrium data showed that the adsorption of naphthalene on studied sorbents follows well the pseudo-second-order kinetic model.

The spectroscopic characterization of the systems obtained before and after modification as well as sorption processes was elaborated. The most important regions of FT-IR spectra of aromatic hydrocarbons and sorbents were studied. The band characteristic of Si-O stretching vibration of red clay is shifted from 979 cm^{-1} to 985, 1032 and 1031 cm^{-1} for Surf_3-red, BTMA-red and PTMA-red, respectively. This is the consequence of the strong ion-dipol interaction of organic cations with H_2O, which is concurrent with the complexation of siloxane oxygen by

H_2O. The sorption of naphthalene on clay, which proceeds probably via π-π bond formation between benzyl and phenyl rings of organic cations and naphthalene, manifests as return of the bands from the positions: 985, 1032, 1031 to 981, 984, 980 cm^{-1}. The strength of interaction of naphthalene with organic cations follows the order: Surf_3<<BTMA=PTMA. There is probably obstacle in the formation of π-π bond between naphthalene and spaciously extended Surf_3 cation. In case of halloysite the sequence of the bands shift is very similar, i.e. the bands shifts of BTMA-, PTMA-hal differ remarkable in comparison with those one for Surf_3-hal.

UV-Vis absorption, emission and excitation spectra were recorded to monitor the adsorbate presence and its luminescence activity due to the various surfactants addition. The best results were obtained for naphthalene adsorbed on halloysite, especially in the presence of PTMA (Figure 1B). The band in the region of 320-335 nm characteristic of naphthalene was noticed. Spectrophotometric measurements confirm the results from the sorption experiments.

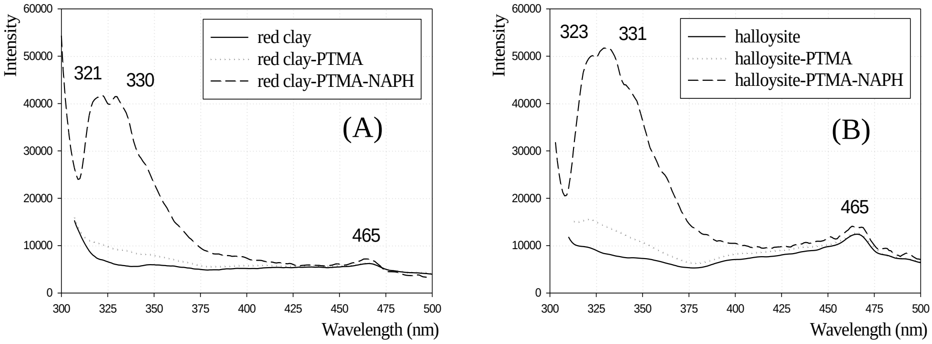

Fig.1. The emission spectra of naphthalene adsorbed on PTMA modified red clay (A) and halloysite (B) (λ_{exc} = 276 nm).

The research was carried out with the equipment purchased thanks to the financial support of the European Regional Development Fund in the framework of the Operational Program Development of Eastern Poland 2007–2013 (Contract No. POPW.01.03.00-06-017/09). We are thankful to PTH INTERMARK (Gliwice, Poland) for the kind delivery of halloysite samples.

References:

[1] C.B. Vidal, A.L. Barros, C.P. Moura, A.C.A. de Lima, F.S. Dias, L.C.G. Vasconcellos, P.B.A. Fechine, R.F. Nascimento, *J. Colloid Interf. Sci.*, **357** (2011) 466.

[2] M.F. Brigatti, L.Medici, L. Poppi, *Appl. Clay Sci.*, **11** (1996) 43.

THE APPLICATION OF MESOPOROUS ORGANOSILICA ADSORBENTS FOR ANALYSIS OF TRANSITION ELEMENTS USING CHOSEN ATOMIC SPECTROMETRY METODS

Joanna DOBRZYŃSKA
DEPARTAMENT OF ANALYTICAL CHEMISTRY
AND INSTRUMENTAL ANALYSIS

The increasing industrial demand of rhodium and other platinum group elements has caused their extensive emission and spread in the environment. Vehicles catalyst containing different combinations of PGEs are found to be the main source of rhodium emission. The elevated concentration of rhodium is often found in the airborne dust collected longwise heavy traffic roads. The accumulation of rhodium in soil and plants may pose a health risk. Therefore, the development of selective and sensitive methods of its determination is required. Due to the low concentration of analyte and composed matrix of analysed samples the separation/ preconcentration of rhodium from environmental samples is often necessary. The introduction of the enrichment step to the analytical procedure results in the improvement of detection limits and elimination of matrix interferences. It may be carried out by extraction of analyte to the solid phase (SPE-solid phase extraction). Among the wide range of sorbents used for the enrichment of PGE, mesoporous organosilica of SBA-15, due to high hydrothermal stability, high surface area and simplicity of modification, seems to be perfectly suited for this purpose.

The aim of this study was the synthesis of modified SBA-15 sorbent exhibiting high adsorption affinity toward Rh(III) ions.

The modified SBA-15 material was synthesized as follows: 2 g of Pluronic 123 was dissolved in 72 mL of 2 M HCl. The mixture was stirred at 40°C for 8 h, then 0,54 mmol of $ZrOCl_2$ and 18 mmol of tetraethoxysilane (TEOS) was dropped. After 15 minutes 2 mmol of 3-mercaptopropyltrimethoxysilane was added dropwised. The mixture was stirred for 24 h at 40°C and aged for 48 h at 100°C. The obtained material was washed with deionized water, filtered and dried at 70°C. Finally, three-time extraction with ethanol at 70°C was carried out. The obtained material was characterized by using of SEM and low temperature nitrogen adsorption/desorption isotherms. It was stated that the addition of $ZrOCl_2$ to the reaction mixture results in the increase of the surface area. Additionally, the presence of $ZrOCl_2$ impacts on the morphology of the obtained MPTMS modified SBA-15 particles, which is presented in Fig. 1.

According to accomplished experiments it was stated that inorganic Rh(III) ions present in model water solutions do not adsorb onto SBA-15 modified by MPTMS, TMPED and APTES. Based on the literature data nitrogen-containing heterocyclic compound 1-(2-pyridylazo)-2-naphthol PAN was selected as an agent for complexing Rh(III) ions. In order to complex Rh(III) ions 0.05% solution of PAN was prepared by dissolving solid in ethanol. The green Rh-PAN complex was created using water-ethanolic solutions at pH 5.1 (acetic buffer). An aliquot of rhodium solution, 8 mL of acetic buffer and 16 mL of 0.05% PAN was placed in a 100mL Erlenmeyer flask and diluted to 50 mLwith distilled water. The mixture was heating for 60 minutes in 90°C in water bath. Before the adsorption studies the obtained Rh-PAN complex was appropriately diluted.

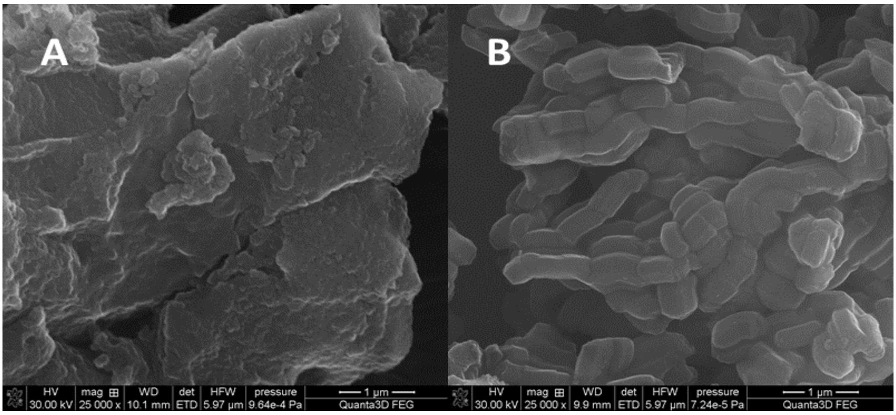

Fig.1. SEM picture of MPTMS-modified SBA-15 synthesized without (A) or in the presence of $ZrOCl_2$ (B).

The adsorption experiments were carried out in the batch mode at pH 5.1 [1]. In the model adsorption system 5 mL of Rh-PAN water-alcoholic solution was shaken with 5 mg of sorbent. After 30 minutes shaking the adsorption equilibrium state was reached (Fig.2). In Fig.3 the adsorption isotherm of Rh-PAN complex onto MPTMS-modified SBA-15 is presented. As one can see the adsorption capacity is 27 mg/g, which substantially exceeds values described in the literature [2]. The described adsorption system due to the high adsorption capacity and fast kinetics may be applied for the enrichment of Rh traces before determination by slurry sampling GF AAS

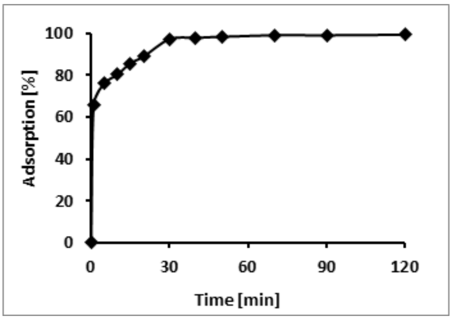

Fig.2. Kinetics of Rh-PAN complex adsorption onto MPTMS-modified SBA-15; m = 0.005 g, V = 5 mL, T = 25ºC, $c_{\text{initial Rh}}$ = 50 mg/L, pH_{initial} = 5.1.

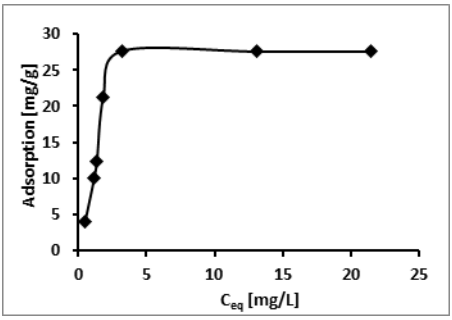

Fig.3. Adsorption isotherm of Rh(III) onto MPTMS-modified SBA-15; m = 0.005 g, V = 5 mL, t = 2 h, T = 25ºC, pH_{initial} = 5.1.

References:

[1] J. R. Stokely, W. D. Jacobs, *Analytical Chemistry*, **35** (1963) 149-152.
[2] S. Ghaseminezhad, D. Afzali, M.A. Taher, *Talanta*, **80** (2009) 168–172.

DETERMINATION OF Pb(II) AND Cd(II) BY STRIPPING VOLTAMMETRY USING NEW TYPE OF ARRANGEMENT TO DOUBLE DEPOSITION AND STRIPPING STEP

Iwona GĘCA
DEPARTMENT OF ANALYTICAL CHEMISTRY
AND INSTRUMENTAL ANALYSIS

Stripping voltammetry is one of the frequently used analytical method for the determination of metals ions and organic compounds. This method belongs to the group of the most sensitive analytical methods thanks to preconcentration step of the analyte on the surface of working electrode. The detection limit of stripping voltammetry has been decreased using chemical, instrumental and mathematical approaches. In 2014 a new way of lowering the detection limit in stripping voltammetry has been proposed – namely the application of double deposition and stripping steps [1-3]. In this study a lowering of the detection limit of Pb(II) ions determination by stripping voltammetry with the use of a new type of arrangement to double deposition and stripping steps has been proposed. The combination of the measurement consisting of two deposition and stripping steps with the application of an innovative set of two working electrodes where a microelectrode is placed in the centre of the macro-electrode will lead to a significant decrease of the detection limit. The application of new type of arrangement in combination with additional deposition and stripping steps in the same voltammetric cell will lead to lowering the detection limit, increasing the selectivity of determinations, facilitating analyses and shortening the measurements time. The miniaturization of the electrochemical cell and the application of environmentally friendly mercury free electrodes are additional advantages of the proposed idea.

The Pb(II) determination procedure consists of the following steps:

The sample was pippeted to the voltammetric cell and the following reagents were added: 1 mL 0.5 mol L^{-1} acetate buffer (pH 4.6) + 1.05 µL 1 g L^{-1} Bi(III). The sample was adjusted to 10 mL with water. Firstly the potential of -1.25 V for 300 s was applied to the first electrode in order to plate a new bismuth film on a impregnated graphite substrate and to simultaneous lead preconcentration. During this stage the solution was stirred using magnetic stirring bar. Next the stirring was stopped, the stirrer was directed near the wall of the vessel using a stir bar retriever placed outside the cell and the electrode was moved near the bottom of the voltammetric cell. After that deposited Pb and Bi were stripped simultaneously from the first electrode surface by applying the potential of 0.3 V for 30 s. When the first stripping step was finished the concentration of lead ions was much higher near working electrodes in comparison to the concentration in the bulk of the solution. The first electrode was disconnected and the potential of -1.15 V for 300 s was applied to the second electrode (ensemble of carbon fibers microelectrodes) in order to plate a bismuth film on the microelectrode surface and then to perform the second deposition step at this electrode. Then, a square wave voltammogram was recorded at a frequency of 20 Hz, while the potential was changed from -1.25 to 0.5

V. The amplitude and the potential step were equal to 50 and 4 mV, respectively. The measurements were carried out from undeaerated solutions. After each measurement a conditioning step of 30 s at 0.3 V (with solution stirring) was used to remove the target metals from both working electrodes before the next measurement.

The procedure optimization

The main parameter influencing the bismuth film formation was the concentration of Bi(III) ions added to the sample solution. The influence of Bi(III) concentration was studied in the range from 2×10^{-7} to 2×10^{-6} mol L^{-1}. For further studies Bi(III) concentration of 5×10^{-7} mol L^{-1} was chosen. Thanks to the bismuth preconcentation on the first working electrode during the first deposition step Bi(III) concentration is much higher in the second deposition step and, consequently, its concentration needed to Pb(II) determination is very low.

The optimum deposition potentials were found to be -1.25 V and -1.15 V at the first and second electrode, respectively. The influence of deposition time on Pb peak current was studied in the range from 60 to 1200 s. It was observed that analytical signal of lead increased linearly in studied range of deposition time. In order to shorten time of measurements further studies were performed at deposition time of 300 s for both working electrodes.

The calibration graph for Pb(II) in the optimized conditions was linear in the range from 1×10^{-10} to 2×10^{-9} mol L^{-1} with the linear correlation coefficient $r = 0.995$. The relative standard deviation from five determinations of Pb(II) at a concentration of 2×10^{-9} mol L^{-1} was 3.9 % ($n = 5$). The detection limit calculated as 3 s/m, where s is a standard deviation for a low Pb(II) concentration and m is the slope of the calibration plot for deposition time of 300 s for both working electrodes was about 2.4×10^{-11} mol L^{-1}.

The interference of foreign ions was studied for a solution containing Pb(II) at a concentration of 1×10^{-9} mol L^{-1}. Deposition time was 300 s for both working electrodes. The results indicate that for 100-fold excess of Cu(II), Fe(III), Zn(II), Mo(VI), V(V), Mn(II) and Ni(II) the interference on Pb(II) analytical signal was not observed. The proposed procedure was used for Pb(II) determination in certified reference material TMRAIN-04 rain water (certified value for lead ions was equal to 0.34 μg L^{-1}). Determinations were carried out using the method of standard additions following deposition time of 300 s for both working electrodes. The obtained result of 0.37 μg L^{-1} with a standard deviation 4.2% ($n = 5$) confirmed the accuracy of the proposed method and indicates that this procedure can be used for Pb(II) determination in environmental water samples.

During the optimization studies of the Cd(II) ions determination procedure it was found that the decrease of the detection limit is not enough satisfying with the use of such a set of working electrodes. The procedure of Cd(II) ions determination requires further optimization.

References:

[1] I. Rutyna and M. Korolczuk, *Sensors and Actuators B*, **204** (2014) 136.
[2] I. Rutyna and M. Korolczuk, *Electroanalysis*, **26** (2014) 2639.
[3] M. Korolczuk, M. Grabarczyk and I. Rutyna, *Talanta*, **130** (2014) 342.

INFLUENCE OF PLASMA ACTIVATION ON THE SURFACE PROPERTIES OF POLYAMIDE 6G

Diana RYMUSZKA
DEPARTMENT OF INTERFACIAL PHENOMENA

Due to the low surface free energy and poor chemical reactivity polymer surfaces are often difficult to wet and bind with other materials. Different types of low-temperature plasma are widely used for modification of chemical and physical properties of polymers and textile materials [1,2]. In addition to the surface chemistry, plasma treatment also often affects the surface topography [3]. These techniques have become a very interesting alternative for different types of methods which allow replacement of the environmentally harmful chemical modification [4]. The interaction of plasma with the polymer surfaces leads mainly to the change of surface polarity, wettability, printability, adhesion, durability, scratch resistance, hardness, biocompatibility and improves their performance in various applications.

In this work, the effect of low-temperature air plasma on the surface properties of polyamide 6G (PA6G – nylon 6 $H–[NH–C_5H_{10}]_n–OH$), which is an aliphatic polyamide obtained via the polycondensation reaction of ε-caprolactam, was investigated. Plasma activation was performed at low pressure of plasma Pico from Diener Electronic Germany. The polyamide plates were treated by the air plasma power 160 V for 10 and 60 s. To determine changes in wetting properties the advancing and receding contact angles of water, formamide and diiodomethane on the bare and modified polymer surfaces were measured using the sessile droplet method because they reflect the interactions at the solid/liquid/gas interfaces. Then, based on the measured contact angles, the surface free energy was calculated from the contact angle hysteresis (CAH model) [5]. The values of the total surface free energy were compared with the energy calculated from the acid-base (LWAB) approach [6].

The advancing and receding contact angles on the polyamide bare (untreated) surface and after 10 and 60 s air plasma treatment are plotted in Fig. 1. As can be seen, the surface modification by plasma decreases the contact angles of probe liquids, especially for water and formamide (Fig. 1). The advancing contact angles of water on the plates modified for 10 and 60 s changed from 81.8±7.8° for the untreated surface to 64.5±7.8° and 21.7±0.9°, respectively. The decrease in the values of the contact angles is mostly caused by the increase of the surface hydrophilicity which is directly related to the polar groups introduced onto the surface during the plasma process. For diiodomethane the contact angles changes were slightly smaller. The contact angle on the untreated surface was 47.4±5.3°, while the lowest one being 17.5±7.4°, was found on the PA plates activated for 60 s.

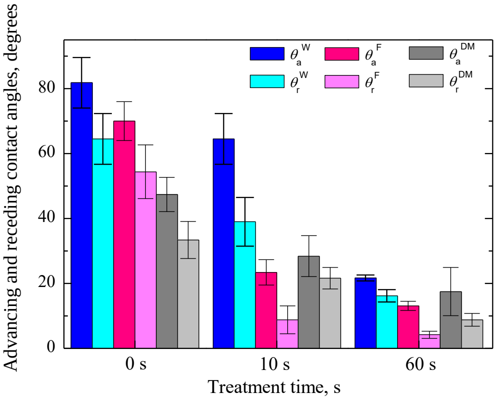

Fig. 1. Advancing (θ_a) and receding (θ_r) contact angles of water (W), formamide (F) and diiodomethane (DM) on the untreated and plasma activated PA6G plates for different period of time of air plasma treatment.

The apparent surface free energy values calculated using two approaches are very similar. The decrease of the contact angles of probe liquids was related with the increasing surface free energy with the plasma treatment time prolongation. The total surface free energy for the untreated surface was 35.7±2 mJ/m^2 from the LWAB approach and 36.3±0.6 mJ/m^2 for the contact angle hysteresis of polar liquids. For the surface treated by air plasma for 10 s the energy was much higher and the amounts about 52.9±1.5 mJ/m^2 and 50.5±4.1 mJ/m^2, respectively. Longer surface activation does not affect significantly the surface free energy.

Air plasma treatment influences the surface properties of PA6G, which can be clearly seen in the changes of wettability and surface free energy. Plasma exposure leads to hydrophicility increase and contact angles decrease, the greater with the longer time of plasma activation. With the increase of modification time, the increasing surface free energy value was observed, mainly resulting from an increase in the polar nature interactions.

References:

[1] M. Collaud Coen, R. Lehmann, P. Groening, and L. Schlapbach, *Appl. Surf. Sci.*, **207** (2003) 276.

[2] C. Canal, R. Molina, E. Bertran, P. Erra, *J. Adhesion Sci. Technol.*, **18** (2004) 1077.

[3] K. Tsougeni, N. Vourdas, A. Tserepi, E. Gogolides, and C. Cardinaud, *Langmuir*, **25** (2009) 11748.

[4] H. Jung, B. Gweon, D.B. Kim and W. Choe, *Plasma Process. Polym.*, **8** (2011) 535.

[5] E. Chibowski, R. Carpio, A. Ontiveros-Ortega, *J. Adhesion Sci. Technol.*, **16** (2002) 1283.

[7] C.J. van Oss, R.J. Good, M.K. Chaudhury, *Langmuir*, **4** (1988) 884.

THERMAL ANALYSIS OF HYDROPHOBIC POLYMER/SILICA FILMS DEPOSITED ON GLASS SURFACE

Diana RYMUSZKA
DEPARTMENT OF INTERFACIAL PHENOMENA

Nowadays glass is a very common support used in everyday life and industry. Protecting optically transparent materials like glass extends their lifetime when exposed to atmospheric conditions (especially water). As a protective coating there can be applied a transparent superhydrophobic layer with the silanized silica which formed nano/micro structures [1]. Frequently covering of the surface by hydrophobic or superhydrophobic layers is not stable because of their poor adhesion to the substrate and because of that using plasma technique for surface modification is justified.

In the previous study the effect of polymer+modified silica film on the air plasma activated glass on its hydrophobic/superhydrophobic properties was studied. During plasma activation polar groups are introduced onto the glass surface which leads to adhesion improvement between the deposited layer and glass support. The layer, deposited by spreading on glass, was composed of PMMA and silica particles silanized at different surface coverages (ϑ from 0.53 to 1.0) with trimethylsilyl (TMS). Changes in the surface properties of glass/polymer+nanocomposite (silica/TMS) layers (wettability, surface free energy and structure) were investigated by the contact angle measurements and SEM images.

Further studies dealt with the thermogravimetric (TG) and derivative thermogravimetric (DTG) analyzed of the PMMA+silica/TMS powders, which were obtained after evaporating of the solvent from the dispersions used for coating of the activated glass. In Fig. 1 the TG and DTG curves obtained for PMMA+silica/TMS powders are presented.

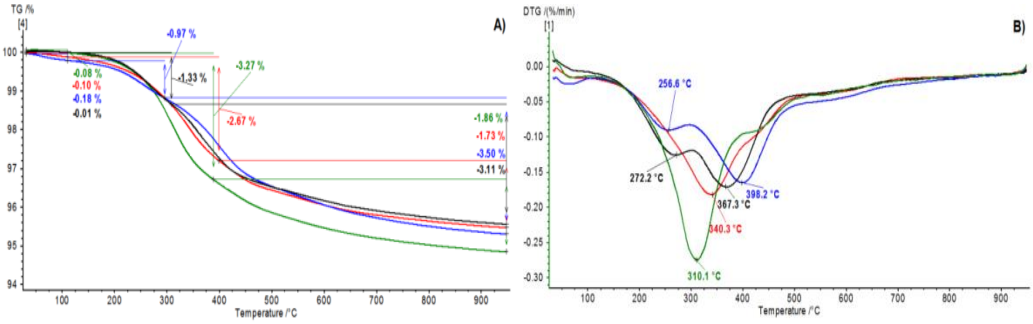

Fig. 1. TG (A) and DTG (B) curves for PMMA+silica/TMS powders at different surface coverages of silica particles: ϑ= 0.53 (green line), ϑ= 0.63 (red line), ϑ=0.86 (blue line), ϑ=1.00 (black line).

Analysis of the obtained curves in the range 30–900°C indicated two main stages of the thermooxidation: first, the weight loss below 100°C corresponds to removal of physically adsorbed water from hydrophobic nanoparticles and second, the exothermic peaks from 120 to 950°C are due to the decomposition of organic molecules. According to Yariv [1] and Landau *et al.* [2] oxidation of organic compounds in the range 200–900°C generally can be divided into three main stages: melting and dehydration (100–250°C), partial oxidation of the hydrogen atoms (250–400°C) and thermooxidation of hydrogen and nitrogen atoms and carbonized residue at 400–900°C. The TG curves (Fig. 1A) of PMMA+silica/TMS powdres revealed a major weight loss in the range of temperature 120 – 500°C which depends on silica surface properties, chemical composition and amounts of polymer and adsorbate-adsorbent interactions. The calculations indicated that this degradation step results in the weight loss of 4.11%, 3.42%, 3.23% and 3.46% for PMMA+silica/TMS$_{0.53}$ (ϑ=0.53), PMMA+silica/TMS$_{0.63}$, PMMA+silica/TMS$_{0.86}$ and PMMA+silica/TMS$_{1.00}$, respectively.

The DTG dependences (Fig. 1B) showed some differences. The degradation of PMMA+silica/TMS$_{0.53}$ and PMMA+silica/TMS$_{0.63}$ starts at 120°C and seems to proceed in a one-reaction stage according to the DTG curves (wide peaks with the minimum at 310°C for PMMA+silica/TMS$_{0.53}$ and 340°C for PMMA+silica/TMS$_{0.63}$. Similar changes were observed by Aymonier *et al.* [3] for the thermal decomposition of PMMA/palladium nanocomposites under air conditions.

It can be concluded that thermal stability decreases with the increasing amount of PMMA in the sample. On the other hand, increase in enthalpy of the reaction suggests that the process which, is predominant in thermal degradation, is polymer combustion.

References:

[1] D. Goswami, S.K. Medda, G. De, *ACS Appl. Mater. Interfaces,* **3** (2011) 3440.
[2] S. Yariv, *Appl. Clay Sci.* **24** (2004) 225.
[3] A. Landau, A. Zaban, I. Lapides and S. Yariv, *J. Therm. Anal. Calorim.,* **70** (2002) 103.
[4] C. Aymonier, D. Bortzmeyer, R. Thomann and R. Mülhaupt, *Chem. Mater.,* **15** (2003) 4874.

ADSORPTION AND AGGREGATION PROPERTIES OF SODIUM DODECYLSULFATE AND RHAMNOLIPID MIXTURE

Diana MAŃKO
DEPARTMENT OF INTERFACIAL PHENOMENA

Capacity of surfactants to adsorb at different interfaces and form micelles promote their application in both everyday life and numerous industries. However, in many practical applications mixtures of different kinds of surfactants are rather used than a single one [1] because appropriately chosen mixtures exhibit synergetic effects in the reduction of water surface tension and formation of mixed micelles.

Recently a special attention has been paid to biosurfactants. Biosurfactants are produced by microorganism. Although they exhibit high surface activity, low critical micelle concentration, high biodegradability [2] they are not frequently applied because of high cost of their production. It seems possible that the addition of even small amounts of biosurfactants to the classical surfactants greatly improves their properties. Thus the purpose of this study was to investigate aggregation and adsorption properties of the mixture of rhamnolipid (RL) which represents biosurfactants with anionic, synthetic sodium dodecyl sulfate (SDDS). This aim was achieved by measurements of surface tension, density and viscosity of aqueous solutions of RL and SDDS mixture.

From the obtained results it can be stated that the values of critical micelle concentration (CMC) of RL and SDDS mixture determined from the surface tension, density and viscosity isotherms are similar but differ from those calculated theoretically from the following equation:

$$\frac{1}{CMC_{12}} = \frac{1-\alpha}{CMC_{SDDS}} + \frac{\alpha}{CMC_{RL}} \tag{1}$$

where CMC_{SDDS} and CMC_{RL} are the CMC of individual surfactants, α is the RL mole fraction in the mixture in the bulk phase.

Such differences indicate that there is no ideal mixing of SDDS and RL in the mixed micelles. This fact was confirmed by the values of standard free energy of micellization (ΔG^{o}_{mic}). It follows from these calculations it results that between the obtained values of ΔG^{o}_{mic} and α there is no straight linear dependence. No ideal behaviour of the RL and SDDS mixtures was also proved by the Hua, Rosen and Rubingh [1] as well as Bergström and Eriksson [3] theories.

The reduction of water surface tension by surfactants is correlated with their adsorption at the water-air interface which can be expressed by the Gibbs surface excess concentration. These values for RL (Γ_{RL}) and SDDS (Γ_{SDDS}) can be determined from the Gibbs isotherm equation based on the surface tension isotherms. As can be seen from Fig. 1 the shape of the Γ_{SDDS} and Γ_{RL} isotherms is typical of classical surfactants and similar to those of individual RL and SDDS in the absence of another surfactant [4].

Fig. 1

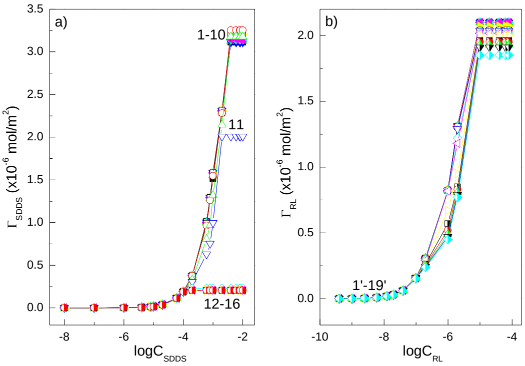

Fig. 1. A plot of the Gibbs surface excess concentration of SDDS (Γ_{SDDS}) and RL (Γ_{RL}) calculated from the Gibbs isotherm equation vs. the logarithm of a) SDDS (C_{SDDS}) and b) RL (C_{RL}) concentration.

The measure of surfactants tendency to adsorb at the water-air interface is the standard Gibbs free energy of adsorption (ΔG^0_{ads}). This energy is very often determined on the basis of the Langmuir equation modified by de Boer and thus this equation was applied in this study. It results from the obtained data it results that in the case when the concentration of one surfactant corresponds to its unsaturated monolayer in the absence of another, the values of ΔG^0_{ads} are constant. On this basis it can be stated that there are no interactions between the RL and SDDS molecules. It should be also noted that the obtained values of ΔG^0_{ads} of SDDS and RL mixture can not be predicted based on this value for individual SDDS and RL.

References:

[1] J.M. Rosen, *Surfactants and Interfacial Phenomena*, Wiley-Interscience, New York, 2004.
[2] Biosurfactants: Production: Properties: Applications (1993). In Kosaric N (ed.) Surfactant Science Series Vol 48. Marcel Dekker New York.
[3] M. Bergström, J. Ch. Eriksson, *Langmuir,* **16** (2000) 7173.
[4] D. Mańko, A. Zdziennicka, B. Jańczuk, *J. Surfactants Detergents*, DOI: 10.1007/s11743-016-1916-6.

ADSORPTION AND AGGREGATION PROPERTIES OF TRITON X-100 AND RHAMNOLIPID MIXTURE

Diana MAŃKO
DEPARTMENT OF INTERFACIAL PHENOMENA

Triton X-100 (TX-100) and rhamnolipid (RL) are very interesting surfactants because of their unique properties and wide practical applications. TX-100 is a typical representative of nonionic surfactants belonging to the alkyl polyethylene oxide family used to solubilize membrane phospholipids, DNA extraction and to purify membrane-bound proteins and enzymes without a loss of their biological activity [1-3]. It is applied in almost every type of liquid, paste, and powdered cleaning compound, ranging from heavy-duty industrial and agrochemical products to gentle detergents [4]. In turn, RL, which is a biosurfactant, is characterized by high surface activity, specificity of action, temperature stability and resistance to pH changes in the whole range. It undergoes biodegradation more readily and is less toxic. Owing to such properties biosurfactants are more and more widely applied in various fields of industry, among others, in cosmetic, agricultural, textile, cellulose and stationary ones. They are also exploited in crude oil mining as well as in remediation and detoxification of soil.

It is known that in practice the mixtures of different kinds of surfactants are more commonly used than individual ones. In many cases the mixtures of surfactants show the synergetic effect in the reduction of water surface tension and micelle formation. In the literature it is difficult to find the data dealing with the adsorption and aggregation properties of the RL mixed with another surfactant. A proper mixture of RL and synthetic surfactant can be interesting not only from the theoretical but also practical points of view. Therefore the purpose of our studies was to determine the adsorption and aggregation properties of TX-100 and RL mixtures. For this purpose in 2015 the surface tension, density and viscosity of aqueous solutions of this mixture at a constant concentration of RL or TX-100 were measured.

In 2016 we made the additional pH measurements of studied solutions. pH of all studied solutions was natural but controlled using a pHmeter Hanna Instuments (HI3220). The obtained results were used to improve our statement that hydrogen ions from the rhamnolipid molecules can be joined with the oxyethylene groups in the hydrophilic part of TX-100. The possibility of joining the oxyethylene group was confirmed by the increase of pH of the TX-100 and RL mixture compared to the individual RL at the same concentration as in the mixture.

Results of these studies were presented at national and international conferences and described in the paper entitled *Composition of surface layer at water-air interfaces and micelle of Triton X-100 and rhamnolipid mixture* that is presently in the reviewing process.

References:

[1] C. Tandford, J.A. Reynolds, Characterization of membrane proteins in detergent solutions, *Biochim. Biophys. Acta*, **457** (1976) 133.

[2] A. Levitzki, Reconstitution of membrane receptor systems, *Biochem. Biophys. Acta*, **822** (1985) 127.

[3] A.A. Ribeiro, E.A. Dennis, Motion in nonionic surfactant micelles and mixed micelles with phospholipids. A carbon-13 spin-lattice relaxation study on p-tert-octylphenylpolyoxyethylene ethers, *J. Phys. Chem.*, **80** (1976) 1746.

[4] J.M. Rosen, Surfactants and Interfacial Phenomena, 3rd edition, Wiley Interscience, New York 2004.

APPLICATION OF CHROMATOGRAPHIC METHODS IN EVALUATION OF ANTIOXIDANT PROPERTIES OF SUBSTANCES

Małgorzata OLSZOWY
DEPARTAMENT OF CHROMATOGRAPHIC METHODS

Generation of reactive oxygen species (ROS) and their negative influence on living organisms and on the stability of food products is the reason of a significant interest, especially over the last 25 years, in substances exhibiting antioxidant properties and in methods used for the estimation of such properties. In most methods used for estimation the antioxidant properties, the ability of antioxidants to neutralize free radicals is measured by monitoring only the depletion of colour radical [e.g. (2,2-diphenyl-1-picrylhydrazyl radical (DPPH) and 2,2-azinobis(3-ethylbenzothiazoline-6-sulphonic acid) cation radical ($ABTS^{\bullet +}$)] after defined incubation time (from several minutes to several hours, most frequently after one hour). As it is know from the literature [1, 2], the reaction of radical neutralization depends on many factor (e.g. metal ions content, hydrogen ions, solvent, time, the presence another antioxidant substances). The antioxidant activity of substances determined by measurements of the radical changes are not reliable and not reflect the “true” mechanism action of antioxidant during radical neutralization. The application of chromatographic measurements for the reaction products monitoring and depletion of “pure” antioxidants during/or after radical neutralization seems to be very useful for better understanding mechanism action of examined antioxidant or antioxidants mixture.

Phenolic compounds, which mainly come from plants (flavonoids, phenolic acids, stilbens, tocopherols, tocotrienols etc.), are the biggest group of exogenous antioxidants. Among them chlorogenic acid (CQA) is especially popular due to its potentially useful in pharmaceuticals, foodstuffs, food additives, and cosmetics due to its recently suggested biomedical activity. Hence, research interest in CQAs properties, including antioxidant properties has been growing.

The report presents the results of research work on the application of chromatographic measurements for the evaluation of antioxidant properties of CQA and for the determination of antioxidant changes and products of radical neutralization reaction: The measurements were carried out by ABTS method and by chromatography which allows to establish the changes of antioxidant and product reaction in the long period time (by 7 days), in differ reaction conditions and at various molar ratio of ABTS cation radical to CQA. The performed experiments shows that CQA is rebuilt after defined time.

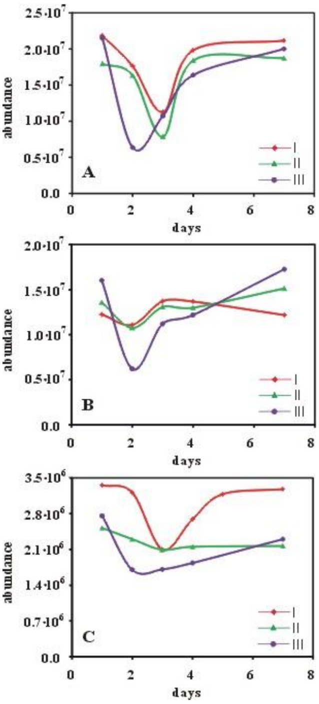

Fig. 1. The concentrations changes of CQA during 7 day reaction in measuring systems containing ABTS cation radical. Reaction enviroment: MeOH (I), aerated MeOH (II) and MeOH with Fe3+ (III). The experiments were performed using different molar ratio of ABTS$^{\bullet+}$ to CQA - 1:2 (A); 1:1 (B) and 2:1 (C).

The obtained results show that CQA, independence of measuring system, is rebuilt after 2-3 days. This process is depends on:

- reaction medium - the highest changes in CQA concentration are observed in system containing metal ions
- molar ratio ABTS$^{\bullet+}$ to CQA - the highest changes in CQA concentration are observed at greater amounts of CQA in measuring system (n ABTS$^{\bullet+}$ to n CQA equals 1:2)

The presented results are the preliminary study for experiments with another phenolic compounds and their mixture. In the future the obtained results will allow better understanding of antioxidant action in free radical neutralization process. The obtained results will be very importance for choosing the best combination of antioxidants which should be taken in consideration when designing functional foods.

References:

[1] A. L. Dawidowicz, D. Wianowska, M. Olszowy, *Food Chemistry*, **131** (2012) 1037.
[2] K. Mishra, H. Ojha, N. K. Chaudhury, *Food Chemistry*, **130** (2012) 1036.

SYNTHESIS AND CHARACTERIZATION OF SILICA MATERIALS SUSCEPTIBLE TO MAGNETIC FIELD

Karolina GDULA
DEPTARTMENT OF THEORETICAL CHEMISTRY

Nanotechnology offers broad opportunities in synthesis of various materials with enhanced properties. Amine-functionalized silica materials with magnetic cores have two main advantages: (1) presence of amine groups in the silica surface ensures adsorption sites for adsorbate molecules [1]; (2) magnetic cores built in the adsorbent structure allow to easily separate the adsorbent from the solution [2].

In this work, we present surface characterization of amine-functionalized magnetic nanoparticles. Herein, three different amine-functionalized polysiloxanes with magnetic core composed of Fe_3O_4 particles, were synthesized by using sol-gel method, based on hydrolysis and co-condensation of TEOS (as silica source) and amine-containing organosilane. Those three oragnosilanes were: (3-Aminopropyl)triethoxysilane (APTES), N-[3-(Trimethoxysilyl)propyl]ethylenediamine (TMPED) and Bis[3-(trimethoxysilyl)propyl]amine (BTMPA). The whole procedure is described in paper [3]. As-synthesized materials were labeled as follows: **A**, **T** and **B**, and characterized by several analytical techniques: nitrogen adsorption/desorption measurements, FT-IR spectroscopy, acid-base titration and XPS spectroscopy. Moreover, parameters characterizing electrical double layer (EDL) on the silica adsorbent/electrolyte solution interface, were also measured. Obtained pH_{IEP} (zeta potential measurements) and pH_{PZC} (surface charge density measurements) were different, when compared with those for pure Fe_3O_4 nanoparticles, playing role of the magnetic cores.

The values of specific surface area, were: 144, 176 and 29 m^2/g for **A**, **T** and **B**, respectively. Each of synthesized materials had characteristic peak at 3270-3370 cm^{-1} region, coming from $-NH_2$ stretching vibrations (FT-IR spectra). What is more, intense and broad absorption band, in the region 550-580 cm^{-1}, corresponds to ν(FeO), can be observed in all spectra (for pristine Fe_3O_4 nanoparticles and each polysiloxane). The amount of amine groups built in the structure of each adsorbent, obtained by acid-base titration measurements, were as follows: 1.83, 2.66 and 1.89 mmol/g for **A**, **T** and **B**, respectively. The XPS results have shown that the highest amount of nitrogen – coming from amine groups present in the material surface – had material **T** (5%), while material **A** and **B** had the same content (3.8%).

The density of surface charge and zeta potential measurements were carried out at the broad pH range, in order to determine pH_{PZC} and pH_{IEP} – parameters characterizing electrical double layer (EDL). It was found that zeta potential for material **A** overall investigated pH range is positive, unlike in the case of material **T** and **B**.

From the carried out researches it was proved, that the sol-gel method leads to obtain materials with high content of amine groups built into their surfaces (in the range 1.8-2.7 mmol/g). IR results, obtained from FT-IR spectroscopy, clearly show that the surface of the synthesized Fe_3O_4 particles is coated by silica layer with amine functional groups.

Thanks to their nanometer size and surface properties (especially, the presence of amine groups which can ensure the electrostatic interaction between surface of adsorbent and molecules of adsorbate), the obtained nanocomposites can be considered as promising adsorbents for metal ions and bioorganic compounds from water solutions.

References:

[1] T. Coradin, M. Boissiere, J. Livage, *Curr. Med. Chem.*, **13** (2006) 99.
[2] S. Singh, K.C. Barick, D. Bahadur, *J. Hazard. Mater.*, **192** (2011) 1539.
[3] I.V. Mel’nik, Yu.L. Zub, B. Alonso, N.V. Abramov, P.P. Gorbik, *Glass Phys. Chem.*, **38** (2012) 96.

THE SURFACE STATE OF COBALT-BASED CATALYSTS UNDER THE ETHANOL STEAM REFORMING CONDITIONS

Sylwia TURCZYNIAK
DEPARTMENT OF CHEMICAL TECHNOLOGY

Cobalt-based catalysts are one of the most extensively studied systems for ethanol steam reforming (ESR) [1]. Among various techniques applied for the characterization of this type of catalysts, the microscopic [2] and spectroscopic techniques; especially XPS [3, 4] should be listed. Indisputable advantage of the XPS spectroscopy is the possibility of the determination of the changes in the elemental composition of the surface layers (top 5 nm), oxidation states of an each catalyst's component, and the local bonding of atoms.

The aim of this study was to supplement so far obtained results, and to identify the oxygen-containing species presence on the surface of the fresh, reduced (H_2/Ar) and spent (EtOH/H_2O=12/1 mol/mol) Co/AO_2 catalyst.

The high resolution spectra of the O 1s region for active phase (A), support (B), and the catalyst (C) are presented in Fig. 1. The most intense signal (O_{latt}; Fig. 1 A-C) on the binding energy scale (530.0±0.2 eV) is related to oxygen from Co_3O_4 and AO_2 lattice. The O_{latt}/Co and O_{latt}/A atomic ratio, calculated on the base of the spectra, was equal 1.6 and 1.9 respectively, giving the value close to the expected one. The component **a** (531.5±0.2 eV) is usually assigned to the presence of the surface adsorbed hydroxyl and/or carbonate species. However, the calculations based on the spectra of C 1s region showed that not the **a** but **b** component is a result of the presence of carbonates (O/C $\approx$ 3). After the reduction, three new components (**c-e**) appear in the A and C spectra: 530.9, 532.0, 533.1 eV. The component **c** is most likely related to the defect in the lattice of cobalt oxide CoO_x, whereas the component **d** can be assigned to the presence of the residual oxygen atoms and hydroxide species (Co(0)-OH and CoO-OH). The last component (**e**) is commonly assigned to the presence of physically adsorbed water and/or organic species.

The comparison of the spectra of the pure active phase, support and the catalyst, led to the conclusion that in the case of the catalyst, the components located at higher binding energy than 530.0 eV (in the O 1s spectra) are related to the cobalt phase.

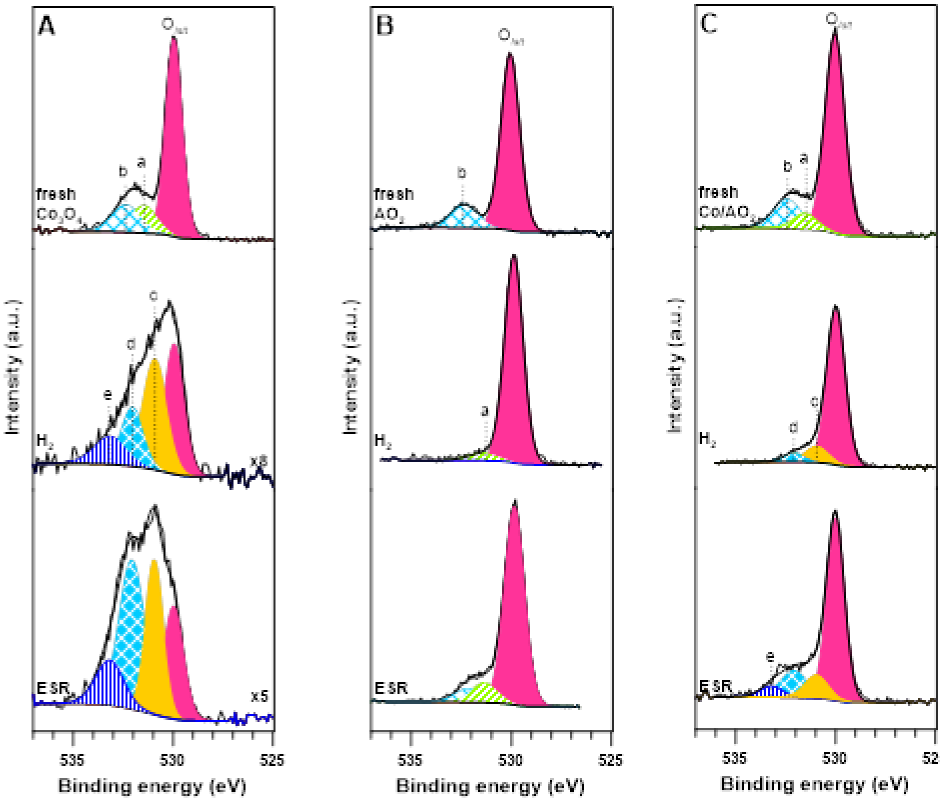

Fig. 1. The high resolution spectra of cobalt active phase (A), support (B), and cobalt-based catalyst (C).

Reference:

[1] G. Słowik, A. Gawryszuk-Rżysko, M. Greluk, A. Machocki, *Catal Lett*, **146** (2016) 2173.

[2] G. Słowik, M. Greluk, A. Machocki, *Mater. Chem. Phys.*, **173** (2016) 219.

[3] I.I. Soykal, H. Song, U.S. Ozkan, *ACS Catal.*, **2** (2012) 2335.

[4] H. Sohn, U.S. Ozkan, *Energy Fuel*, **30** (2016) 5309.

PREPARATION AND CHARACTERIZATION OF PROMOTED COBALT-BASED CATALYSTS FOR ETHANOL STEAM REFORMING

Sylwia TURCZYNIAK
DEPARTMENT OF CHEMICAL TECHNOLOGY

This study was carried out in order to determine the influence of the impregnation order on physico-chemical properties of oxide-supported (AO_2) cobalt-based catalysts, promoted with the compound further abbreviated as M.

Fig. 1 presents the scheme of the catalysts preparation. The catalysts were obtained by the impregnation of the support with water solution of cobalt(II) nitrate hexahydrate or metal (M) nitrate (M/AO_2). After the drying and calcination, the catalysts precursors were once again promoted with metal nitrate ($M/Co/AO_2$) or cobalt(II) nitrate hexahydrate ($Co/M/AO_2$). The catalysts were dried and calcined.

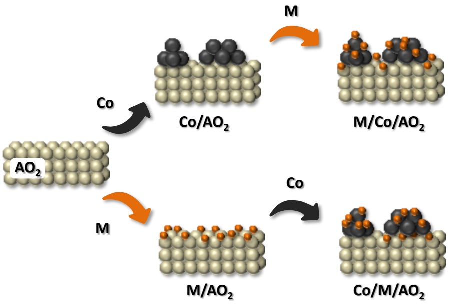

Fig. 1. The scheme of the catalysts preparation.

Table 1 shows that the cobalt loading (9 wt.%) was very similar for both catalysts. On the basis of the XRD it was confirmed that cobalt phase occurs in the form of spinel (Co_3O_4). Studies showed that the catalysts differ only slightly in terms of the physico-chemical properties (Table 1).

Table 1. The catalysts characterization.

Catalyst	**Total surface area, m^2/g[a]**	**Pores volume cm^2/g[a]**	**Pores diameter, nm[a]**	**Cobalt wt. content, %[b]**	**Cobalt dispersion, %[c]**	**Cobalt crystallites size, nm[c]**	**Cobalt surface area, m^2/g sample[c]**	**Cobalt surface area, m^2/g metal[c]**
$M/Co/AO_2$	27.72	0.13	15.12	8.75±0.26	2.59	38.53	1.53	17.49
$Co/M/AO_2$	30.40	0.13	14.11	8.95±0.27	2.76	36.09	1.67	18.68

[a] On the basis of nitrogen adsorption, [b] On the basis of XRF, [c] On the basis of hydrogen chemisorption.

To determine the influence of the impregnation order on the reducibility of both catalytic systems, the temperature-programmed reduction studies (TPR) were performed. The first, very intense maximum on the TPR profiles (Fig. 2) is related to the gradual reduction of cobalt spinel phase: $Co_3O_4 \rightarrow CoO$ (247°C). In the temperatures range of 300−450°C the reduction of cobalt(II) oxide to metallic phase occurs ($CoO \rightarrow Co^0$) [1]. Above 600°C proceeds the reduction of the support surface. A slight asymmetry of the $Co/M/AO_2$ TPR profile towards higher temperatures might be an evidence of a weakness of the metal-support interaction. Very similar shape of the TPR profiles can suggest that the significant amount of the M-compound migrated onto cobalt crystallites as a result of calcination. In order to confirm this suggestion, microscopic studies should be performed.

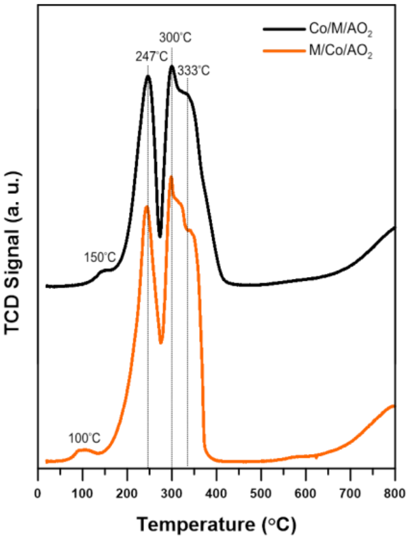

Fig. 2. TPR profiles obtained for Co/M/AO$_2$ and M/Co/AO$_2$.

Basing on so far obtained results, it was stated that the order of the support's impregnation with cobalt and metal M salts only slightly influences physico-chemical properties of the catalytic system. In the further stage of this project the studies of the surface state (by means of the X-ray Photoelectron Spectroscopy) and catalytic performance under the ethanol steam reforming over the pre-reduced samples will be performed.

Reference:
[1] S. Tuti, F. Pepe, *Catal. Lett.*, **122** (2008) 196.

SELECTIVITY AND ACTIVITY STUDY OF SUPPORTED COBALT-NICKEL CATALYSTS IN THE STEAM REFORMING OF ETHANOL

Grzegorz SŁOWIK
DEPARTMENT OF CHEMICAL TECHNOLOGY

Shortage of fossil fuel in the near future will cause serious energy problems. Therefore, there is a growing interest in energy production from renewable sources. Today, as a fuel of the future hydrogen is mostly considered. Hydrogen is a clean energy source that does not emit CO_2 or NOx, and its demand as a fuel for fuel cells is increasing. The steam reforming of ethanol (SRE) $C_2H_5OH + 3H_2O \rightarrow 6H_2 + 2CO_2$ is a very effective way of hydrogen obtaining from easy to transport and storage liquids. Ethanol can be produced from renewable raw materials (e.g. biomass). The catalyst plays an important role in achieving complete and selective ethanol conversion in the SRE. Depending on the catalyst nature, the method of its preparing and the SRE reaction conditions, conversion of ethanol and hydrogen production are significantly different. In contrast to the highly active catalytic systems of noble metals proposed for the SRE, supported nickel and cobalt catalysts are less costly alternative. For these reasons, they are often proposed for many reactions, including those whose the goal is production of hydrogen (e.g. for the steam reforming of ethanol).

The aim of the studies was determination of the relationship between conversion of reactants and selectivity of the steam reforming of ethanol process and its temperature and determination of the stability of potassium promoted cobalt and nickel catalytic systems in the steam reforming of ethanol by testing under isothermal (420°C) conditions.

The catalysts containing 10% nickel and 10% cobalt and promoted with potassium were prepared by two-step impregnation of the CeO_2 support. Before testing of the selectivity and activity, catalysts were reduced with hydrogen directly in the reactor at 400°C. The activated nanomaterials were used in the steam reforming of ethanol (the ratio of reactants was 12 mole of water/1 mole of ethanol) to obtain hydrogen.

Studies show that at the initial phase of testing both of catalysts provides 100% conversion of ethanol (Fig. 1) but after 24 hours of work in the steam reforming of ethanol only the catalyst with nickel active phase provide 100% conversion of ethanol (Fig. 2). Both of catalysts showed high selectivity for hydrogen. The nickel catalyst were more selective to methane than cobalt catalyst. Significant amounts of acetaldehyde and acetone were formed on the catalyst with cobalt active phase. Acetaldehyde and acetone produced on the KCo/CeO_2 catalyst during the steam reforming of ethanol belongs to a main carbon deposit precursors contribute to the production of amorphous carbon which can block active sites and cause catalyst deactivation. The most stable system was proved to be the catalyst containing 10% of nickel. The hydrogen yield over that catalyst not changed during 24 hours of the steam reforming of ethanol.

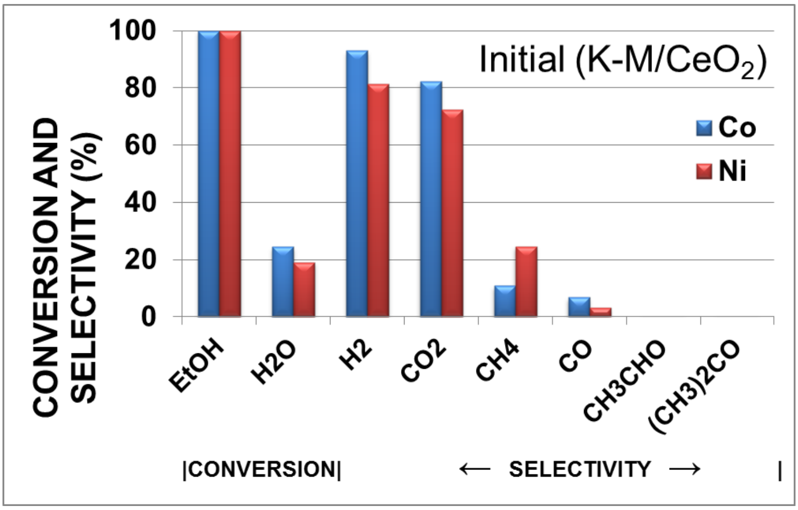

Fig. 1. Initial EtOH and H_2O conversions and selectivity in the steam reforming of ethanol on potassium promoted cobalt and nickel catalysts.

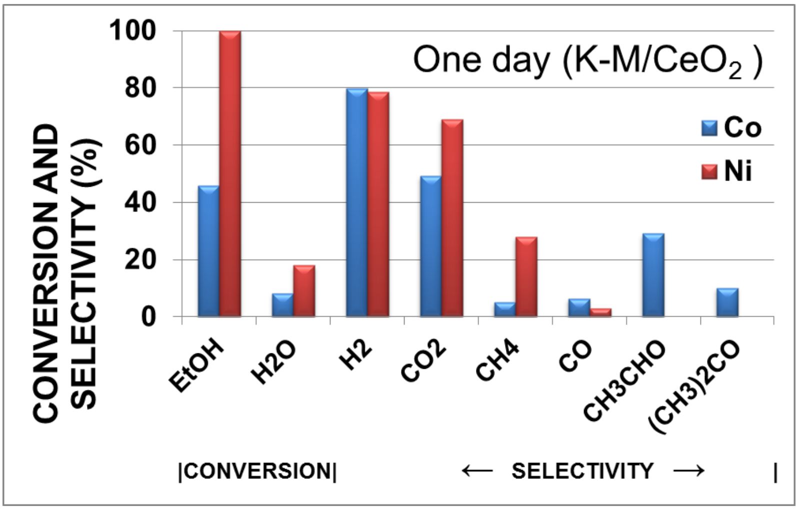

Fig. 2. Conversions of EtOH and H_2O and selectivity in the steam reforming of ethanol after one day on potassium promoted cobalt and nickel catalysts.

OPTIMIZATION OF CHEMISORPTION ON THE CATALYSTS FOR STEAM REFORMING OF ETHANOL

Grzegorz SŁOWIK
DEPARTMENT OF CHEMICAL TECHNOLOGY

Heterogeneous catalysts through their irreplaceable role in chemicals and fuels production constitute a high interest research topic. In the steam reforming of ethanol (SRE) besides operating conditions, the use of suitable catalyst plays a crucial role in achieving selective, efficient and economically profitable process. The commonly used in the SRE heterogeneous catalysts are cobalt-based ones, usually highly dispersed on inorganic oxide supports, which show a high activity and stability, relatively low cost and a high selectivity for the most desirable reaction products. Among supports of the active phase, cerium oxide was used very often in various catalytic systems.

The catalytic properties of catalysts depend on their key parameters, such as crystallites size, structure and morphology. Dispersion of the metallic active phase is one of the most important parameters characterizing the heterogeneous catalysts, which are essential for the activity, selectivity and stability of catalytic processes. The catalytic activity of a supported catalysts depends on the degree of dispersion of the metallic active phase and its active surface area, and it usually increases with increasing dispersion of metal. The crystallites size of metallic active phase are usually determined by hydrogen chemisorption, X-ray diffraction (XRD) or TEM (Transmission Electron Microscopy), but sometimes different results are found from various methods for the same catalyst. The differences in measurements of the crystallites size can result from methods limitation.

The evaluation of dispersion of the active phase, on the basis of hydrogen chemisorption data is a common, simple and cheap method. However, literature show that temperature of hydrogen chemisorption measurements can significantly influence on obtained results.

From three methods (H_2 chemisorption, TEM and XRD) used for crystallites size determination, only TEM shows distinct advantages for the direct measurement of crystallites size in comparison with other methods, because the metal active phase crystallites can be quite clearly distinguished from the catalyst support and directly measured [1].

The aim of studies provided in the project is (i) determination, on the basis of the results obtained with different methods (H_2 chemisorption, TEM and XRD), the optimum temperature H_2 chemisorption and evaluation of the proper use of data for the total or strong chemisorption to determine the average crystallite size of cobalt active phase, which should be consistent with the results of microscopic examination. An additional objective is also to (ii) determine the effect of addition of the potassium promoter to the Co catalyst on the optimum temperature of H_2 chemisorption, appropriate to determine the average crystallite size of the active phase.

Cobalt catalysts with CeO_2 support, unpromoted and promoted with potassium were prepared by an impregnation method. Reduced catalysts were subjected to hydrogen chemisorption at different temperatures in the range of 313-453 K. Studies have shown that calculated Co crystallites size depends on the temperature of chemisorption. Comparison of the average size of the cobalt-based crystallites measured by TEM, H_2 chemisorption and XRD methods proved that the good agreement between values obtained from total chemisorption and TEM data is possible (Fig. 1 and Table 1). The total hydrogen uptake on the potassium-free catalyst, measured at 383 K, leads to the estimation of the size of crystallites compatible with the values measured by the most objective, microscopic method. When potassium is present in the catalyst, the optimum of hydrogen chemisorption temperature is higher by c.a. 30 K, i.e. 413 K.

The average size of cobalt-based crystallites estimated from XRD data is congruous with that measured by the TEM method only in the case when among crystallites there are no very small ones [1].

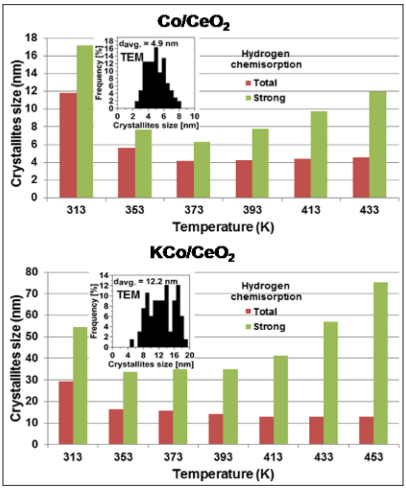

Fig. 1. TEM and hydrogen chemisorption measurements of cobalt crystallites size.

Table 1 Comparison of the average size of crystallites determined by TEM, XRD and hydrogen chemisorption for reduced (at 673 K) Co/CeO_2 and KCo/CeO_2 catalysts.

Catalyst	**TEM [nm]**	**XRD [nm]**	**Hydrogen chemisorption [nm]**
	reduced	**reduced**	
Co/CeO_2	4.9 ± 0.3	7.8 ± 0.4	4.1 ± 0.3*
KCo/CeO_2	12.2 ± 0.7	15.2 ± 0.8	12.5 ± 0.3**

Measured at *383K/ **413K

References:

[1] G. Słowik, A. Gawryszuk-Rżysko, M. Greluk and A. Machocki, *Mater. Chem. Phys.*, **146** (2016) 2173.

STUDY OF THE MECHANISM OF OXIDATION OF SOOT FROM DIESEL EXHAUST GASES ON THE SURFACE OF THE COBALT CATALYST WITH USE OF STABLE ISOTOPES OF OXYGEN

Marek ROTKO
DEPARTMENT OF CHEMICAL TECHNOLOGY

The removing (oxidation) of soot from diesel exhaust gases is a very important issue due to the negative impact of this type of pollution on human health and climate of our planet. Diesel soot is carcinogenic [1] and contributes to the greenhouse effect [2]. Therefore, many countries have introduced limits on the emission of soot and still are exacerbated. In order to decrease the content of soot in the engine exhaust, a diesel particulate filter (DPF) is widely mounted in vehicles. For the proper functioning of such filters, a regeneration step is required. One of the most promising ways of the diesel particulate filter regeneration is employed of catalytic substances, which permit to remove (oxidize) soot in the exhaust gas temperature. For this purpose, catalysts, which demonstrate high activity and selectivity to carbon dioxide and high resistance to operating conditions, are proposed. One of them is Co_3O_4 [3], whose catalytic properties are connected with the mobility of oxygen on the surface and in the bulk. Therefore, the main aim of this study was the analysis of these properties with use of stable isotopes of oxygen ($^{16}O_2$ and $^{18}O_2$).

The cobalt catalyst was prepared from an aqueous solution of cobalt acetate by the precipitation method. The catalyst precursor was calcined at 400^{o}C by 2 h. Its basic physicochemical parameters were determined by the N_2 adsorption/desorption experiment and X-ray diffraction spectroscopy (Table 1). The activity of the cobalt catalyst was measured in the “tight contact” using model soot (Printex U) and the reaction mixture containing 10 vol.% of O_2 and inert gases (argon and helium). The studies were conducted in a quartz reactor filled with 50 mg of the catalyst-soot mixture (45 mg of catalyst and 5 mg of soot) and 450 mg of finely ground quartz. The effects of soot oxidation were analysed by a mass spectrometer. Moreover, the temperature-programmed exchange experiment was performed from 150^{o}C to 550^{o}C with the ramp rate – 10^{o}C/min. During this experiment, the mixture containing 5 vol% of $^{18}O_2$ and inert gases (helium and krypton) was dosed into the reactor with the catalyst bed.

Table 1. The basic physicochemical parameters determined for the cobalt catalyst.

Total BET surface area (m^2/g)	Mean pore size [nm]	Total pore volume (cm^3/g)	Content of Co_3O_4 (%)	Mean size of crystallites (nm)
44.5	19.71	0.222	100	20

The process of soot oxidation on the cobalt catalyst begins at about 285°C, and the maximum rate is observed at about 395°C, whilst the process of oxidation of soot without employing a catalyst needs much higher temperature (Fig. 1).

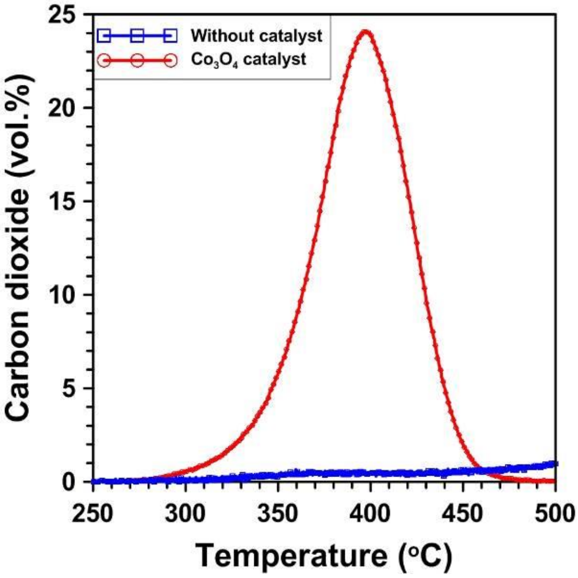

Fig. 1. Concentration of CO_2 in the post-reaction mixture during soot oxidation.

The process of oxygen exchange between the gas phase and the catalyst lattice begins at about 180°C, but its rate is low until to 400°C (Fig. 2). After exceeding 400°C, the fast increase of $^{16}O^{18}O$ concentration is observed. The process of oxygen exchange begins much earlier (180°C) than soot oxidation (285°C), but when the temperature exceeds 290°C the process of oxygen exchange accelerates.

Further studies will be conducted in 2017.

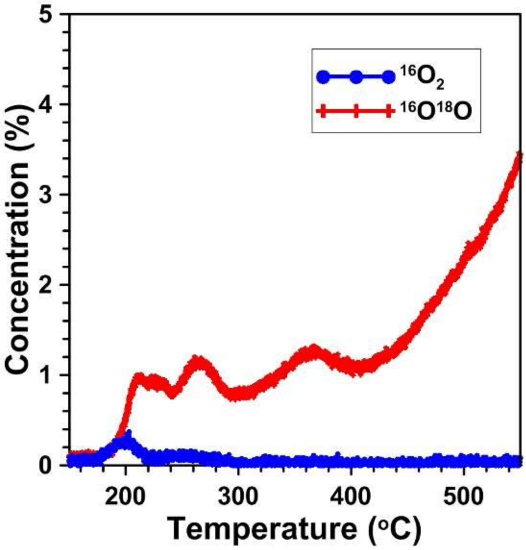

Fig. 2. Effects of temperature-programmed exchange experiment with use of $^{18}O_2$.

References:

[1] M. Knaapen, P.J.A. Borm, C. Albrecht, R.P.F. Schins, Inhaled particles and lung cancer, *Internat. J. Cancer*, **109** (2004) 799.

[2] M.Z. Jacobsen, Strong radiative heating duo to the mixing state of black carbon in atmospheric aerosol, *Nature*, **409** (2001) 695.

[3] G. Mul, F. Kapteijn, C. Doornkamp, J. A. Moulijn, Transition metal oxide catalyzed carbon black oxidation: a study with $^{18}O_2$, *J. Catal.*, **179** (1998) 258.

PREPARATION AND CATALYTIC CHARACTERISTICS OF ACTIVE NANOMATERIALS FOR STEAM REFORMING OF ETHANOL

Magdalena Greluk
DEPARTMENT OF CHEMICAL TECHNOLOGY

The electrochemical conversion of hydrogen to power via polymer electrolyte membrane (PEM) fuel cell technology may alleviate global dependence on fossil fuels, as well as decrease emissions of greenhouse gases and other atmospheric pollutants. Among the available resources, bioethanol is one of the most attractive options, as it is easily produced via well advanced technique of fermentation of biomass or agricultural waste products. Additionally, it is non-toxic, easy to store and transport, and has the advantage of offering a nearly closed carbon loop as the carbon dioxide produced during its conversion may be consumed during biomass growth [1, 2].

Obviously, the catalysts play a crucial role in the reactivity toward complete conversion of ethanol. However, various catalysts induce different reaction pathways and, therefore, the selection of a suitable catalyst plays a vital role in the ethanol conversion for H_2 production. An active catalyst should maximize hydrogen selectivity and productivity and inhibit coke formation as well as CO production. Accordingly, non-expensive active metals and supports with non-acid character of their surface are considered the best option. Among several studied metallic active phases, cobalt based catalysts have been widely investigated due to their low cost, low working temperature, low generation of by-products and smaller C–C bond cleavage ability than those indicated by noble metal or nickel-based catalysts.

The aim of this work was to study the catalytic properties of the supported cobalt catalyst under steam reforming of ethanol conditions.

The reaction of ethanol conversion with water was carried out under atmospheric pressure in a fixed-bed continuous-flow quartz reactor over the catalyst (0.1 g; 0.15-0.3 mm) reduced in situ with hydrogen at 400°C for 1 hour, prior to the reaction. The aqueous solution of ethanol (H_2O/ethanol=12/1) was supplied to an evaporator (150°C) and the reactant vapours, without diluting with any inert gas, and were fed to the reactor at a flow rate of 100 mL×min-1. The catalytic performance was tested in the temperature range of 390-480°C. The analysis of the reaction mixture and the reaction products (all in gas phase) were carried out on-line by means of two gas chromatographs. One of them, Bruker 450-GC was equipped with two columns, the first filled with a porous polymer Poropak Q (for all organics, CO_2 and H_2O vapor) and the other one—capilary column CP-Molsieve 5 Å (for CH4 and CO analysis). Hellium was used as a carrier gas and a TCD detector was employed. The hydrogen concentration was analyzed by the second gas chromatograph, Bruker 430-GC, using a Molsieve 5 Å, argon as a carrier gas and a TCD detector.

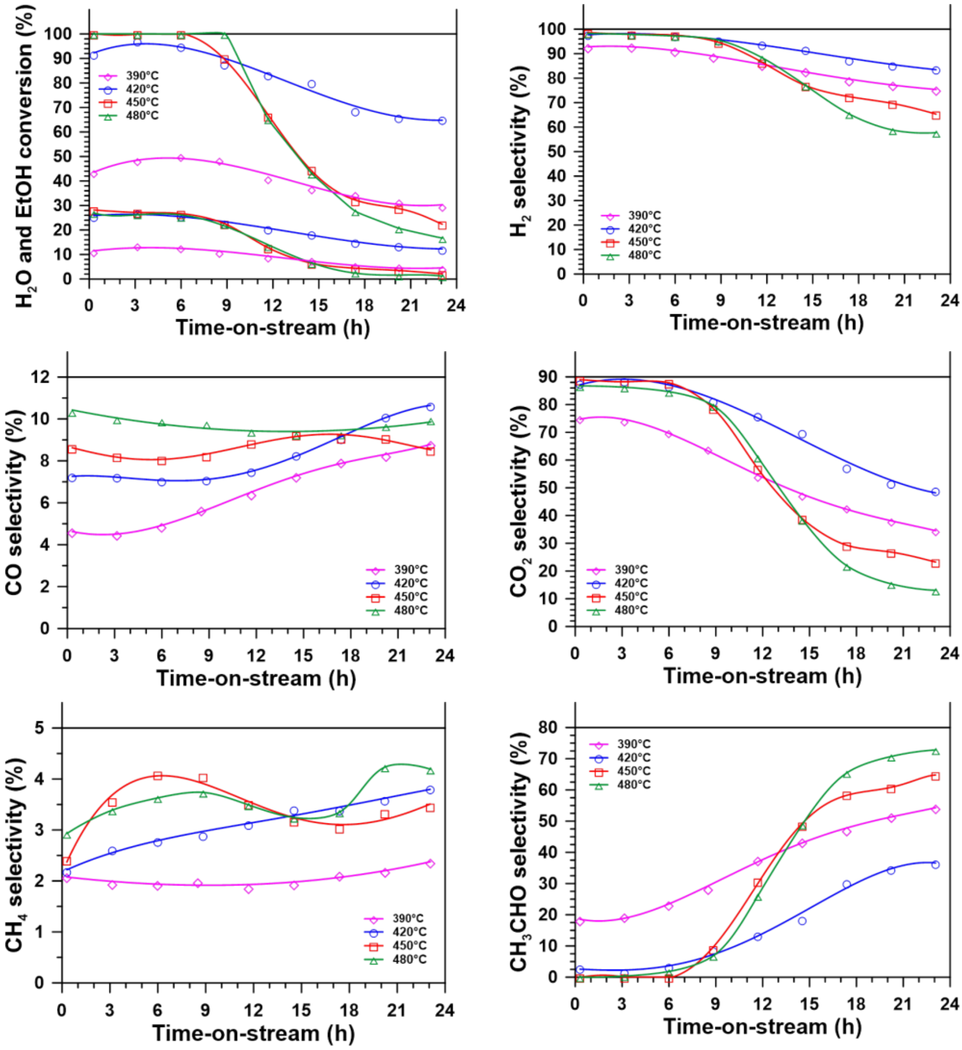

Fig. 1. Effect of the reaction temperature on ethanol and water conversion and selectivity to products over A catalyst under SRE conditions.

Steam reforming of ethanol (EtOH/H2O =1/12) over 2 catalyst showed that the temperature of 420°C was the most advantageous for this process. The catalyst indicated the high SRE process selectivity to two most desirable products of reaction, hydrogen and carbon dioxide and amounts of carbon monoxide, methane and acetaldehyde formed in side reactions were much smaller.

References:

[1] S. M. De Lima, I. O. Da Cruz, G. Jacobs, B. H. Davis, L. V. Matos, F. B. Noronha, *J. Catal*., **257** (2008) 356-368.

[2] N. Srisiriwat, S. Therdthianwong, A. Therdthianwong, *Int J.Hydrog Energy*, **34** (2009) 2224-2234.

SYNTHESIS AND EXAMINATION OF PROPERTIES OF BIMETALLIC CATALYST FOR METHANOL STEAM REFORMING

Justyna PAWLONKA
DEPARTMENT OF CHEMICAL TECHNOLOGY

Growing demand for energy has forced development of fuel cell technology and thereby increased interest in the process of hydrogen production by the steam reforming of methanol. In order to improve the efficiency of the process new catalysts are designed and examined. Hence it is known that the structural and surface properties of support, crystallite size, and dispersion of the active phase significantly affect the activity and selectivity of the catalysts. For this reaction bimetallic palladium-zinc catalyst seems to be promising. Moreover the synthesis of bimetallic alloy could be easily performed in reverse micelles – specific nanoreactors. Thanks to this method it is possible to obtain catalyst with controlled crystallite size and high dispersion which is one of the major challenges. It could be achieved by simple adjustment of the amount particular microemulsion components and synthesis conditions. The aim of the studies was to determine the influence of synthesis conditions on the surface and structural properties of bimetallic palladium-zinc catalysts.

Palladium supported zinc oxide catalysts were prepared by microemulsion method. Microemulsion consisted out of cyclohexane, isopropanol, aqueous solution of metal salts and Triton-X-100 as surfactant. The catalysts were synthesized by hydrazine reduction method of palladium and palladium-zinc ionic species within reversed micelles, respectively. The obtained nanoparticles were next deposited on commercial zinc oxide support. The properties of the catalysts were investigated by X-ray fluorescence (XRF), X-Ray diffraction (XRD) and low-temperature nitrogen adsorption methods (ASAP). Catalysts prior to the catalytic tests in the steam reforming of methanol were reduced *in situ* with H_2 at 350°C for 1 h.

Physicochemical properties of two catalysts are presented in the Table 1. In spite of the use of the same support, Pd/ZnO-A has characterised with higher specific surface area and simultaneously lower average pore diameter than PdZn/ZnO-B catalyst.

Table 1. Physicochemical properties of catalysts.

Catalyst	**S_{BET} (m^2/g)**	**Average pore diameter (nm)**	**Palladium content (wt.%)**	**PdZn average crystallite size (nm)**	**Pd average crystallite size (nm)**
Pd/ZnO-A	8.9	14.3	4.36	31.1	34.1
PdZn/ZnO-B	6.9	24.3	4.42	45.2	-

XRD studies showed that palladium-zinc alloy phase was present in Pd/ZnO-A and PdZn/ZnO-B catalysts, but Pd/ZnO-A has additional monometallic palladium phase. Although Pd/ZnO-A exhibited smaller PdZn alloy crystallite size than PdZn/ZnO-B, the size of crystallites was relatively large and both catalysts showed low active surface area. This resulted in the low activity of catalysts in methanol steam reforming reaction. Conversion of methanol for both catalysts did not exceed 25 % even at the temperature of 420°C. It was observed that PdZn/ZnO-B catalysts showed higher activity and lower selectivity to carbon monoxide than Pd/ZnO-A catalysts. This indicate that simultaneous reduction of ionic species in reversed micelles can be beneficial. However further studies of palladium-zinc microemulsion systems are necessary to improve the performance of catalysts.

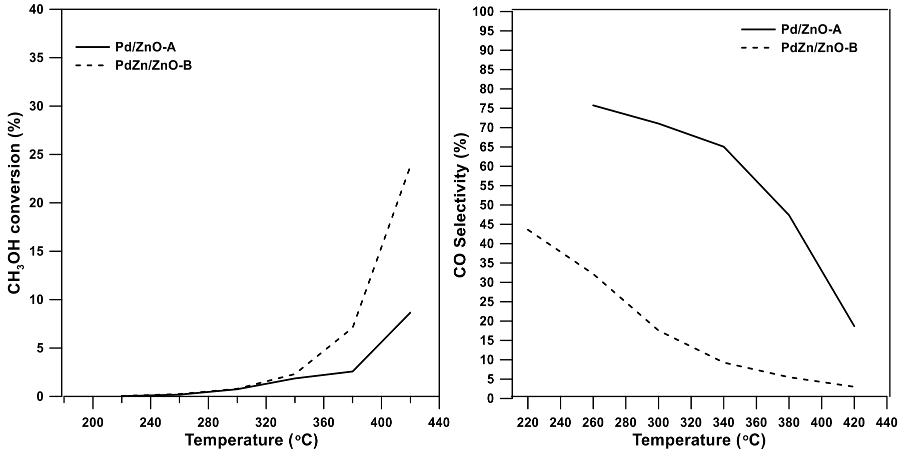

Fig. 1. Activity and selectivity of the catalysts in methanol steam reforming reaction (H_2O/CH_3OH = 1.5 mol/mol).

PHOTOCATALYTIC DEGRADATION OF TRICLOSAN, CHLORAMPHENICOL AND DICLOPHENAC USING Ti/SBA-15 PHOTOCATALYSTS

Tomasz OLEJNIK
DEPARTMENT OF CHEMICAL TECHNOLOGY

Ordered SBA-15 mesoporous silica supports have been synthesized and used for incorporation of titanium with different Ti/Si weight ratio via incipient wetness impregnation. Titanium tetraisopropoxide (TTIP) was used as a source of Ti.

Obtained catalysts were characterized to investigate the chemical framework and morphology by nitrogen sorption measurements, powder X-ray diffraction (XRD), X-ray fluorescence elemental analysis (XRF), transmission electron microscopy (TEM), UV-VIS diffuse reflectance spectroscopy (UV-VIS DRS) and Fourier transform photoacoustic infrared spectroscopy (FT-IR/PAS).

The photocatalytic degradation of phenol and methylene blue water solutions were selected as a probe reactions to test the photoactivity of prepared samples and to verify the potential application of these materials for water purification. Ordered mesoporous SBA-15 type with textural porosity has a major effect on the structural properties and photocatalytic activity.

The results demonstrate that the order of the SBA-15 framework was maintained upon impregnation by titanium tetraisopropoxide. The increase of titanium amount led to decrease of the surface area and random dispersion of titanium nanoparticles inside the channels of SBA-15 thus narrowing parts of the SBA-15 mesopores.

The results of photodegradation activity indicate the influence of TiO_2 content on the photocatalytic activity of the TiO_2/SBA-15 materials. Ti-Si mesoporous materials exhibit potential application in the photodegradation of toxic pollutants in environment.

THE PHYSICO-CHEMICAL PROPERTY STUDIES OF MOLECULAR MAGNETS OF d- AND f- TRANSITION METAL IONS WITH ISATIN

Dariusz OSYPIUK
DEPARTMENT OF GENERAL AND COORDINATION CHEMISTRY

Isatin with formula presented in Fig. 1a is a substrate, which can be used for synthesis of a large variety of heterocyclic compounds, such as indoles and a raw material for drug synthesis. Due to its “stiff” molecule structure, isatin doesn’t easily coordinate with metal ions. In order to induce the process of transition metal bindings, the amino acids may be joined to it. Isatin connected with amino acids is a typical carbon-nitrogen double bond compound with anti-malarial, anticancer, antibacterial and antimicrobial activities. The transition metal ions also show interesting biochemical properties thus they may be useful in many areas of modern medicine. The studies of the structure and the physico-chemical properties of isatin compounds with various metal ions are interesting because of their applications. Therefore it was decided to synthesize some of isatin with 2-aminobutric and glutamic acids (L_1 and L_2 ligands, respectively) complexes with Mn(II), Co(II), Ni(II), Cu(II), Zn(II) and to study their magnetic properties at 77–300 K and 2–300 K, thermal stability in air (TG/DSC method), to record their FT-IR, TG-FTIR and X-ray spectra and to try to determine their structures.

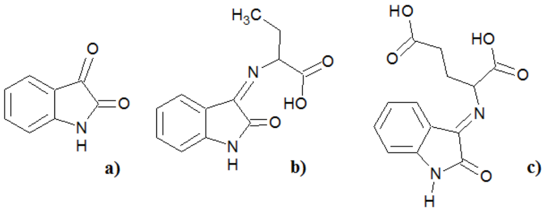

Fig. 1. The formulae of **a)** isatin, **b)** L_1 and **c)** L_2 ligands .

The ligands were synthesized by refluxing isatin (0.01 M, 1.47 g) with 2-aminobutric acid (L_1) (0.01 M, 1.03 g) and glutamic acid (L_2) (0.01 M, 1.47 g) in 50ml of methanol and water for 2-3 hours in the presence of two-three drops of glacial acetic acid (Fig. 1b, 1c). Synthesis of metal complexes was carried out in methanol. Alcoholic solutions (50ml) of metal salts ($MnCl_2 \cdot 4H_2O$, $CoCl_2 \cdot 6H_2O$, $NiCl_2 \cdot 6H_2O$, $CuCl_2 \cdot 2H_2O$ and $ZnCl_2$) were mixed with warm alcoholic solution (50ml) of L_1 and L_2 ligands in ratio of 1:2 for L_1 and 1:1 for L_2. The pH of reaction mixture was adjusted to 7 by adding ammonia. Resulting reaction mixtures were refluxed for 5 to 6 hours. Next they were filtered off, washed with methanol and dried at 303 K.

The new complexes of L_1 and L_2 with Mn(II), Co(II), Ni(II), Cu(II) and Zn(II) crystallize as solids in monoclinic or triclinic systems. They have general formulae: $M(L_1)_2 \cdot H_2O$ for Mn(II) and Zn(II) and $ML_1Cl \cdot nH_2O$ for Co(II), Ni(II) and Cu(II) (where n=1 for Ni(II) and Cu(II) and n=2 for Co(II)) and $M(L_2)_2 \cdot nH_2O$ for Mn(II), Ni(II) and Zn(II) (where n=1 for Zn(II), n=3 for Ni(II) and n=4 for Mn(II) and $ML_2 \cdot nH_2O$ for Co(II) and Cu(II) (where n=1 for Cu(II) and n=2 for Co(II)). The compounds were investigated by elemental analysis, FTIR spectroscopy, magnetic and thermogravimetric TG-DSC, TG-FTIR studies and also by X-ray powder diffraction (XRD) measurements.

The FTIR spectra for analysed compounds were recorded. The bands in these spectra with the maxima at 3480–3372 cm^{-1} for L_1 and at 3440–3332 cm^{-1} for L_2 characteristic for ν(OH) vibrations confirm the presence of crystallization water molecules in complexes. The stretching vibration bands of ν(C=O) at 1688cm^{-1} in L_1 and L_2 ligand spectra are shifted to 1664 – 1708 cm^{-1} and 1692 – 1712 cm^{-1} respectively, in their FTIR spectra. The spectra bands at 580 – 672 cm^{-1} for L_1 and 580 – 680 cm^{-1} for L_2 indicate the ionic metal – oxygen stretching bond vibrations respectively and those at 460 – 496 and 416 – 488 cm^{-1} of their ionic metal – nitrogen ones. The analysis of the IR spectra of the ligands and its complexes shows that the complexation process occurred. From the obtained data it appears that the compounds may have the various structure and different physico-chemical properties.

Heated to 1173 K the complexes are stable up to 310 – 414 K. Their dehydration processes are connected with endothermic effects (DSC curves). The complexes dehydrate in one step and form anhydrous compounds that next are decomposed to the oxides of appropriate metals with intermediate product formations.

The analysis of TG-FTIR spectra of complexes shows that with the rise of temperature the hydrates release the water molecules the presence of which in the gaseous mixture is confirmed by the bands in the range of 3900 – 3400 cm^{-1}. During further heating the organic ligand decomposes releasing the molecules of CO_2, CO and hydrocarbons (Fig. 2).

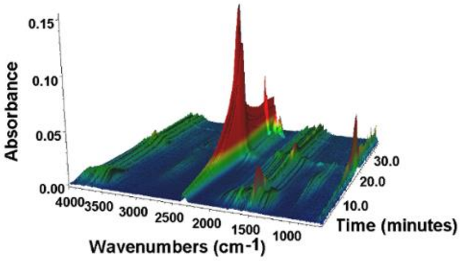

Fig. 2. The FTIR spectrum of gaseous products evolved during the decomposition of Ni(II) with glutamic acid and isatin complex.

The complexes of Mn(II), Co(II) and Ni(II) with L_1 and L_2 ligands obey the Curie–Weiss law [1]. The magnetic moment values of Cu(II) compound suggest its to be dimer. The environments around central ions in the rest of complexes (Mn(II), Co(II) and Ni(II)) depends on the kind of cation and carboxylate group characters.

References:

[1] S. F. A. Kettle, *Physical Inorganic Chemistry: A Coordination Chemistry Approach*, Oxford University Press, Oxford, 2000.

2-BENZYLSULFANYLACETIC ACID IN TERMS OF QUANTUM CHEMICAL CALCULATIONS IN CONJUCTION WITH EXPERIMENTAL DATA

Justyna SIENKIEWICZ-GROMIUK
DEPARTMENT OF GENERAL AND COORDINATION CHEMISTRY

The 2-benzylsulfanylacetic acid is an aromatic monocarboxylic compound containing three potential binding sites, namely two acidic ″hard″ oxygen donor atoms and one basic/alkaline ″soft″ sulphur donor atom. The compound in question has applications in the synthesis of coordination polymers thanks to the high plasticity of thioacetate group affecting on versatile coordination behaviour of this ligand with respect to the metal ions, like cooper(II), cadmium(II) and zinc(II). This compound is also used in organic chemistry as a key intermediate for the synthesis of 3-(4-methoxy-benzylidene)-isothiochroman-4-one belonging to the spiro-heterocyclic compounds, which can act as anti-tumorous, anti-tubercular and anti-HIV agents. It is also involved in the enantioselective synthesis of 4-(2-hydroxy-(1*R*)-phenylethyl)-thiomorpholin-3-one derived from the group of 2-substituted thiomorpholin-3-ones figured as pharmacophores in the ligand-based drug design.

Taking into consideration the application aspects of 2-benzylsulfanylacetic acid, in particular the possibility of its using as an organic ligand for construction of metal-organic coordination polymers, the determination of its structural, spectroscopic, thermal and electronic characteristics became the primary aim of this research. The first part of presented research was to develop the efficient method of synthesis of this acid as a pure phase product in the solid state, and then to determine its structural, spectroscopic and thermal properties by using different experimental measurement techniques, like SC XRD technique, elemental analysis, melting point measurement, XRPD analysis, IR and ^{1}H and ^{13}C NMR spectroscopy as well as thermal analysis (TG/DSC). The second part of this study was to provide a comprehensive DFT characteristics containing information on the geometrical and electronic structure of the acid in the ground state along with the structure-chemical reactivity relations and infrared and Raman vibrational spectroscopic analysis. Thus, the quantum chemical calculations have been performed using the density functional theory (DFT) at the B3LYP functional consisting of Becke's three-parameter (B3) hybrid exchange functional with non-local correlation provided by the Lee-Yang-Parr expression (LYP) together with the 6-311++G(d,p) basis set function employing Gaussian 03W and GaussView 4.1.2 program package.

The acid in question was synthesized on the basis of three-step synthesis route consisting in: (a) reaction of benzyl chloride and thiourea resulting in isothiouronium chloride; (b) transformation of isothiouronium salt into benzylthiol; (c) conversion of benzylthiol into 2-benzylsulfanylacetic acid. The synthesized product in the form of white powder was re-crystallized from pure methanol resulting in the formation of well-shaped crystals of the acid. The SC X-ray analysis confirmed that the title compound crystallizes in the monoclinic space group $P2_1/c$ with one molecule in the asymmetric unit of the crystal. The acid molecule adopts bent conformation in the solid state. The crystal structure of the acid is stabilized by numerous intermolecular interactions, including O−H···O, C−H···O, C−H···S and C−H···π_{phen} contacts. Very good fit between the simulated and experimental powder diffraction patterns confirmed the phase purity and good crystalline quality of the sample. The appearance of four proton and seven carbon signals in the recorded ^{1}H and ^{13}C NMR spectra unambiguously proved the structure of the compound. The presence of hydrogen-bonded carboxylic groups derived from the neighbouring molecules of acid is reflected in the registered IR spectrum. Thermal study indicates that the analyzed material is resistant to thermal degradation up to about 150 ºC and the melting point is 64 ºC [1].

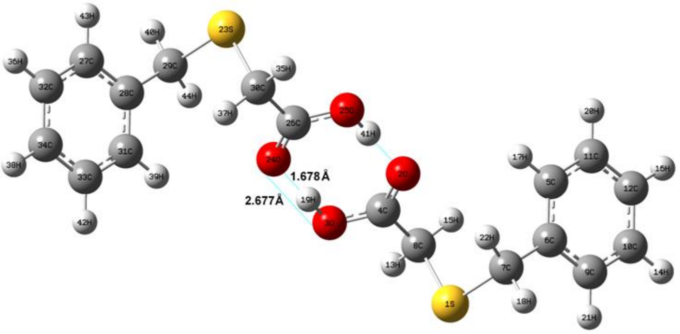

Fig.1. The optimized dimer structure of 2-benzylsulfanylacetic acid in the ground state.

The molecular structure of the acid belongs to C_1 point group symmetry. The minimum energy of most stable conformer of monomer and dimer structure was assessed by DFT calculations as –897.80610050 hartree (–2357189.91686 kJ/mol) and –1795.63703103 hartree (–4714445.02497 kJ/mol) respectively. In the case of optimized dimeric structure (Fig. 1), the appearance of two equivalent stable hydrogen-bonded O3–H19···O24 and O25–H41···O2 intermolecular contacts results in increased stabilization of dimeric structure in comparison to monomeric one. The intermolecular hydrogen bonds are almost linear (the O–H···O angle equals 179 °). The measured distances O3···O24 and O25···O2 is equal 2.677 Å and they are lying within the range <3 Å for hydrogen interaction. The O–H bond length and the bond angle C–O–H involved in hydrogen bonding causes an increase of 0.030 Å and 3.13 ° with respect to the isolated molecule. The optimized model of the dimeric structure showing the simulated system of two equivalent O–H···O hydrogen bonds significantly improves the convergence of carboxylic geometrical parameters in relation to the experiment. Despite some obvious discrepancies resulting from the different physical states, the optimized geometric parameters show reasonable agreement with the experimental data.

References:

[1] J. Sienkiewicz-Gromiuk, B. Tarasiuk and L. Mazur, *J. Mol. Struct.***, 1110** (2016) 65.

THE MODIFICATION OF POLYMERIC MICROSPHERES WITH THE USE OF RAFT POLYMERIZATION

Marta GROCHOWICZ
DEPARTMENT OF POLYMER CHEMISTRY

The presence of functional groups in the chemical structure of the polymer network determines the application of polymeric microspheres. Functional groups can be introduced into the structure of crosslinked polymers in two ways. The first involves the synthesis of microspheres from a crosslinking monomer and a functional monomer having appropriate functional groups. Another one is connected with the modification of the microspheres' surface. Such approach involves the presence of appropriate functional groups able to react in different chemistries on the surface of microspheres. A convenient group that can react with a great number of nucleophiles is the epoxy group [1, 2]. The aim of the project was the functionalization of surface of copolymeric microspheres obtained with glycidyl methacrylate (GMA) and 1,4-dimethacryloyloxybenzene (1,4DMB) with the use of linear polymeric chains of poly(geranyl methacrylate) (poly(GM)) which were obtained via RAFT polymerization.

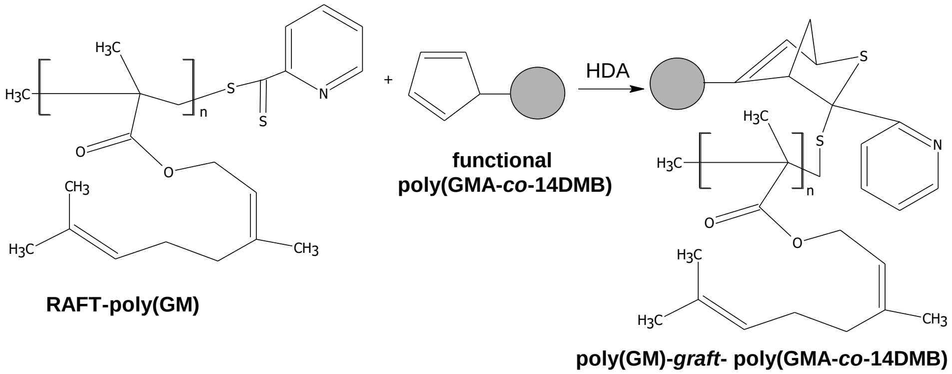

Scheme 1. The modification reaction of microspheres.

Copolymeric microspheres poly(GMA-co-1,4DMB) with permanent porous structure and monodisperse particle diameters were obtained via radical seed swelling polymerization of functional glycidyl methacrylate and crosslinker 1,4-dimethacryloyloxybenzene. Microspheres which possessed in their structure epoxide groups were reacted with sodium cyclopentadienide. The chemical modification of such prepared microspheres was carried out with hetero Diels Alder reaction, according to overall synthetic route presented in Scheme 1. As a dienophile the RAFT poly(geranyl methacrylate) chains were used. The 'grafting to' approach was chosen for grafting polymeric chains on the surface of the microspheres.

In the ATR-FTIR spectra of primary and modified microspheres presented in Fig 1 significant changes are observed. After the reaction with sodium cyclopentadienide a decreasing of the absorption band at 907 cm^{-1} attributed to epoxide ring vibration and increasing of the absorption band at 3467 cm^{-1} attributed to –OH vibration was observed. The grafting process of poly(GM) caused the changes in the region of C-O-C group vibration (1171 cm^{-1} and 1122 cm^{-1}). Moreover, in the course of the research thermal characteristic in inert conditions of prepared materials was made. As it is seen from Fig 2, on TG curve of poly(GM)-*graft*-poly(GMA-*co*-1,4DMB) three mass losses are observed: the first at 120°C connected with evaporation of unreacted geranyl methacrylate, the next at 250°C related to the decomposition of grafted poly(GM) and the last one with maximum at 430°C where crosslinked part of the material decomposed. These stages are also reflected in the 3D FTIR diagram of gasses evolved during modified microspheres degradation.

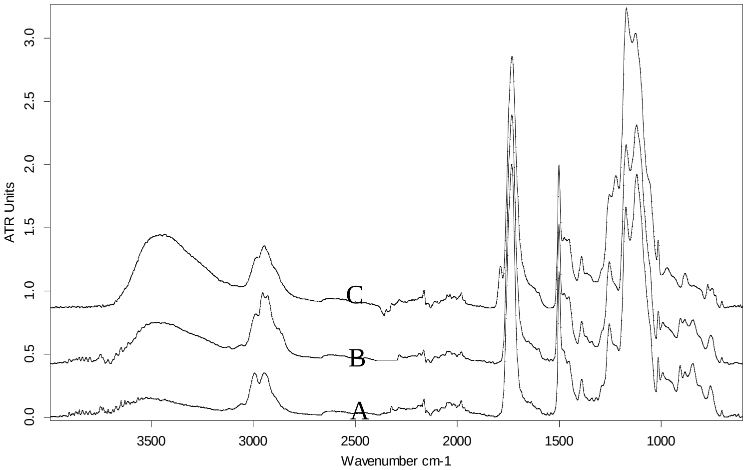

Fig.1. ATR-FTIR spectra of primary and modified copolymers: A – poly(GMA-*co*-1,4DMB); B – poly(GMA-*co*-1,4DMB)-Cp; C – poly(GM)-*graft*-poly(GMA-*co*-1,4DMB)

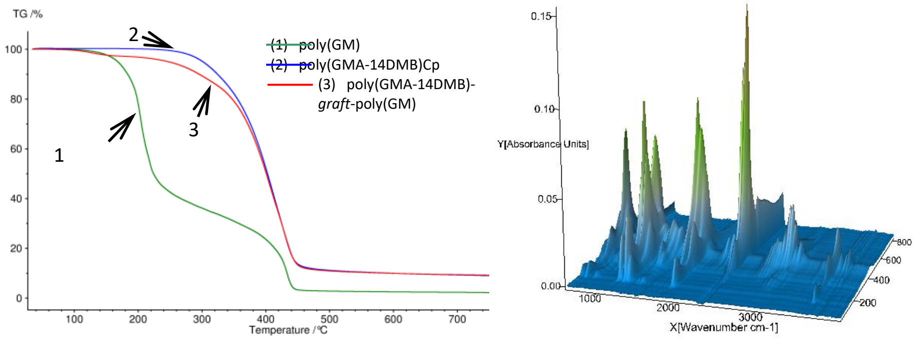

Fig.2. TG curves of studied polymers (left) and 3D FTIR diagram of gasses evolved during decomposition of poly(GMA-1,4DMB)-*graft*-poly(GM) (right)

References:

[1] A. S. Goldmann, L. Barner, M. Kaupp, A. P. Vogt, C. Barner-Kowollik, *Prog. Polym. Sci.*, **37** (2012) 975.

[2] M. Grochowicz, P. Pączkowski, B. Gawdzik, *Adsorpt. Sci. Technol.*, **33** (2015) 677.

SYNYHESIS OF POROUS MICROSPHERES FUNCTIONALIZED WITH LINEAR POLYMERIC CHAINS AND THEIR APPLICATION AS HPLC COLUMN PACKINGS

Marta GROCHOWICZ
DEPARTMENT OF POLYMER CHEMISTRY

The shell-functionalization is an attractive tool for modifying the surface of polymeric microspheres. In general, two different approaches can be mentioned, the ‘grafting to’ and the ‘grafting from’ approach [1]. In the ‘grafting to’ technique a reactive terminal group on a functional polymer chain reacts with the activated surface of microspheres. The already attached chains lead to a steric hindrance for following chains to diffuse to the surface. Such an approach suffers from low grafting rates. The benefit of the ‘grafting to’ technique is that usually the reactive groups necessary to achieve the ‘grafting to’ process do not dictate the kind of polymer chemistry employed, allowing a great versatility of polymers to be immobilized on the particle’s surface. Moreover, the employed linear polymer can be thoroughly characterized before the conjugation (with regard to molecular weight, polydispersity or functionality). As a polymerization method for obtaining polymeric chains, reversible addition-fragmentation polymerization is often used. The dithioester moiety of a RAFT agent serves two purposes. Initially, the dithioester moiety functions as a RAFT agent for obtaining polymer chains of predetermined molecular weight carrying RAFT end groups; subsequently these dithioester functionalities can be employed as a reactive heterodienophile in heteroatomic Diels Alder cycloaddition reaction (HDA) with a functionalized diene.

The aim of the project was the functionalization of surface of copolymeric microspheres obtained with glycidyl methacrylate (GMA) and 1,4-dimethacryloyloxybenzene (1,4DMH) with the use of linear polymeric chains of poly(2-hydroxyethyl methacrylate) which were obtained via RAFT polymerization and their subsequent use as column packings in HPLC.

Primary poly(GMA-co-14DMH) microspheres with permanent porous structure and monodisperse particle diameters were obtained via radical polymerization of methacrylate monomers: functional glycidyl methacrylate (GMA) and crosslinking agent 1,4-dimethacryloyloxybenzene (1,4DMH). Seed polymerization was chosen as an efficient method for the preparation of such particles with diameters about 8.61 μm (RSD – 2.47%). The poly(GMA-co-1,4DMH) microspheres which possessed in their structure epoxide groups were reacted with sodium cyclopentadienide which is able to react as diene in the Diels–Alder reactions. As a result of RAFT polymerization of 2-hydroxyethyl methacrylate poly(HEMA) chains were obtained. RAFT-poly(HEMA) macromolecules with Mn equal 4800 Da possessing thiocarbonyl groups on the chain ends were reacted with polymeric microspheres by hetero Diels Alder reaction according Scheme 1.

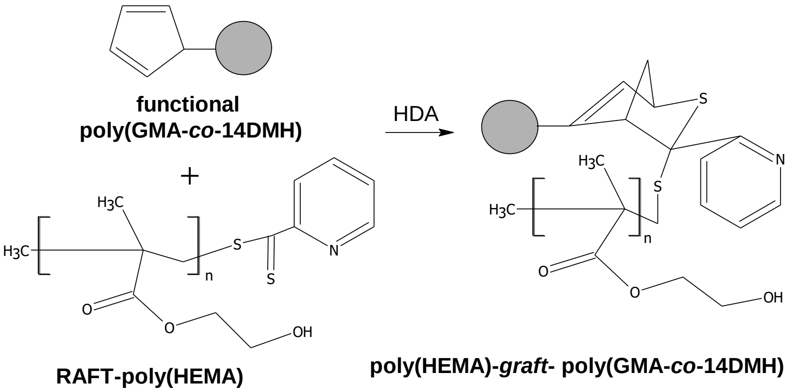

Scheme 1. The modification reaction of microspheres.

To evaluate the chromatographic properties of new porous packing the Smith method was applied [2]. The retention indices of five sets of homologous compounds and the selectivity test compounds (toluene, nitrobenzene, p-cresol, 2-phenylethanol, N-methylaniline) were measured. The exemplary chromatograms of separation of alkyl aryl ketones and chlorophenols are presented in Fig 1. Using ACN/buffer (50/50 v/v) mobile phase isocratic separation of alkylbenzenes was achieved with satisfactory resolution on 100 x 4.6 mm i.d. column. Theoretical plate number exceeding 20350 m^{-1} could be obtained with benzene as the analyte. The conducted research show that microspheres of poly(GMA-co-14DMH) grafted with poly(HEMA) can be applied as column packings for reversed phase HPLC.

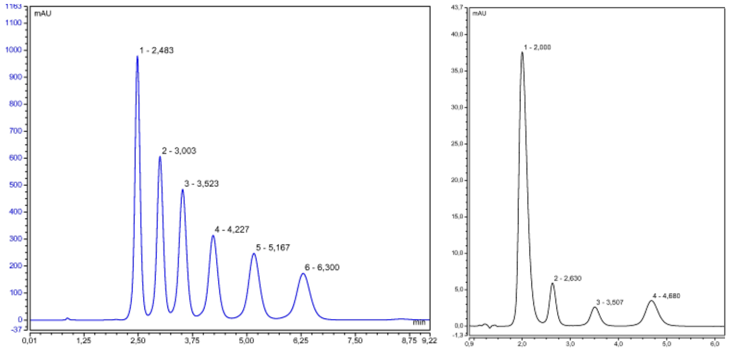

Fig. 1. Chromatograms of alkyl aryl ketones (left) and chlorophenols (right). Conditions: column 100 × 4.6 mm id; ACN concentration 50%; mobile phase ACN/buffer; 1mL/min; UV detector 254 nm. (1) acetophenone, (2) propiophenone, (3) butyrophenone, (4) valerophenone, (5) hexanophenone, (6) heptanophenone; (1) 2,4,6-trichlorophenol, (2) phenol, (3) 2,4-dichlorophenol, (4) 2-chlorophenol.

References:

[1] L. Barner, *Adv. Mater*, **21** (2009) 2547.
[2] M. Grochowicz, Ł. Szajnecki, B. Gawdzik, *Adsorpt. Sci. Technol.*, **33** (2015) 609.

STRUCTURAL STUDIES OF COUMARIN DERIVATIVES

Ilona MATEREK
DEPARTMENT OF CRYSTALLOGRAPHY

Coumarins isolated from natural sources and used in the folk medicine have a lot of therapeutic effects. The following biological activities of these compounds have been listed: vasodilatory, antiviral, anticancer, antiproliferative, anti-inflammatory, analgesic, antifungal and many others.

The molecular and crystal structure of new hydroxyl derivatives of pyranocoumarins was investigated. They can be divided into two groups, viz. seselin and alloxanthyletin derivatives.

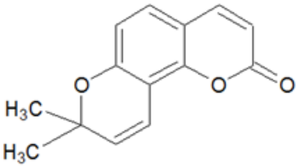

seselin

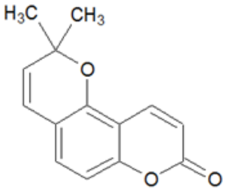

alloxanthyletin

Furthermore, the Hirshfeld surface analysis was performed for better understanding the nature of intermolecular interactions in the supramolecular crystalline network of analyzed compounds. The most important non-covalent interactions indicated by the Hirshfeld surface analysis for the investigated crystals are: O-H…O, C-H…O, and C-H…π. Aromatic π-π stacking between the rings may also contribute to the stabillization of the network.

The contribution of each type of interaction to the crystal networks for the constitutional isomers **S1** and **A1** is comparable (see table below).

	interaction	*%*		*interaction*	*%*
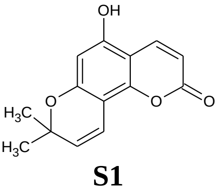 **S1**	C…C	11.2	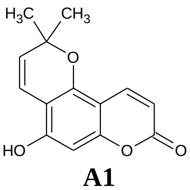 **A1**	C…C	15.1
	C….H/H…C	8.0		C….H/H…C	5.6
	O…H/H…O	27.8		O…H/H…O	29.7
	C…O/O….C	2.6		C…O/O….C	3.8
	H…H	48.5		H…H	44.6

Molecules connected by intermolecular hydrogen bonds can form planar chains, 8-membered rings and centrosymmetic dimers.

Moreover, both compounds have been evaluated for their cytotoxicity and anti-HIV activity, as well as for antiproliferative activity against human lung carcinoma and melanoma cell lines.

OPTIMIZATION OF MICROSTRUCTURED OPTICAL FIBERS DRAWING TECHNIQUE

Grzegorz WÓJCIK
LABORATORY OF OPTICAL FIBERS TECHNOLOGY

During realization of the investigations several technology stages were planned and realized. The most important steps were related with manufacturing and measurements of optical characteristics of different kinds of classical and microstructured optical fibers. The main goal was to identify and characterize mechanisms of propagation losses – especially micro-bending losses in fibers with unusual – asymmetric cross-section.

The first optical fiber produced during the research was classic single-mode fiber, with geometrical parameters identical to commercially available optical fibers. The classic preform was fabricated with MCVD method, preforms core was made from syntetic pure silica glass doped with 4% GeO_2. Next on the drawing tower fiber was drowned in two versions with different coating: intermediate and hard. Motivation of using different coatings was to expose micro-bending losses effect in the hard coating fiber.

In the following steps next preforms with various cross-sections, have been fabricated with different technology methods. By the stacking method was produced full solid hexagonal shape preform where the doped core and the outer fiber shape was hexagonal, geometrical parameters of this fibers was related to the classical single-mode fiber. The third preform was characterized by hexagonal shape of the core and circular outer fibers shape. This preform was produced using the mixed method – an internal part of cross-section was prepared by the stacking method, then the outer part of fibers clad was placed in the overcladding process on the MCVD machine. The last manufactured single-cell microstructured preform was produced by the stacking method with the use of silica rods and capillaries. All manufactured fibers was produced in two coating versions – intermediate and hard. The length of drowned fibers sections was no less than 1000m.

Figure 1 presents the electron microscope pictures of cross-section of all manufactured fibers.

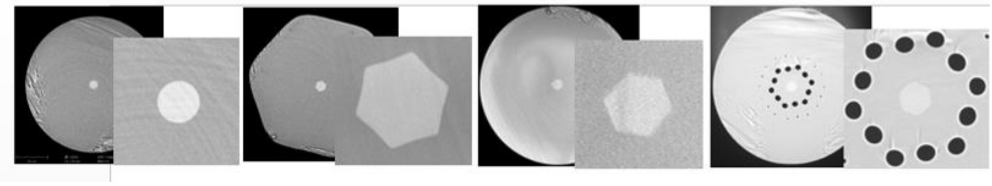

Fig.1 SEM pictures of cross-sections manufactured fibers, from the left: classic single-mode fiber, hexagonal single-mode fiber, mixed type single-mode fiber, single-cell microstructural single-mode fiber.

The final stage were loss measurements of all fibers in the climatic chamber. According to recommended by International Electrotechnic Commission in the Technology Report TR 62221 “Optical fibers – Measurements methods – Microbending sensivity”, sections of 60m length fibers were rewound with directly set nonzero force on the silica glass tube and placed in the climatic chamber in the temperature range from -40^{O}C to 60^{O}C. All produced fibers were measured using the reflectometer worked at wavelength 1620nm.

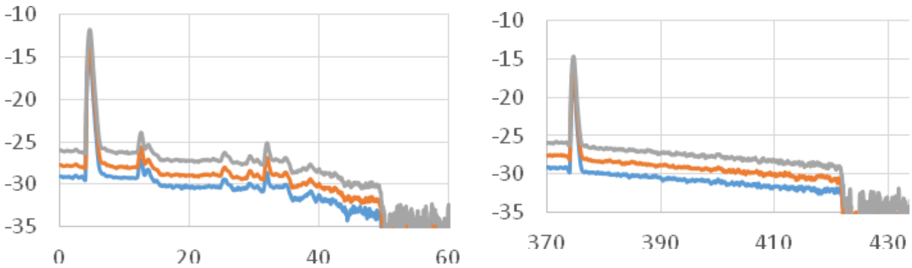

Fig.2 Comparison of mixed type single mode fibers characteristics gained in the climatic chamber microbending test. On the left side results for - hard coat fiber, on the right – intermediate coat fiber. On the both characteristics: blue lines refers to (-40^{O}C), orange lines refers to (10^{O}C), grey lines refers to (60^{O}C).

PLASTICS AS CARRIERS OF ORGANIC CONTAMINANTS IN AQUEOUS ENVIRONMENT. PHYSICO-CHEMICAL AND ECOTOXICOLOGICAL ASPECTS

Aleksandra BOGUSZ
DEPARTMENT OF ENVIRONMENTAL CHEMISTRY

Civilisation development has caused a notable increase in the global production of plastics. In 1950 it amounted to 1.5 million tons, while in 2012 as much as 288 million tons, which gives an average annual increase of about 9%. The storage of plastics constitutes a burning problem for the world economy. Statistics show that the polymers most frequently used in industry include low density polyethylene (LDPE), polypropylene (PP), poly(vinyl chloride) (PVC) and poly(ethylene terephthalate) (PET). From the economy and environmental viewpoint the storage of waste plastics constitutes an important problem, as they are characterised by a high volume to mass ratio, which generates increasing demand for new areas for their storage. The demand for plastics in the economy, and thus the amount of generated wastes migrating to the natural environment, assumes a growing tendency. While the problem of controlled storage of plastics has already been partially solved and the main problem in this respect is the organisation of new storage sites, a new growing problem has been observed in recent years, related with the migration of waste plastics to the environment. The first reports concerning environmental pollution with microplastics appeared at the turn of the seventies and eighties of the 20th century and referred to the area of North Pacific. Research shows that 10% of the amount of plastics produced end up in sea and ocean waters where they accumulate. This problem is of special importance as plastics particles drifting in water may become food for aquatic animals, causing their maiming and death. Numerous model experiments have been conducted which demonstrated that aquatic organisms such as invertebrates, zooplankton and larvae of echinoderms are capable of swallowing microplastics. In recent years it is also noted that apart from the direct exposure of organisms to waste microplastics there is also the danger of adsorption of contaminants on their surface. For example, it has been demonstrated that microplastics can play the role of a medium for the transport of inorganic and organic contaminants to living organisms. Ingestion of small particles of plastics, together with contaminants accumulated on their surface, by aquatic organisms entails the risk of desorption of chemicals from the surface of the plastics into the organism.

The research was conducted in three stages. In the first stage residues of plastics (LDPE, PET) was aged in the controlled laboratory conditions in the water from the karst lake Firlej. The purpose of ageing was the simulation of natural conditions occurring in the environment, which would permit the recreation of real processes to which polymers might be subject. In the next stage, study of the process of adsorption of selected PAHs on polymers before and after the process of ageing was performed. The last step involved the ecotoxicological tests on *Dapnia magna.*

For the experiment polyethylene (LDPE) and poly(ethylene terephthalate) (PET) were selected and incubated from June of 2015 in water collected from karst lake Firlej. After one year of incubation the polymer probes were collect to check the level of ageing. On the basis of analysis adsorption/desorption of nitrogen was confirmed that the specific surface area of studied plastics grown at about 15% in case of LDPE and 20% in case of PET. It was important information because the physical sorption as a primary mechanisms in sorption of PAHs is mentioned. While in the adsorption/desorption of nitrogen the structural changes after ageing of plastics were visible, this effect was completely unnoticeable in case of FTIR analysis. After confirming the changes in the structure of materials began to study the adsorption of selected PAHs, i.e. phenanthrene (PHE) and pyrene (PYR). The adsorption experiment was conducted follow by the procedure on passive samplers (POM) described by Zielińska et al. The values of partitioning coefficients $\log K_d$ obtained using a third-phase partitioning method showed that both plastics exhibits higher sorption capacities in case of PYR ($\log K_{d,LPDE}=4.58$, $\log K_{d,PET}=5.37$) than PHE ($\log K_{d,LPDE}=3.42$, $\log K_{d,PET}=4.92$). Furthermore, within the plastics, the higher sorption capacity in case of both PAHs was observed in case of aged PET. For the comparison, the adsorption tests were also performed for “raw” plastics. It was proved that aged materials had higher adsorption ability to studied PAHs ($\log K_d$ for aged materials were even 1.1 times higher). As a last stage of project, the ecotoxicological test on *Daphnia magna* was conducted. The Daphtoxkit F test was performed in the accordance with the test procedures of OECD Guideline 202 and ISO 6341. The increase of the toxicity of the plastics was observed with the increase in their concentration in the solution. The highest toxicity towards *Daphnia magna* was characteristic for PET than LDPE, what was correlated with higher content of adsorbed PAHs on PETs surface.

References:

[1] Plastics – the Facts 2013, An analysis of European latest plastics production, demand and waste data.
[2] K. Betts, *Environ. Sci. Technol.,* **42** (2008) 8995.
[3] L.M. Rios et al., *Mar. Pollut. Bull.,* **54** (2007) 1230–1237.
[4] A. Zielińska et al, *Chemosphere,* **153** (2016) 68-74.

POROUS POLYMERS AS AN ENVIRONMENT FOR HYDROLYSIS AND CONDENSATION OF INORGANIC OXIDE PRECURSORS

Agnieszka KIERYS
DEPARTMENT OF ADSORPTION

Porous resins produced by the suspension polymerization exist primarily in the form of spherical beads which are insoluble both in organic and inorganic solvents but they swell in them to a certain extent [1]. Individual polymer bead possesses very complex internal structure which may be considered as a continuous pore network set within a continuous polymer phase of a specific chemical character. The pore network which consists of interconnected free volumes of different size may be regarded as a specific microreactor where different chemical reactions can take place. Indeed, polymer-supported reactions gained considerable interest, especially in the context of organic combinatorial syntheses [2]. However, it has previously been shown that porous polymers may be regarded as a system in which precursors of inorganic oxides (e.g. silica [3, 4]) can undergo the process of transformation which involves hydrolysis and condensation. Although, these processes conventionally takes place in aqueous solutions of desired pH, they can also occur when catalysts are provided in the vapour phase of the desired composition [5].

The present paper describes the synthesis of polymer-silica composites by *in situ* transformation of different silica precursors (i.e. tetramethyl (M), tetraethyl (E), tetrapropyl (P) and tetrabutyl (B) orthosilicates) within the porous polymer support in the presence of the mixture of NH_3 and H_2O in the vapour phase. The Amberlite XAD7HP (XAD7) resin has simultaneously served as microreactor for the sol-gel process and the polymer support. The properties of final products have been presented.

The dry XAD7 beads rapidly swell in the liquid precursors which leads to the increase of their size. The maximum amount of the absorbed precursor depends on its type. And from the study it follows that the investigated XAD7 which is of moderately polar character, absorbs by about 25 % more tetramethyl ortosilicate then tetrabutyl ortosilicate. Exposure of the XAD7 saturated with precursor to the catalyst initiates and accelerates the precursor hydrolysis and polycondensation reactions. This in turn, leads to formation of the silica gel which is of amorphous character, as it may be concluded from the presence of the peak at about $2\theta = 22°$ the XRD pattern of composites (Fig. 1). The polymer-silica composites derived from the appropriate precursors (MC, EC, PC, BC, respectively) differs significantly in respect to the silica gel content as well as to the parameters characterizing their porosity (Table 1).

As it follows from Table 1, the higher the silica gel content is, the lower S_{BET} and V_p values for composites are.

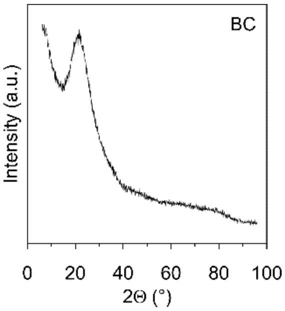

Fig. 1. XRD pattern of the representative composite BC.

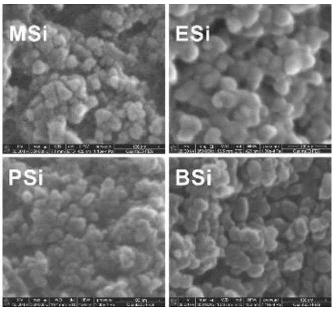

Fig. 2. SEM micrographs of the silica gels.

Table 1. Parameters characterizing the porosity obtained from N_2 sorption at 77 K: S_{BET}, the specific surface area; V_p, the total pore volume. The SiO_2 content was evaluated by the thermogravimetric measurements (% wt).

Sample	SiO_2 cont (% wt.)	S_{BET} (m^2/g)	V_p (cm^3/g)	Sample	S_{BET} (m^2/g)	V_p (cm^3/g)
XAD7	0	458	0.56			
BC	27	432	0.78	BSi	151	0.66
PC	29	412	0.64	PSi	239	0.83
EC	35	339	0.58	ESi	329	1.45
MC	43	119	0.32	MSi	261	0.79

After removal the polymer support during a high temperature treatment of the polymer–silica nanocomposites in air, spherically shaped silica gel particles (MSi, ESi, PSi, BSi, respectively), were obtained. SEM micrographs (Fig. 2) reveal the complex character of their interior and confirm that silica particles consist of tiny microparticles. Although, the differences between the internal structure of silica gels are hardly visible, they differ significantly in S_{BET} and V_p values between each other as well as in comparison the initial composites (Table 1). To sum up, the presented vapour phase synthesis route gives opportunity to obtain polymer-silica composites which contain very high content of silica oxide and highly developed internal surface. The amount of absorbed precursor depends on interactions between silica precursor and the polymer support.

References:

[1] D.C. Wu, F. Xu, B. Sun, R.W. Fu, H.K. He and K. Matyjaszewski, *Chem. Rev.*, **112** (2012) 3959-4015.
[2] P. Hodge, *Chem. Soc. Rev.*, **26** (1997) 417-424.
[3] A. Kierys, M. Dziadosz, J. Goworek, *J. Colloid Interf. Sci.*, **349** (2010) 361-365.
[4] A. Kierys, R. Zaleski, W. Buda, S. Pikus, M. Dziadosz, J. Goworek, *Colloid Polym. Sci.*, **291** (2013) 1463-1470.
[5] I. Halasz, A. Kierys, J. Goworek, *J. Colloid Interface Sci.*, 4**41** (2015) 65-70.

SYNTHESIS OF SANDWICH-TYPE COMPOSITES FOR SELECTIVE AND REVERSIBLE MACROMOLECULES ADSORPTION

Andrzej SIENKIEWICZ
DEPARTMENT OF ADSORPTION

The ability of Amberlite resins to swell in contact with liquid silica precursors creates unique opportunity to produce silica-polymer composites [1]. Setting swollen beads of polymer in atmosphere rich in ammonia or HCl vapours initiates processes of hydrolysis and condensation of the silica precursors within and around Amberlite matrix [2]. The above mentioned process results in creation of the silica-polymer composite. However, when polymeric beads imbibe mixture of the organic silica precursors that have Si-C bound, which is not susceptible to hydrolysis, the structure of the obtained hybrid silica-polymer composite is more complex. The final material consists of hydrophobic polymer matrix covered with hydrophilic silica to which hydrocarbon chains are bounded (organic-inorganic-organic). The material having these three domains should exhibit high affinity towards adsorption of polar, nonpolar and amphiphilic molecules. The aim of this work is to produce the composite with usage of Amberlite XAD7HP resin (XAD7) and two silica precursors (3-(2-Aminoethylamino)propyl]trimethoxysilane) – APTS, tetramethyl orthosilicate – TMOS) for specific adsorption of macromolecules.

The synthesis procedure began with the XAD7 dry beads immersed in the mixture of APTS and TMOS. The amount of alkoxysilanes was adjusted so that the polymer spheres imbibed it totally (without any external liquid). The swollen particles were aged for 24 h in closed container at room temperature. Subsequently wetted with alkoksysilanes XAD7 particles were exposed to ammonia vapors for 72 h. During this time silica precursors had hydrolyzed and condensed to form silica species within and outside the polymeric matrix. Next, the new materials were dried for 10 h at 80°C. Composite samples were named M05 and M10 which corresponds to the APTS:TMOS molar ratio – 1:5 and 1:10 respectively.

The hybrid silica-polymer composites and commercially available unmodified materials i.e. Amberlite XAD7HP and silica gel Si 100 (which were used for the comparative purposes) were characterized in terms of their structural parameters. The specific surface area (S_{BET}) and the total pore volume (V_p) were determined by the measurements of nitrogen adsorption-desorption at 77 K. For evaluation of interactions between macromolecules and the composites, static adsorption experiment of bovine serum albumin (BSA) from buffer solution (pH=7.4) was performed. The detection of the protein was done on UV-Vis spectrometer at 278 nm. Additionally scanning transmission electron microscopy (STEM) micrographs of material with and without adsorbed protein was taken.

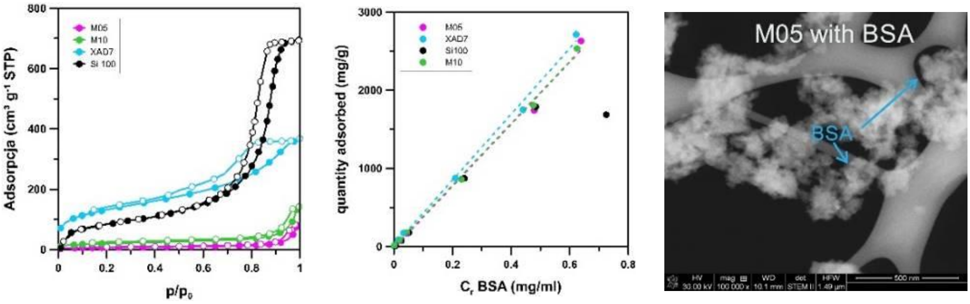

a) b) c)

Fig. 1. The nitrogen adsorption (filled points) and desorption (empty points) isotherms of Amberlite XAD7HP (XAD7), pure porous silica (Si 100), composite M05 and M10 (a), the adsorption isotherm of BSA on all materials under study (b) and STEM micrograph of M05 material with adsorbed BSA (c).

The low temperature nitrogen adsorption-desorption experiment reveals that the obtained hybrid silica-polymer composites have much smaller specific surface area ($S_{BET,M05}$ = 24 m^2/g, $S_{BET,M10}$ = 71 m^2/g) in comparison to the parent polymer ($S_{BET,XAD7}$ = 469 m^2/g). Also, the total pore volume decreases by about 77% and 61% for M05 and M10, respectively. Based on the hysteresis loops on nitrogen adsorption-desorption isotherms for XAD7, M05 and M10, it may be stated that bottle shaped pores in parent polymer are transformed into slit-like pores during the synthesis. It may be assumed that condensing silica species occupy free volumes in XAD7. The structure of a newly formed hybrid silica is less porous and, in consequence, the S_{BET} of the composites is significantly lower. The results of static adsorption of BSA on materials under study are somewhat surprising. While curvature of BSA adsorption isotherm on silica gel (Si 100) has Langmuir profile, the shape of BSA adsorption on XAD7, M05 and M10 is linear (Fig. 1b). Despite the fact that composites have much smaller S_{BET} than XAD7 the quantity of the BSA adsorbed is at the same level. This is probably due to the fact that polymeric matrix is still available for hydrophobic interactions between the protein and the adsorbent. What is more, proteins have tendency to unfold when adsorbed and to create multilayers on the surface of the adsorbent .

As a conclusion it can be stated that obtained composites have potential to adsorb large molecules. However further research should be more focused on molecules smaller than proteins e.g. drugs and on the investigation of mechanism of hydrolysis and condensation of silica precursors within swollen polymer matrix.

References:

[1] A. Kierys, M. Dziadosz, J. Goworek, Polymer/silica composite of core-shell type by polymer swelling in TEOS, *J. Colloid Interf. Sci.*, **349** (2010) 361-5.

[2] I. Halasz, A. Kierys, J. Goworek, Insight into the structure of polymer-silica nano-composites prepared by vapor-phase, *J. Colloid Interf. Sci.*, **441** (2015) 65-70.

TEMPERATURE-DEPENDENT MODIFICATION OF POLYMER MATRIX BY INORGANIC OXIDES

Patrycja KRASUCKA
DEPARTMENT OF ADSORPTION

The spherically shaped hybrid materials composed with polymer and inorganic silica are of great interest due to their unique properties and various application e.g. in adsorption, chromatography, catalysis, energy storage and pharmaceutical industry [1]. In the recent years, we have synthesized the spherically shaped polymer-silica composite by swelling of the polymer (Amberlite XAD7HP) in the silica precursor (TEOS, tetraethoxysilane) at room temperature [2]. After combustion of the organic component, pure silica gel in the form of beads was received. Aforementioned composites are also promising supports for drugs in controlled release system. In all these systems the drugs are fixed on support surface by impregnation of the polymer in a drug solution of desired concentration. Independently of synthesis conditions, composite preparation is connected with swelling of polymer in TEOS. Silica precursor transformation and SiO_2 creation may go *in situ* in surrounding of fixed pH. Transformation of TEOS is evidently dependent on temperature. In the case of *in situ* transformation maximum temperature is low and oscillates around 37°C. In that temperature we were measured the release of insoluble in water Naproxen from pure polymer support and from XAD7 with pores filled with liquid TEOS. The main factors influencing the drug desorption process were porosity of the composite and pH of release solution. Therefore, it is essential to test how the temperature of TEOS and polymer mixing followed by silica gelation influences porosity of the composite support.

Combination of polymer and silica component out of human system may be realized up to temperature of decomposition of polymer i.e. even above 200°C. We synthetized new polymer-silica composite in TEOS-polymer mixing temperature 150°C, which is XAD7 glass transition (Tg) temperature. Our preliminary experiments of mixing of TEOS and polymer above Tg temperature indicates that both components are perfectly mixed and homogeneous phase of the composite is formed. The porosity parameters of this new material are still high and comparable to those for the pure polymer or the composite prepared at room temperature.

For illustrative purposes Figure 1 presents the SEM micrographs of the particle interior of composites and silicas received at room temperature (POLY-Si, SiO_2) and those prepared above glass transition temperature (POLY-SiT, SiO_2T). Table 1 shows porosity parameters of all materials under study (POLY-pure XAD7).

Table 1. Parameters characterizing the porosity of received samples obtained from nitrogen adsorption/desorption isotherms at 77 K: S_{BET} – the specific surface area, V_p – the total pore volume, $D_{PSD1,2}$ – the pore diameter at the peak of PSD [3].

Sample	**S_{BET} [m^2/g]**	**V_p [cm^3/g]**	**$D_{PSD\ 1;2}$ [nm]**
POLY	458	0.56	3.8; 9.4
POLY-Si	430	0.26	3.8
SiO_2	756	1.27	9.5; 15
POLY-SiT	363	0.31	3.8
SiO_2T	995	0.75	3.8

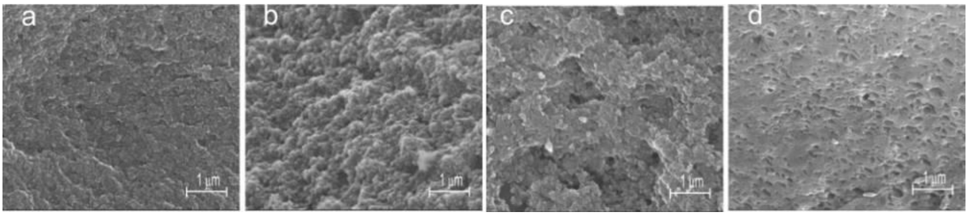

Fig. 1. SEM micrographs of a - POLY-Si composite, b - SiO_2, c – POLY-SiT composite, d– SiO_2T [3].

The SEM images and the porosity parameters indicate that the high-temperature synthesis is an interesting approach for preparation of new composite and silica materials of high porosity and unique structure.

References:
[1] H. Zou, S.S Wu, J. Shen, *Chem. Rev.*, **108** (2008) 3893–3957
[2] A. Kierys, M. Dziadosz, J. Goworek, *Colloid Interf. Sci.*, **349** (2010) 361–365.
[3] P. Krasucka, R. Zaleski, K. Skrzypiec, J. Goworek, M*icropor. Mesopor. Mat.*, **237** (2017) 210-221.

ANALYSIS OF PROTEINS ADSORPTION ON MESOPOROUS MATERIALS: INFLUENCE OF PORE SIZE AND ADSORBENT SURFACE STRUCTURE

Agnieszka CHRZANOWSKA
DEPARTMENT OF PHYSICOCHEMISTRY OF SOLID SURFACE

Investigation of biomolecules adsorption (proteins, enzymes, pharmaceuticals) from solutions on solid surfaces is of great importance with regard to prominent role in biology, medicine and bio- nanotechnology [1]. Therefore, it is important to understand mechanisms of sorption processes of compounds showing biological activity at different solid surfaces as well as study practical use of the modified biological materials in many areas (BioSS - Surface Biological Science) [2].

The mesoporous silica materials like MCF (mesocellular foam) with desirable and unique properties (highly ordered pore structure, high surface area and pore volume, possibility of functionalizing and changing surface properties) are very attractive group of adsorbents which can be very useful in the processes involving substances with large molecular sizes, including albumins. For large protein molecules the rate of adsorption process is controlled by their diffusion in pore system of a solid, therefore the studies on the effect of pore sizes on the kinetics of these processes are very important.

The main aim of the studies was synthesis, physicochemical and structural characterization of MCF materials with differentiated porosity for adsorption of albumin molecules as well as detailed analysis of morphology/topography and physico/electrochemical properties of composite surface of protein/silica system. In this study, the adsorption processes of selected BSA and OVA proteins (Bovine serum album, Ovalbumin) from aqueous solutions at pH=7.4 on the series of MCF materials with different porosity are investigated. The MCF adsorbents with various structures were prepared by using the non-ionic tri-block Pluronic copolymers as a template and trimethylbenzene as a pore expanding agent according to a modified procedure described in the papers [3,4]. The equilibrium adsorption isotherms and concentration vs. time profiles were determined from UV–Vis spectra [5,6]. The dependences between pore diameter and kinetic rate were analyzed. It was observed that protein adsorption process on mesoporous silica support is slow and limited by diffusion of biomolecules into internal adsorbent porous structure and is strongly dependent on the pore size of MCF material (Fig. 1).

Structure of the protein/silica composites was investigated using nitrogen adsorption/desorption isotherms. The basic porous structure parameters of the studied silica supports as well as protein/silica composites: the BET specific surface area (S_{BET}), the micropore area (S_{mic}), the external surface area (S_{ext}), the total pore volume (V_t), the micropore volume (V_{mic}), the average pore diameter (D_{av}), the average hydraulic pore diameter (D_{hy}) were determined. Analysis of porous structure of the MCF material after adsorption of both albumins shows that all porosity parameters (S_{BET}, S_{ext}, V_t, V_{mic}, D_{av}, D_{hy}) are reduced.

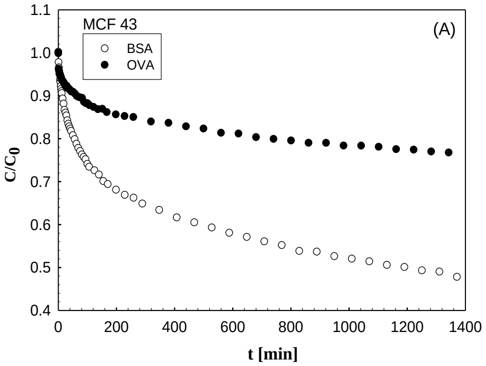

Fig. 1. (A) Comparison of concentration profiles for BSA and OVA adsorption on MCF-43 material; (B) Comparison of concentration profiles for BSA adsorption on MCF-24 (pore size:7 nm) and MCF-43 (pore size:16 nm) (relative concentration~time).

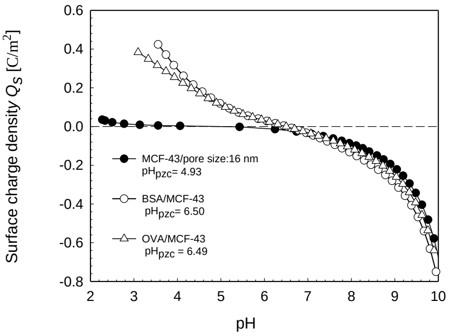

Fig. 2. Dependence of surface charge density on pH for the MCF-43 and BSA/MCF-43 and OVA/MCF-43 samples.

The electrochemical character and surface charge of the native MCF material and protein/silica composites were studied by potentiometric titration. It was stated that the electrochemical character of the silica surface with adsorbed BSA and OVA is clearly different than for pure silica surface (Fig. 2). Native MCF supports have point of zero charge, pH_{pzc}, near 4.9, however, upon proteins adsorption, their surfaces change electrochemical properties (become amphiphilic), with pH_{pzc} near 6.5 (close to pH_{pzc} of proteins).

The morphology and micro-nanostructure of MCF surface with adsorbed protein were monitored by using the atomic force microscope (AFM) and optical profilometer (OP). The results show that the surface roughness and waviness after protein adsorption is lower than for the native silica material. The analysis of surface topography and the elemental composition (Si, C, O, N) of the silica materials with adsorbed proteins was performed by using transmission electron microscopy (TEM) and energy dispersive X-ray spectroscopy (EDX).

In Fig. 3 the TEM micrographs of surface structure of pure MCF silica material and with adsorbed proteins are presented. The TEM analysis before and after protein adsorption confirm the structure and presence of the adsorbed proteins on the surface of porous material. Generally, TEM/EDX results markedly confirm that the BSA adsorption changes surface topography and local concentration of chemical elements of MCF material to a larger extent than in the case of ovalbumin adsorption.

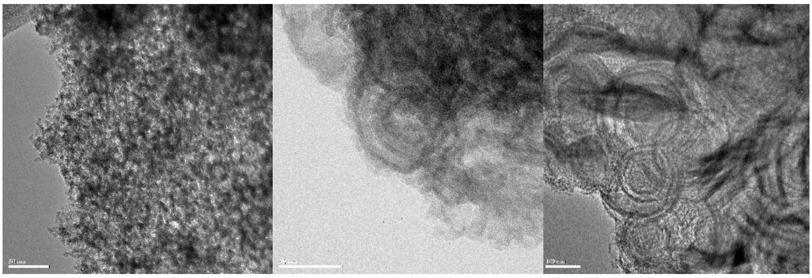

Fig. 3. TEM micrographs showing the surface structure of pure MCF silica (A) and covered by BSA (B) and OVA molecules (C).

References:

[1] J.J. Kirkland, F.A. Truszkowski, R.D. Ricker, *J. Chromatogr. A*, **25** (2002) 965.

[2] C.E. Giacomelli, W. Norde, *J. Colloid Interface Sci.*, **233** (2001) 234.

[3] P. Schmidt-Winkel, W.W. Lukens Jr., D. Zhao, P. Yang, B.F. Chmelka, G.D. Stucky, *J. Am. Chem. Soc.*, **121** (1999) 254.

[4] A. Derylo-Marczewska, A.W. Marczewski, I. Skrzypek, S. Pikus, *Pol. J. Chem.*, **82** (2008) 205.

[5] A.W. Marczewski, *J. Colloid Interface Sci.*, **361** (2011) 603.

[6] A.W. Marczewski, A. Derylo-Marczewska, A. Slota, *Adsorption*, **19** (2013) 391.

SYNTHESIS AND PHYSICO-CHEMICAL CHARACTERIZATION OF SILVER-CARBON NANOCOMPOSITES

Małgorzata ZIENKIEWICZ-STRZAŁKA
DEPARTMENT OF PHYSICOCHEMISTRY OF SOLID SURFACE

Nanocomposite materials as well as other hybrid structures, due to their rare and significant physical and chemical properties, are of great interest in many applications. This work raises questions related with nanomaterials, which, due to the rapid development of nanotechnology are becoming increasingly common in almost all areas of our life. Problems related to safety of nanomaterials, potential threats in relation to health of living organisms and the environment become noticeable. The concern potential impact of nanocomposites and their nano-sized components on living cells, microorganisms and biomolecules. On the other hand, the immobilization of the nanoparticles by embedding them in common and harmless adsorbents may be a method of reducing their number in nature and more safety applications.

In this work, the highly porous activated carbon RIAA (Norit n.v., Amersfoort, Netherlands) was applied as a host phase. The activated carbon adsorbent was highly porous (S_{BET}=1440 m^2/g, pore volume 0.80 cm^3/g) with significant amount of micropores ($S_{BET,MIC}$=1040 m^2/g, micropore volume about 0.49 cm^3/g). Silver nanoparticles solution was obtained according to the reduction of silver nitrate by $NaBH_4$ in the presence of poly(vinyl pyrrolidone) (PVP) and sodium citrate ($C_6H_5Na_3O_7$) as a stabilizer of the nanoparticles. Finally, yellow-orange solution of colloidal silver was obtained. Color of solution indicates the presence of small silver nanoparticles. Performed synthesis procedure allowed us to obtain a stable system without visible effects of agglomeration. Silver-carbon composites were prepared by deposition of specified amount of silver nanoparticles onto the activated carbon by 24-hour incubation of the mixture at 25ºC. The resultant sample was then rinsed with distilled water and dried in an air atmosphere. The obtained silver-carbon composites were characterized by nitrogen adsorption-desorption analysis and imaged by transmission electron microscopy. The thermal stability of silver modified carbon materials were also evaluated. After deposition of the silver nanoparticles significant changes of the porous structure of activated carbon were observed. It should be emphasized significant reduction of specific surface area and limiting the availability of micropores due to their blocking by larger particles of silver nanoparticles. After deposition of silver nanoparticles, the specific BET surface area decreased by 207 m^2/g. Surface area of micropores and pore volume was also significantly lower (by 405 m^2/g and pore volume lower by 0.14 cm^3/g. This suggests that small pores of activated carbon are especially sensitive to the presence of silver nanoparticles which size is comparable or larger with the current micropores.

The TEM images (Fig. 1) show that the visible aggregates of silver nanophase consist of small nanoparticles with well-defined crystallinity.

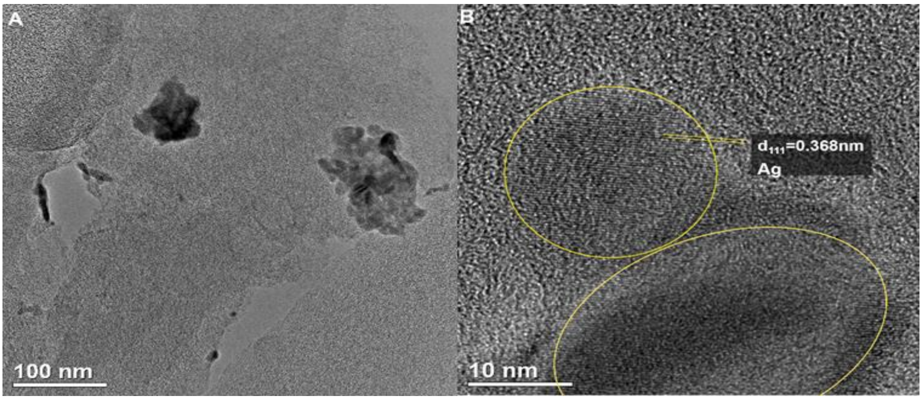

Fig. 1. TEM images of silver nanoparticles deposited on activated carbon. High resolution TEM image of silver crystallites.

Silver nanoparticles are visible as dark objects on the carbon surface. The distribution of silver phase is not uniform and the size of silver crystallites can be differentiated depending on the investigated area. Over aggregates, individual silver nanoparticles exist as crystallites with size below 50 nm. HRTEM images confirmed that this way of preparation of the silver-carbon nanocomposites ensure the creation of composites where silver phase forms well defined crystallites with quite well singled lattice planes.

Thermal stability of investigated samples was evaluated by thermogravimetric (TG) analysis before and after silver nanoparticles incorporation. The weight loss started from 500°C to 650ºC. The total weight loss at 950°C was estimated as 86%. The presence of silver ions had no significant effect on thermal stability of the composites. The remaining missing loss of weight is related to the presence of silver nanoparticles and confirmed their proportional content in the nanocomposite (14 %).

PROCESSES OF ADSORPTION OF BIOACTIVE COMPOUNDS ON MODIFIED CARBON ADSORBENTS

Małgorzata ZIENKIEWICZ-STRZAŁKA
DEPARTMENT OF PHYSICOCHEMISTRY OF SOLID SURFACE

Among new functional materials, the nanocomposites based on natural polymers such as chitosan provides obtaining materials with advanced physicochemical properties and new possible applications. Great importance of chitosan based nanocomposites is the effect of their multi-functionality, biocompatibility, wide range pH stability as well as activity as bioadsorbents [1-4]. With the purpose to build new nanocomposite materials with natural polymer and porous solid phase, activated carbons and silica adsorbents were investigated for enhance the mechanical properties of the composite scaffolds. In this work, the carbon/chitosan (C/CS) and chitosan/silica (CS/silica) composites were prepared and used as support for silver nanoparticles. C/CS composites were prepared by impregnation of the activated carbon granules (RIAA, Norit, n.v., Amersfoort, The Netherlands) in chitosan/acetic acid mixture. CS/silica nanocomposite materials were synthesized by electrospinning to produce the polymer fibers. Electrospinnig procedure was not possible in the case of activated carbon due to the lack of possibility to get a homogenous carbon/chitosan mixture with suitable properties for electrospinning. Based on C/CS and CS/silica composites, the silver modified nanocomposites were prepared by impregnation of the supports by silver ions in the form of ammine complexes ($[Ag(NH_3)_2]OH$) as well as before-prepared silver nanoparticles.

C/CS/Ag composite has an amorphous structure typical for activated carbons, whereas the silver phase is visible as white objects on the surface. The size of the silver phase is about 20 nm, but there are also visible much larger aggregates with size above 100 nm (Fig. 1E). Final silica/chitosan composites are three-dimensional randomly oriented fibrous mesh with fibers with diameters ranging from 100 nm to 500 nm. The diameter of individual fibers varied along their length. Furthermore, the fibers have a well-defined solid surface with some irregularities. Large interconnected voids in the nanocomposites improves their usefulness as membranes or adsorbents. Characterization of morphology of the nanoparticles and their dispersion degree is an important in nanocomposites investigation. The effect of differentiation of dimensions of metal phase is observed depending on form of the type of solid adsorbent as well as silver precursor, and reinforced by the properties of the porous materials/chitosan nanocomposites. The sizes of electron density inhomogeneity generated by Ag NP was at first noticeable by SAXS and equals around 210Å in the case of silica/chitosan/AgNP. Similar size was achieved for C/CS materials. When the silver ions were applied, the electron density inhomogeneity related to silver structures is very slightly outlined on SAXS patterns and suggests significantly smaller size of the formed silver phase. The differences in the particle size was confirmed by powder wide range XRD analysis. The full-width at half-maximum (FWHW) of diffraction peaks illustrate the size of the crystallite and directly describes the size of silver phase. The average size of silver crystallites for C/CS materials from XRD patterns is significantly greater and equals ~ 50 nm. This may suggest that silver phase on C/CS surface have ability to create more agglomerated phase than in the case of composites containing silica phase In the case of silica/chitosan/Ag_{ions} nanocomposite, the broad XRD peaks with big FWHW value according to nanosize effect and smaller silver crystals was observed. Finally, the nanoparticle size effect was confirmed by scanning probe microscopy (AFM) and Scanning Electron Microscope (Fig. 1).

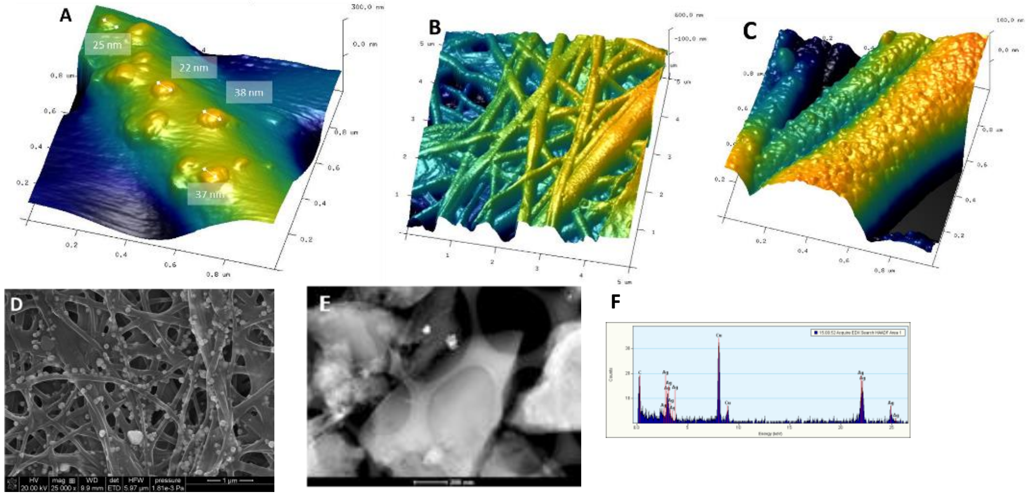

Fig.1. (A) 3D AFM images representing the topography of silica/chitosan/AgNP nanocomposite, (B, C) AFM images of silica/chitosan/Ag_{ions} sample, (D) SEM image of the silica/chitosan/AgNP material, (E) TEM of carbon/chitosan/AgNP composite, (TEM/EDX analysis from Fig. 1E).

The obtained results suggest, that the polysaccharide as a mild reducing agent can be responsible for obtaining extremely-small silver nanoparticles. Diffusion of Ag^+ is limited by the polymer network and the positions of Ag^+ are fixed by coordination to the amino groups of chitosan. Therefore, the possible interactions between silver phase and silica/chitosan surface were also evaluated using X-ray Photoelectron Spectroscopy. Detailed XPS spectra, registered with a high resolution permits analysis of chemical composition, chemical shifts and chemical state of N1s, Ag3d and O1s elements. In the case of silica/chitosan/Ag_{ions} nanocomposite, the shift of binding energy for N1s peak from 399.3 eV (typical for amine NH2 groups) to 398.6 eV corresponding to Ag-N interaction [5]. The possible interaction between silver phase and carbon from C/CS composite were not yet analyzed.

References:

[1] M. Auta, B.H. Hameed, *Chemical Engineering Journal*, **237** (2014) 352.
[2] W. S. Wan Ngah, L.C. Teong, M. A. K. M. Hanafiah, *Carbohydrate Polymers*, **83** (2011) 1446.
[3] M. N. V. R. Kumar, *Reactive and Functional Polymers*, **46** (2000) 1.
[4] G. Crini, P. M. Badot, *Progress in Polymer Science,* **33** (2008) 399.
[5] N. Maiti, *RSCAdv.*, **6** (2016) 56406.

EXPERIMENTAL ANALYSIS OF ADSORPTION KINETICS IN MULTICOMPONENT SYSTEM

Małgorzata SĘCZKOWSKA
DEPTARTMENT OF PHYSICOCHEMISTRY OF SOLID SURFACE

Adsorption methods using activated carbon are commonly used in the technology of water and wastewater treatment. Adsorption is a multistep process and each phase takes place at different times. The rate of the whole process will be determined by the slowest step. The efficiency of adsorption is influenced by many factors related to the properties of adsorbent (specific and external surface area, type and volume of pores, surface charge) and adsorbate (molecular size, solubility, ability for dissociation), process conditions (pH), temperature and the presence of other substances [1-7]. In order to estimate the usefulness of an adsorbent in a given technological system it is necessary to define its adsorption capacity and rate, especially in the case of multicomponent solutions containing compounds of various molecular size and physicochemical properties.

The main aim of this study was experimental analysis of the adsorption kinetics in single- and multicomponent systems. Measurements of adsorption kinetics of methylene blue (MB; Sigma-Aldrich) and Ibuprofen (IBP; Sigma-Aldrich) on granular activated carbon GAC 1240W (Norit; S_{BET}=900 m^2/g, V_t=0.52 cm^3/g, V_{mic}=0.2 cm^3/g) in single and binary systems were performed. The initial solution concentrations were established at a level convenient for measurements without additional dilution. The UV-Vis spectrophotometer with flow cell working in a closed loop was applied to determine the adsorbate concentrations. The measurement technique allowed to obtain high-quality experimental data. The profiles *concentration ~ time* and *adsorption ~ time* for single-component systems were analyzed by using several empirical equations and kinetic models: first, second and mixed 1,2-order equations (FOE, SOE, MOE) [8-11], Langmuir kinetics (IKL) [10,12], intraparticle diffusion (IDM) and pore diffusion models (PDM) as well as multi-exponential (m-exp) equation [8-12]. In order to determine the parameters of the kinetic equations and models general multivariate LSQ optimization procedures were applied.

In Fig. 1 the concentration and adsorption profiles are compared for adsorption of methylene blue and Ibuprofen from single- and bi-component solutions. The influence of co-adsorbate on adsorption rate is found, however, the observed effects are not very pronounced. Generally, comparing the kinetic curves for both compounds measured in one- and two-component systems, one can state that adsorption processes are slower in presence of other substances in solutions. However, taking into account relatively small differences between concentration and adsorption profiles measured from single- and bi-component systems one can conclude that at relatively low concentrations adsorption of methylene blue and

Ibuprofen is partly independent as a result of filling the pores of various sizes (Ibuprofen has smaller molecular size in comparison to methylene blue). However, stronger mutual influence of co-adsorbates related to their competition may be expected at higher concentrations of both solutes.

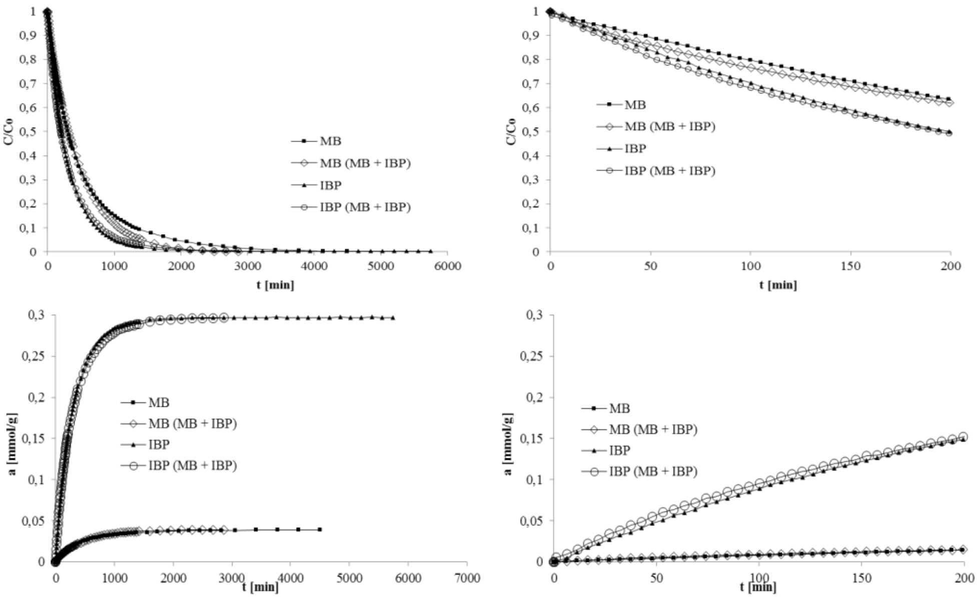

Fig. 1. Comparison of adsorption kinetics of MB and IBP on GAC in single and multi-component systems, 298 K. All kinetic curves are fitted by multi-exponential equation (m-exp).

References:

[1] S. Chiron, A. Fernandez-Alba, A. Rodriguez, E. Garcia-Clavo, *Water Res.*, **34** (2000) 366.

[2] L. Clausen, I. Fabricius, L. Madsen, *J. Environ. Qual.*, **30** (2001) 846.

[3] M. Zahoor, J. Chem. *Soc. Pak.*, **33** (2011) 305.

[4] T.M. Ward, F.M. Getzen, *Environ. Sci. Technol.*, **4** (1970) 64.

[5] K. Ebie, F. Li, Y. Azuma, A. Yuasa, T. Hagishita, *Water. Res.*, **35** (2001) 167.

[6] A. Deryło-Marczewska, A.W. Marczewski, *Appl. Surf. Sci.*, **196** (2002) 264.

[7] A.W. Marczewski, M. Seczkowska, A. Deryło-Marczewska, M. Blachnio, *Adsorption*, **22** (2016) 777.

[8] A.W. Marczewski, *Appl. Surf. Sci.*, **253** (2007) 5818.

[9] A.W. Marczewski, *Appl. Surf. Sci.*, **256** (2010) 5145.

[10] A.W. Marczewski, *Langmuir*, **26** (2010) 15229.

[11] A.W. Marczewski, A. Derylo-Marczewska, A. Slota, *Adsorption*, **19** (2013) 391.

[12] A.W. Marczewski, *J. Colloid Interface Sci.*, **361** (2011) 603.

DETERMINATION OF BIOLOGICAL ACTIVITY OF ORGANIC COMPOUNDS USING *IN VITRO* AND *IN SILICO* METHODS

Katarzyna STĘPNIK
DEPARTMENT OF PLANAR CHROMATOGRAPHY

Due to a large number of chemical substances in everyday use, high costs and long time of investigations on their toxicity estimation as well as ethical aspects connected with experiment on animals, it is necessary to apply a fast and inexpensive methods of determination of toxic substances and develop methods alternative to those *in vivo* of the preliminary determination of potential toxic properties of studied substances. The obtained results of the determination of different biological activity descriptors indicate that various chromatographic methods can be treated like a screening tool especially in the first stage of the research. One of the methods alternative to the *in vivo* ones is micellar chromatography, particularly BMC which combined with the *in silico* methods can be used for preliminary screening estimation of compounds biological activity.

Many researchers in their experiments base on the assumptions of the Hansch model obtaining values of actual descriptors of biological activity close to those obtained under *in vivo* conditions. To determine biological activity of compound by means of *in vitro* and/or *in silico* methods, steric, electronic and lipophilic parameters of the molecule must be taken into account. It is widely recognized that the Hansch approach initiated research on the quantitative relationship between the structure of a compound and its biological activity, QSAR.

The Hansch analysis correlates the biological activity values with physicochemical properties by linear, linear multiple or nonlinear regression analysis; thus, the Hansch analysis is indeed a property-property relationship model. It is sometimes called the linear free energy-related (LFER) approach therefore Abraham parameters are frequently used in the interpretation and prediction of retention data in diverse chromatographic modes. According to a multi-parameter Hansch approach to a number of biochemical issues, biological activity of a compound is conditioned by its physicochemical properties, mainly by its lipophilicity. The Hansch analysis can be used to describe complex biological data where several different transport processes and equilibria contribute to the overall structure-activity relationship. Correspondingly, all different kinds of biological activities have been correlated with the linear free energy-related parameters using the Hansch analysis.

As regards *in silico* methods, they involve computer simulations connected with the particular fields of biological activity with the use of mathematical models constructed on the basis of experimental data. *In vitro* methods are led in systems imitating biological environment. One of the *in vitro* methods which describe biological activity of many compounds is micellar chromatography, MLC (especially Biopartitioning chromatography, BMC). BMC (MLC) micelle is generally recognized as a biological membrane model.

Many important biological activity parameters can be calculated using both *in vitro* and *in silico* methods. These descriptors concern such processes as: blood-brain barrier permeation, skin permeation, jejunum absorption, Caco-2 absorption (Caco-2 is cell line imitating human intestine epithelium), toxicity (expressed as the expected effect on organisms tested), ecotoxicity, mutagenicity, genotoxicity, human serum albumin binding and many others, equally important.

In the study the determination of the free ampicillin fraction as well as percutaneous absorption have been investigated using different chromatographic methods including MLC, BMC, ISRP, IAM, etc. The micellar method involved the direct injection of the protein-drug solutions and pure drug solutions (without the existence of HSA) to the chromatographic system. The optimized MLC systems were used in the evaluation of the influence of the type of surfactant in mobile phase (using the same stationary phase) and the type of stationary phase (using the same mobile phases) on free drug fraction.

The study recognized that micellar with direct sample injection (DSI) method can be successfully applied in the determination of the concentration of free drug fraction as well as percutaneous absorption, provided the appropriate optimization of the MLC systems. As before, it is necessary to compare the value of the free drug fraction concentration obtained using MLC with the appropriate values obtained using other well-known methods. The system consists of CTAB and RP-8e column which proved to be the most useful in the evaluation of the concentration of the free ampicillin fraction in HSA solutions (the obtained values were the most similar to the values obtained by the use of adsorption method: RP-HPLC and spectrophotometric analyses).

DETERMINATION OF BIOLOGICAL ACTIVITY OF ORGANIC COMPOUNDS BY THE USE OF CHROMATOGRAPHIC METHODS

Katarzyna STĘPNIK
DEPARTMENT OF PLANAR CHROMATOGRAPHY

To determine biological activity of organic compounds by means of chromatographic methods, steric, electronic and lipophilic parameters of the molecule must be taken into account. Many researchers in their experiments base on the assumptions of the Hansch model obtaining values of actual descriptors of biological activity close to those obtained under *in vivo* conditions. It is widely recognized that the Hansch approach initiated research on the quantitative relationship between the structure of a compound and its biological activity, QSAR.

Biological data of all different kinds can be used in the QSAR approach. The Hansch analysis correlates the biological activity values with physicochemical properties by linear, linear multiple or nonlinear regression analysis; thus, the Hansch analysis is indeed a property-property relationship model. It is sometimes called the linear free energy-related (LFER) approach therefore Abraham parameters are frequently used in the interpretation and prediction of retention data in diverse chromatographic modes.

According to a multi-parameter Hansch approach to a number of biochemical issues, biological activity of a compound is conditioned by its physicochemical properties, mainly by its lipophilicity. The Hansch analysis can be used to describe complex biological data where several different transport processes and equilibria contribute to the overall structure-activity relationship. Correspondingly, all different kinds of biological activities have been correlated with the linear free energy-related parameters using the Hansch analysis.

To determine biological activity of compound by means of *in vitro* and/or *in silico* methods, steric, electronic and lipophilic parameters of the molecule must be taken into account. Many researchers in their experiments base on the assumptions of the Hansch model obtaining values of actual descriptors of biological activity close to those obtained under *in vivo* conditions.

In silico methods involve computer simulations connected with the particular fields of biological activity with the use of mathematical models constructed on the basis of experimental data. *In vitro* methods are led in systems imitating biological environment. One of the *in vitro* methods which describe biological activity of many compounds is micellar chromatography, MLC (especially Biopartitioning chromatography, BMC). BMC (MLC) micelle is generally recognized as a biological membrane model.

To estimate the biological activity of the compounds tested, the significant bioactivity descriptors should be determined *in silico* or *in vitro*. These descriptors concern such processes as: blood-brain barrier permeation, skin permeation, jejunum absorption, Caco-2 absorption (Caco-2 is cell line imitating human intestine epithelium), toxicity (expressed as the expected effect on organisms tested), ecotoxicity, mutagenicity, genotoxicity, human serum albumin binding and many others, equally important.

In the study the determination of the free ampicillin fraction as well as percutaneous absorption have been investigated using different chromatographic methods including MLC, BMC, ISRP, IAM, etc. The micellar method involved the direct injection of the protein-drug solutions and pure drug solutions (without the existence of HSA) to the chromatographic system. The optimized MLC systems were used in the evaluation of the influence of the type of surfactant in mobile phase (using the same stationary phase) and the type of stationary phase (using the same mobile phases) on free drug fraction.

The study recognized that micellar with DSI method can be successfully applied in the determination of the concentration of free drug fraction as well as percutaneous absorption, provided the appropriate optimization of the MLC systems. As before, it is necessary to compare the value of the free drug fraction concentration obtained using MLC with the appropriate values obtained using other well-known methods. The system consists of CTAB and RP-8e column which proved to be the most useful in the evaluation of the concentration of the free ampicillin fraction in HSA solutions (the obtained values were the most similar to the values obtained by the use of adsorption method: RP-HPLC and spectrophotometric analyses).

The obtained results of the determination of different biological activity descriptors indicate that various chromatographic methods can be treated like a screening tool especially in the first stage of the research. Due to a large number of chemical substances in everyday use, high costs and long time of investigations on their toxicity estimation as well as ethical aspects connected with experiment on animals, it is necessary to apply a fast and inexpensive methods of determination of toxic substances and develop methods alternative to those *in vivo* of the preliminary determination of potential toxic properties of studied substances. One of the methods alternative to the *in vivo* ones is micellar chromatography, particularly BMC which combined with the *in silico* methods can be used for preliminary screening estimation of compounds biological activity.